Master Thesis, Department of Geosciences

Spatial variability of snow and avalanche conditions along a climatic gradient in Central Spitsbergen, Svalbard

Mikkel Arne Kristiansen

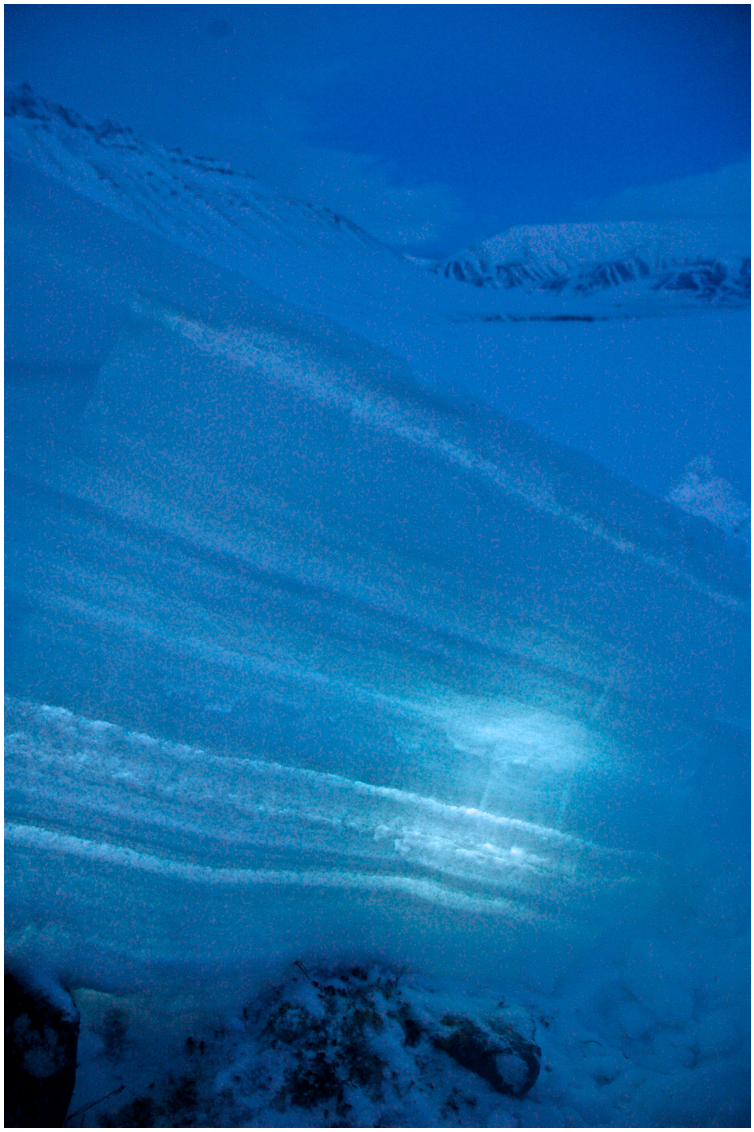

UNIVERSITY OF OSLO

FACULTY OF MATHEMATICS AND NATURAL SCIENCES

Spatial variability of snow and avalanche conditions along a climatic gradient in Central Spitsbergen, Svalbard

Mikkel Arne Kristiansen

Master Thesis in Geosciences

Discipline: Physical Geography

Department of Geosciences / Department of Arctic Geology (UNIS)

Faculty of Mathematics and Natural Sciences

University of Oslo

01.09.14

Supervisor: Ole Humlum, Department of Geosciences, University of Oslo

Supervisor: Hanne H. Christiansen, Department of Arctic Geology, UNIS

Front page photo: Backlit snowpit, Todalen, February 2014. Photo: Mikkel Arne Kristiansen

This work is published digitally through DUO – Digitale Utgivelser ved UiO

http://www.duo.uio.no

It is also catalogued in BIBSYS (http://www.bibsys.no/english)

0.1 Preface

This study never could have taken place without the financial support from Forskningsrådet. The Arctic Field Grant 2014 financed fully the logistics needed to execute regular field work throughout the 2014 late winter season.

0.2 Acknowledgments

First and foremost I would like to thank my family for help and support during my five years as a university student. I wouldn't have succeeded without your motivation and kindness.

Secondly I give my appreciations to Hanne H. Christiansen, my superviser at UNIS, for providing me the opportunity to live and study for two years on Svalbard. Through you I was introduced to the amazing scientific community at UNIS, which further provided me the needs to go explore and study the place I feel privileged to have called home for two years. Thank you! I also give my thanks to Ole Humlum, superviser at UIO, for giving me great freedom and help when necessary.

Marcus Eckerstorfer provided the initial idea for this study, and further helped me develop it into a master study. I greatly appreciate your input.

I would also like to thank everybody at UNIS who have helped me out along the way: Berit the librarian for helping me with hard to find literature and for being super friendly, all fellow students I have enjoyed lunch and coffee breaks with, logistic's staff for helping me organize field work, field assistants for helping me execute field work, and Venke at the reception for making my bad days go from rock bottom to nothing but smiles.

My good friend Henning Åkesson has since my first semester at the university inspired my academic conquest. You are one of my best friends and I can truly say that I never could have come this far without you. Ba-zaow! and I wish you good luck with the rest of the journey, have fun with your PhD!

Last, but certainly not least, I thank my girlfriend, Ida. Hanging out with you on top of mountains, before skiing down, are some of my fondest memories of Svalbard.

0.3 Abstract

Spatial variability of the snow properties in the areas surrounding Longyearbyen, Svalbard has not yet been studied on a larger scale. This first attempt study will research how snow properties varies within a areal 106km^2, around Longyearbyen (78°N). Attempts were made to connect measured snow properties to local climatic gradient, from areas near an ice-free fjord to higher elevation inland areas. Field measurements were conducted regularly from late January to mid May 2014. Coarse resolution snow property measurements and meteorological data were used to describe the spatial and temporal variability of snowpack conditions, and the environmental processes acting on the snow cover. The study provided insight into how regions within the study area were affected differently by weather events, such as mid-winter warm spells. This variability resulted in regional patterns of snowpack instabilities relevant for slab avalanches, and arguably identified higher elevation snowpack conditions as most unstable.

Contents

List of Figures

List of Tables

Chapter 1

Introduction

1.1 Introduction and study aims

Avalanches are a threat to human life and infrastructures in mountainous snow climates.

The arctic archipelago of Svalbard (74°-81°North and 10°-35°east) has long winters due to the cold arctic climate, and there is typically a continuous snow cover from October through May. Characteristic of the Svalbard landscape during this season are snow avalanche activity on the steep mountain- and valley sides that characterizing the landscape. Avalanches are observed near the settlements of Svalbard every year, and people traveling in Svalbard are frequently exposed to avalanche prone terrain. Avalanches have killed four people during the last 20 years, all in areas close to Longyearbyen, the largest town in Svalbard. All accidents were related to recreational snow scooter activity, an activity that is increasing in popularity by both tourists and residents of Longyearbyen. To better understand the avalanche threat in the wilderness and the settlement of Longyearbyen, in an increasingly unpredictable climate, there is growing need for increased understanding of the snow cover in the region of Longyearbyen.

The high latitude northern regions have been pin-pointed as a focus area for future economic potential, as sea-ice is diminishing and opening new areas for potential oil exploration, fishery and shipping routes. The easy access of Svalbard will make the settlements there a natural hub for logistical support to these areas, and is therefore also expecting growth in number of activities related to this.

This introductory chapter will first give a summary of the previous snow studies conducted on Svalbard, then describe the study aims and goals of this master thesis study, and finally introduce the geography and climate of Svalbard.

1.1.1 Previous snow avalanche studies in Svalbard

Early snow avalanche research on Svalbard focused on frequency and the geomorphological print of slush avalanches on Spitsbergen (André 1990a; 1990b). The geomorphological imprint of snow avalanches were continued as a research area, and is still relevant for studies of landform development. Humlum (2007) studied an avalanche derived rock glacier, where ice and rock content was supplied by cornice fall avalanches. Cornice fall avalanches were also studied as a source of rockwall erosion and sediment transport by Eckerstorfer et al. (2013). They studied the slope system of Gruvefjellet, a well known mountain above the Longyearbyen settlement where numerous cornice fall avalanches occur annually.

Avalanche conditions, mechanics and triggers have later also been studied as the settlements on Spitsbergen, the largest and only inhabited island on Svalbard, has seen the need to better understand the avalanche threat. The cornice system mentioned above was also studied by Vogel et al. (2012), who focused on the dynamic growth and collapse of cornices, and connected meteorological parameters to the development of cornices. The avalanche climate was further researched through a PhD thesis, leading to six papers published by Marcus Eckerstorfer including the aforementioned paper (Eckerstorfer et al. 2013) focusing on geomorphology. Eckerstorfer and Christiansen (2011b) studied the topographical and meteorological controls on all forms of snow avalanches observed through an avalanche-monitoring research project (Cryoslope), connecting topographical conditions and weather patterns to avalanches. Their study identified cornice fall avalanches as the dominating type of snow avalanche in the region around Longyearbyen. Cornice fall avalanches are governed by the flat plateau mountains and frequent high winds that transport snow across the flat mountain tops and deposits it on the lee sides of the plateau edges. Meteorological data was used to identify weather patterns leading to natural slab avalanches releases, the second most dominant form of avalanche, in a third paper by Eckerstorfer and Christiansen (2011c). Their findings identified snowdrift as the best predictor for days with natural slab avalanche releases. Eckerstorfer and Christiansen (2012) also studied mid-winter slush and wet slab avalanche periods by identifying meteorological, topographic and snow-pack conditions leading to the studied avalanche events. This study focused on two warm spell cycles leading to slush and wet slab avalanches, and identified the topography of the avalanches, the meteorological conditions leading up to the avalanches, and the snowpack conditions prior to the releases.

Lastly, Eckerstorfer and Christiansen (2011a) described the snow climate based on meteorological data and snowpack studies over two winter seasons (2007/2008 and 2008/2009), and proposed an additional snow climate: "The High Arctic Snow Climate". The snow climate class was suggested as an addition to the existing classification systems developed by Sturm and others (1995) and was a good expansion, as the the snow

climate of Svalbard did not fit in to any of the existing classes. This snow climate was described as a very thin and cold snowpack, a basal layer of depth hoar with wind slabs and ice layers on top (Eckerstorfer and Christiansen 2011a). The paper also includes types of weak layers identified through the studied seasons. Description of the snow climate and the other classifications by Sturm and others (1995 , including additions are found in Appendix II.

Another doctoral thesis focusing on avalanches was completed by Louis Delmas (2013) titled "Spontaneous Avalanche Releases in Svalbard, Influence of Climate Parameters on Snow Mechanical Properties", focusing on the mechanical properties of snow in regards to the changing arctic climate on Svalbard. The thesis concluded, among other things, that a changing climate could have implications for the future avalanche climate on Svalbard.

Furthermore, Eckerstorfer and others (2014) studied avalanche triggering zones on wind-affected slopes at three small slopes on Svalbard, and found that surface topography combined with snowpack development and extreme weather events were important for understanding slab avalanche triggering zones. The study found an inverse relationship between stability and slab thickness for weak layers developed early in the season, as weak layers were discontinuous over a slope and preserved in topographical depressions (Eckerstorfer et al. 2014).

A MSc project (Farnsworth et al. 2013) studied spatial variability on small, wind affected slopes, and how surface topography influences snowpack stability. Farnsworth (2013) supported the idea that weak layers in thin sections of the snow cover (caused by horizontal concave surface profiles) are potentially more easy to trigger. The study also suggested an inverse relationship between snow depth and instabilities, as deeper snow sections of a slope often hold more weak layers.

Lastly there are three avalanche incident reports by the Norwegian Geotechnical Institute (NGI.no), which describe avalanches with fatalities. These reports carry some scientific relevance, as they outline the type of avalanche and the meteorological conditions leading up to the event.

1.1.2 Research aim

This study aimed to investigate the spatial variability of snow properties along a climatic gradient, from near fjord areas to higher elevation inland areas. In an area of 106km^2, between 15 to 616 m a.s.l., were seven snow pits regularly surveyed from January to May 2014, and data from six meteorological stations analyzed (Fig. 3.1). This study structure facilitated description of the environmental gradient within the study area.

By these methods the thesis wishes to answer the following research questions:

- What characterized the environmental gradient, from fjord proximal areas to higher elevation inland areas, through the mid-winter season of 2013-2014, and how did this season compare to previous seasons?
- How did snow properties vary along the climatic gradient through the season, and did they reflect the environmental gradient described by meteorological data?
- Did the variable snow properties result in temporal and spatial patterns of snowpack instabilities?

1.2 Thesis structure

This thesis is structured as follows: Chapter 1, Introduction introduces the environment of Svalbard and why avalanche studies are important in this area. Following are previous snow studies of the region briefly described and research aims manifested through three research questions. Last in this chapter is general geography and climate of Svalbard introduced. Chapter 2, Theory, establishes the theoretical base needed for this thesis. It covers topics on snow climates to snow metamorphism, and avalanches. Chapter 3, Methods, described the methods used in the field, of how digital data was obtained, and of how data was further analyzed and classified. Chapter 4, Results, provides all data presented through the thesis, including meteorological data and snow measurements. Most data are provided through figures and tables, but are also in large described in the text. Chapter 5, Discussion, discusses the results presented, relates the results to theory and discusses their significance. This chapter also includes a brief discussion on Spatial variability and research methods. Chapter 6, Results, concludes the thesis and attempts to answer the research questions. Last is Appendix (I-III) including figures of relative fractions of snow types per pit, overview of seasonal snow climates on the ground, and all snow pits in a digital format.

1.3 The Geography and Climate of Svalbard

In the following sections will the geography and climate of Svalbard be described as an introduction to the topography and climate relevant for this study.

1.3.1 Geography

Svalbard is an arctic archipelago located between 74°to 81°N and 10°to 35°E see fig. 1.1. It is surrounded by four seas: the Barents Sea to the east, the Greenland Sea to the west, the Norwegian Sea to the south and the Arctic Ocean to the north. The archipelago has an areal of 62 160 km^{2}and its principal islands are Spitsbergen, Nordaustlandet,

FIGURE 1.1: Svalbard's location and permafrost distribution in the northern hemisphere. The archipelago is within an areal of 62 000 km^2. Its principal islands are Spitsbergen, Nordaustlandet, Edgeøya, Barentsøya, Kong Karls Land, Prins Karls Forland, and Bjørnøya. Red frame show location of Svalbard. Source: maps.grida.no 2014

Edgeøya, Barentsøya, Kong Karls Land, Prins Karls Forland and Bjørnøya, see fig. 1.2 . The main settlement on Svalbard is Longyearbyen, which is located on the largest island, Spitsbergen (39 044 km^2). Spitsbergen's topography is mountainous, with glacially derived valleys and fjords, and includes many valley glaciers and ice caps. Svalbard's highest peak, located on Spitsbergen, is Newtontoppen 1717 m a.s.l.

Svalbard is one of few land areas in the high Arctic that have permanent settlements throughout the year. All settlements on Svalbard have originally been formed in connection to coal exploration, but most of them have adapted past the company-style town to support the new industries that flourish in the area. Svalbard has lately become a hot-spot for arctic- tourism and science, which are now competing with coal exploration in revenue.

1.3.2 Currents and sea ice

Two ocean currents with relatively different surface water properties, namely The Eastern Spitsbergen Current (ESC) and The Western Spitsbergen Current (WSC), Fig. 1.2 flows south along the eastern coast and north along the western coast of Spitsbergen respectively. The currents strongly affects the climate in Spitsbergen and Svalbard (**hanssen1990**). WSC is the northernmost extension of the warm Norwegian Current, and flows towards the west coast of Spitsbergen. This current brings warm and salty

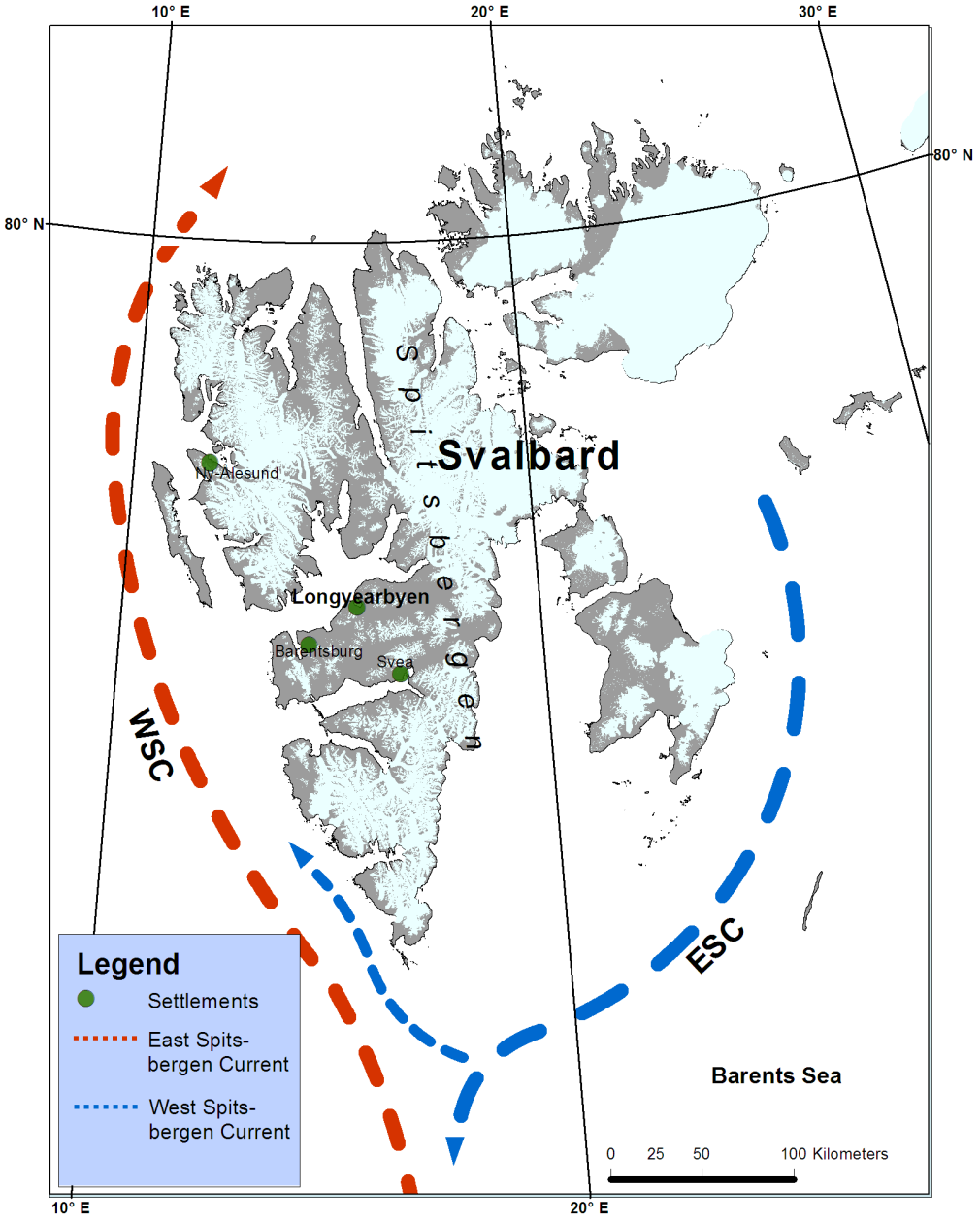

FIGURE 1.2: Overview of Svalbard's glacier distribution, surrounding seas and ocean currents

surface water that causes the world's northernmost open sea area with ice-free conditions during winter months. To the east of Spitsbergen, ESC flows southwest along the east coast, bearing cold waters with low salinity, which frequently carry pack ice. ESC partly deflects where the two currents meet, at Sørkapp, and flows north between the west coast and the WSC, often carrying pack ice and causing foggy conditions along the west coast during summer (Harland et al. 1997). This situation normally causes western Spitsbergen to be mostly ice-free during the winter while the east coast is dominated by sea ice.

Bernestad and others 2002 concluded that there is a connection between sea ice cover and local climate on Svalbard. While sea ice insulates the ocean from the atmosphere, open waters transfer a substantial amount of heat to the atmosphere. Open waters cause the coastal climates to be warmer than continental inland climates, like e.g. the coast of western Spitsbergen. This implies a strong climatic gradient from the coastal areas to the relatively more continental inland areas, along the ice free coast of west Spitsbergen.

1.3.3 Climate and meteorology

The weather on Svalbard is controlled by two weather systems with opposing characteristics. The pressure gradient between the semi-permanent low-pressure area east of Iceland and the relatively high-pressure area over Greenland governs the amount of warm air masses transported from lower latitudes towards Svalbard, i.e. the North Atlantic Cyclone Track (**hanssen1990**). When the low-pressure systems from the south reach Svalbard they bring relatively high temperatures, humidity and cause strong winds (see Fig. 1.3) . This is in contrast to high-pressure scenarios, which causes cold and dry arctic air masses to extend over Svalbard, typically flowing in over Spitsbergen from northeast. The difference in air temperatures over Svalbard, during these two opposing weather scenarios, can be large, and cause sudden large temperature rises/drops.Temperature changes of 20°C is not uncommon, and temperatures above zero with rain can occur even mid winter (Eckerstorfer and Christiansen 2011c).

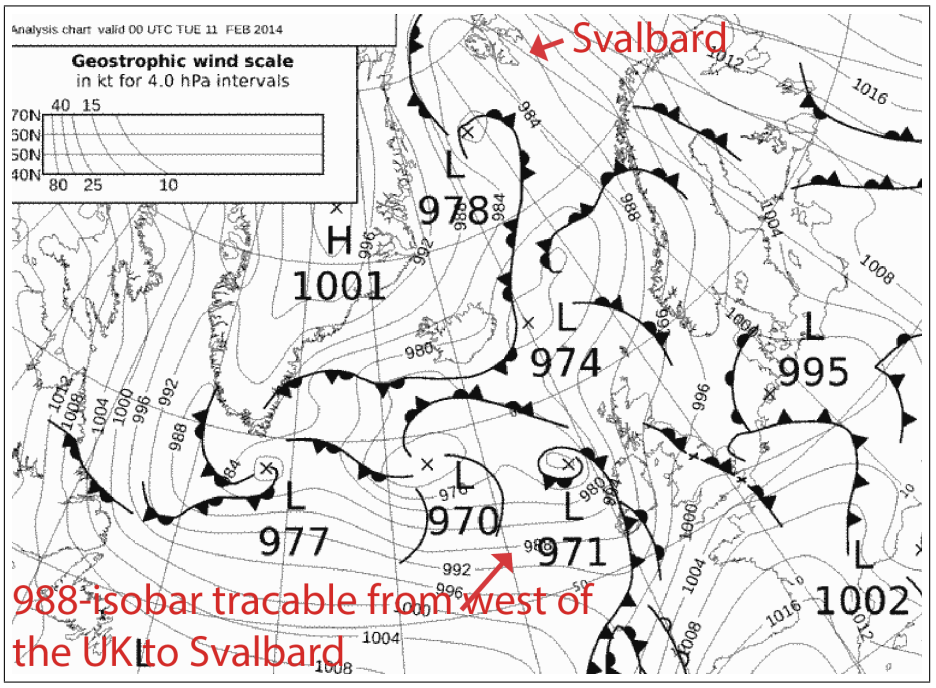

(A) Low pressure scenario causing mid-winter warm spells on Svalbard, recorded February 11th 2014. Winds, traceable along the isobars from lower latitudes of central Europe towards north and over Svalbard, carry warm air masses in an anti-clockwise movement towards the low pressure center located south-west of Spitsbergen. UK = United Kingdom.

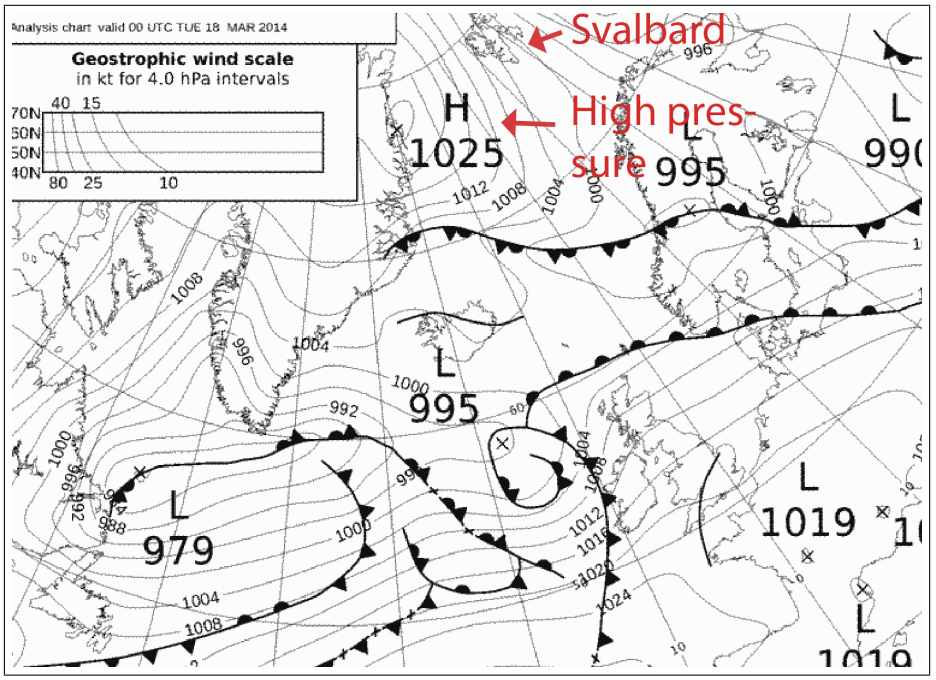

(B) High pressure scenario, recorded March 18th 2014, causing periods of cold calm weather on Svalbard. High pressure center located south-west of Spitsbergen transport air masses from north and towards Svalbard.

FIGURE 1.3: Maps of location of pressure centers, over the North Atlantic, during two distinct weather types on Svalbard. Map (A) show a typical scenario of low pressure centers causing mid-winter warm spells, and (B) show how high pressure systems cause calm cold-weather periods. Maps downloaded from: www.wetterzentrale.de.

Weather systems associated with cold-weather and warm-weather periods on Svalbard can be illustrated by maps of pressure centers over the north Atlantic (see Fig. 1.3). Map A in Fig.1.3 show a low-pressure center located southwest of Svalbard, a typical scenario for mid-winter warm spells on Spitsbergen. Winds follow the pressure isobars, which in the low-pressure scenario (map A, 1.3), can be traced from lower latitudes of central Europe, up along western north Europe and over Svalbard. These air masses often carry mild temperatures, and can cause positive temperatures on Svalbard mid-winter. Map B, Fig.1.3 show a high pressure scenario associated with calm cold-weather periods on Svalbard. The high pressure center on the map, located just southwest of Svalbard, caused cold air masses to extend down from high north latitudes, reaching Svalbard.

Longyearbyen has a long record of meteorological data, see Fig. 1.4. The recent normal period (1961-1990) mean annual temperature was -6,7 °C, but temperatures have increased by 1.04 °C per decade from 1975 to 2011, with the highest increase during winter and spring months (Humlum et al. 2003).

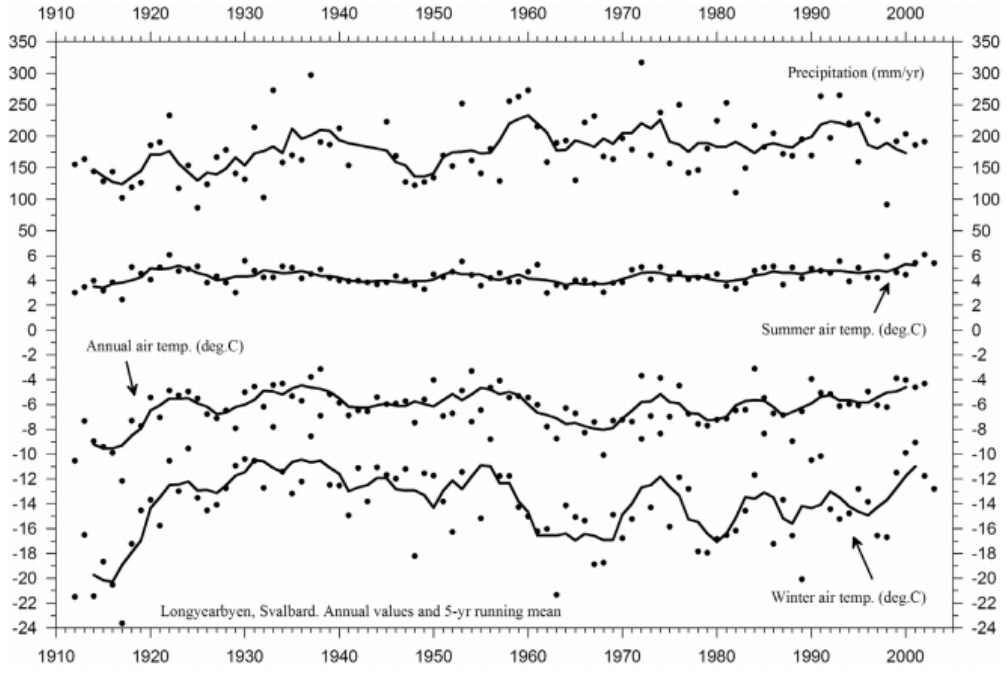

FIGURE 1.4: Meteorological record from Flyhavnen (Svalbard airport), 1910 - 2003. Source: Humlum et al. 2003

Precipitation data from the station is considered inaccurate due to issues with solid precipitation, often in combination with strong winds, leading to wind-induced under-catch (Adam and Lettenmaier 2003). This systematic bias, and the weather station's low representation due to its locality, undermines the relevance of the data. Nonetheless, *Humlum (2002) used a 100 % adjustment to the recorded precipitation values, and modeled a 15-20 % precipitation vertial (per 100 m) precipitation gradient in coastal regions, and a 5-10% gradient in the inland environments.*

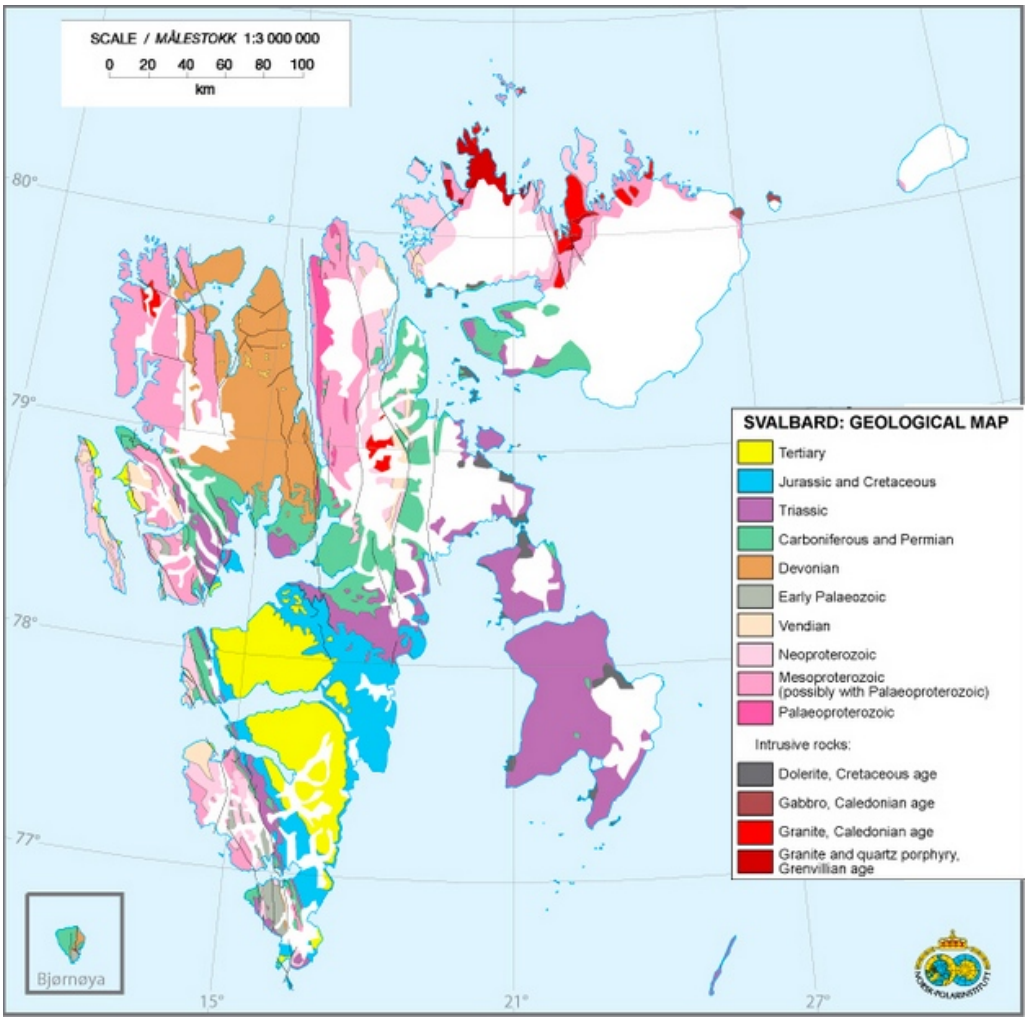

FIGURE 1.5: Overview map of Svalbard's bedrock geology. Longyearbyen is within the area of Tertiary. From npolar.no

1.3.4 Geology

Svalbard is an uplifted area of the northeast Barents Sea, and contains a large geological archive. The archive of Svalbard is rare as it is one of the few places on Earth that contains such long geological record within a relatively small area, which spans from Precambrian granites to Tertiary sedimentary rocks (Worsley, 2008), see Fig. 1.5. Each sedimentary succession reflects its geological depositional environments, and can be studied to increase the understanding of the Earth's climate and tectonic history. Relict fault zones, rift basins and orogenically deformed strata show that the area has been tectonically active (Harland et al. 1997). The majority of the archipelago has drifted from lower latitudes at Devon, nearby the equator, to the present high arctic latitudes, and is still drifting north towards the geographic North Pole.

1.3.5 Glaciation and permafrost

Glaciers cover 60 % of Svalbard, and the remaining land areal in continuous permafrost (Humlum et al. 2003). In general the permafrost varies in thickness from about 100 meters in the valleys to up to 400-500 meters in the mountains (Christiansen et al. 2005). The permafrost greatly affects natural systems such as hydrology, biology, and snow cover, but also man made structures such as fundaments and pipelines. Landforms associated with glaciers and permafrost are abundant all over the landscape of Svalbard, e.g. ice cored moraine complexes, rock glaciers, pingos and ice wedge polygons (Humlum et al. 2003).

Chapter 2

Theory

2.1 Snow avalanches

Snow avalanches are masses of snow that rapidly tumbles, slides and/or flows down slopes. There are four different sub-categories: (1) slab avalanches are cohesive slabs of snow that loosens from the snow cover and avalanches downslope; (2) loose snow avalanches are point triggered flows of low density snow; (3) slush avalanches are water saturated masses of snow; and (4) cornice fall avalanches are big pieces of dense snow released from a cornice that tumble down a slope, and potentially also trigger additional snow for avalanching (McClung and Schaerer 2006).

This thesis focuses on the underlying conditions for slab avalanches, i.e. how meteorology, thermal conditions and topography affect the snow cover in respect to potential slab avalanche hazard. Only an introduction to slab avalanches is therefore included here.

2.1.1 Slab avalanches

Slab avalanches release when a weak layer or interface underneath a cohesive thick layer of snow (known as a slab) fails and initiates fracture propagation. If the fracture propagates and releases the slab from the snow cover, and the slope is steep enough to overcome the friction between the slab and the sliding plane, the mass of snow start sliding down slope (Schweizer 1999).

Most slab avalanches occur during or right after storms, and contain only the newly deposited snow, and are typically small in size (McClung and Schaerer 2006). This type of avalanches is called direct-action avalanches, and is triggered by shear-failure in the old-new-snow interface. Slab avalanches are also often triggered by the failure of layers with kinetic-growth crystals (see section 2.2.4) deeper in the snowpack, and are often

known as climax avalanches (McClung and Schaerer 2006). These types of weaknesses in the snow stratigraphy are called persistent weak layers. The layers can develop within the snowpack or on the surface if buried by subsequent snowfall, and can persist for long periods of time after a storm (McClung and Schaerer 2006).

Persistent weak layers are problematic when forecasting avalanche events, as they are highly unpredictable and remains hidden from the surface as traps waiting to be sprung (McClung 2002). Common persisting weak layers found within the snow cover are horizons of faceted grains, depth hoar and buried surface hoar. Faceted crystals develop post-deposition due to high temperature gradients; depth hoar commonly form at the bottom of the snowpack in the early season due to very high temperature gradients in a shallow snow cover; and surface hoar is the frozen equivalent of dew, and can persist as weak layers if they are buried by subsequent snow fall (Birkeland 1998). Slabs, weak layers and interfaces between layers are all typical elements of the stratified snow cover that builds up throughout winter season, and their properties results from an interconnecting relationship between weather, ground thermal regime, topography and post-deposition snow development (Schweizer et al. 2008). Snow crystals are in a dynamic state after deposition, and change form and size through recrystallization. This process is known as snow metamorphism and will be explained in detail through the next sections.

2.2 Snow properties

2.2.1 Snow metamorphism

Snow on the ground can be seen as a porous fine-grained material with constantly changing properties due to external influences (Pielmeier and Schneebeli 2003). Transformation of snow crystals and their properties is called snow metamorphism, and includes how the seasonal snow cover, from each individual snow grain to bulk masses of snow, transforms in size, shape and cohesion over time (Colbeck 1982). The snow cover is always developing, starting right at deposition and ending at melt-out in spring. Initial changes to snow crystals are caused by wind shattering and environmental conversion (from the atmosphere to the ground surface). Post-deposition, snow grains develop further in shape and size because of processes that operate within the snowpack. Some grains grow large, while others might disappear completely on the expense of other crystals growing (Colbeck 1982). Rate of crystal type transformation and growth depend the environment within the snowpack and external driving forces (Colbeck 1991). Air temperature, wind and solar radiation are the most important external forces that affects snow metamorphism, as they regulate the temperature gradient within the snowpack (McClung and Schaerer 2006). The temperature gradient within the snowpack is an important cause of recrystallization of snow grains, as it drives water vapor flux.

Water vapor is transported from relative warmer areas to colder areas of the snowpack along the temperature gradient, and consequently re-shape snow grains into different crystal types, depending on the amplitude of the driving force and/or the concentration of excess water vapor (Colbeck 1982).

Water vapor travel from relatively warm to colder areas of the snowpack, along the naturally occurring temperature gradient, and consequently transforms the shape of snow grains through recrystallization as water vapor deposits onto crystals in cold areas (Colbeck 1982). Temperature measurements is often used in the field for identifying areas of potential large water vapor fluxes within the snowpack (McClung and Schaerer 2006). And as snow has a low thermal conductivity, there will almost always be a temperature gradient within the snow cover, as the ground below the snow cover will be insulated from the air above (McClung and Schaerer 2006). This typically causes a warmer base than the top part of the snowpack, as the snowpack typically cools from above.

2.2.2 Water vapor transport

How mass is transported between snow grains has been studied through the last decades, and is considered to be a very complex interplay of processes (e.g. Yosida et al. 1955; Sommerfeld and LaChapelle 1970; Colbeck 1993; Schneebeli and Sokratov 2004). The process causing water vapor to move along a temperature gradient is still not fully understood (Pinzer et al. 2012). The process governs how snow crystals recrystallize and alter the physical properties of the snowpack, and is thus important for understanding why, when and where certain crystals appear. Water vapor moves in two ways within the snow cover: (1) by diffusion in the pore spaces in between snow grains, and (2) by conduction from snow grain to snow grain (McClung and Schaerer 2006). However, it is not clear if one way is more dominant than the other, or if one excludes the other under certain conditions. Pinzer and others (2012) published the first high resolution time lapse video of snow metamorphism, which showing how snow grains loose mass, grow and reshape by the process described as sublimation-deposition in the opposite way of a high temperature gradient. The paper concluded that one no longer should think of high-temperature snow metamorphism as a result of growing snow grains but rather growth by replacement, as they observed that the mass of some grains would all sublimate within few days and deposit in the opposite direction, favoring vertical structures (i.e. depth hoar). However, it is important to note that the finding by Pinzer and others (2012) does not exclude mass transport by conduction.

To fully understand and describe how water vapor moves within the snowpack is outside the scope of this study. For this study it is sufficient to acknowledge that temperature gradients drive water vapor transport, and depending on whether or not a temperature gradient is weak or strong, the snow crystal develops into different shapes with different

properties. The two contrasting processes and crystal types will be described in the following sections.

2.2.3 Equi-temperature metamorphism and the curvature effect

The initial change in newly deposited precipitation snow crystals is the *curvature effect*, which is not controlled by the temperature gradient within the snowpack, but rather differences in water vapor concentrations above different areas of the snow crystal (McClung and Schaerer 2006). To understand the curvature effect it is convenient to visualize the crystal shape of a stellar dendrite, a common type of precipitation snow crystals (see Fig. 2.2). Developed in an environment with high water vapor saturation, the stellar dendrite takes a form that require high energy to sustain, and is thus in disequilibrium with its environment once deposited on the ground (where the air has a much lower water vapor saturation) (Furukawa and Wettlaufer 2007). The snow crystal will therefore inevitably transform into a more energy-efficient structure, which is a sphere because of smallest surface area to volume ratio (LaChapelle 1969). The shape of the stellar dendrite has series of convex and concave surfaces (branches and in between branches respectively). There is a differences in water vapor pressure between surface parts of snow grains; as higher vapor pressure was recorded above convex parts than concave parts (Sommerfeld and LaChapelle 1970). This difference implies that concave parts are colder, and that water vapor above convex surfaces favorably deposit on concave surfaces (Sommerfeld and LaChapelle 1970). This net transport of mass leads to rounded spherical crystal shapes, commonly known as rounds (see Fig. 2.2) (Colbeck 1982). This process also strengthens bonds between neighboring snow grains, as there often will be a concave profile at the connection points between grains. Lab experiments show that rounding of snow crystals due to the curvature effect is very slow when there is no temperature gradient present, compared to other recrystallization processes (Colbeck 1982).

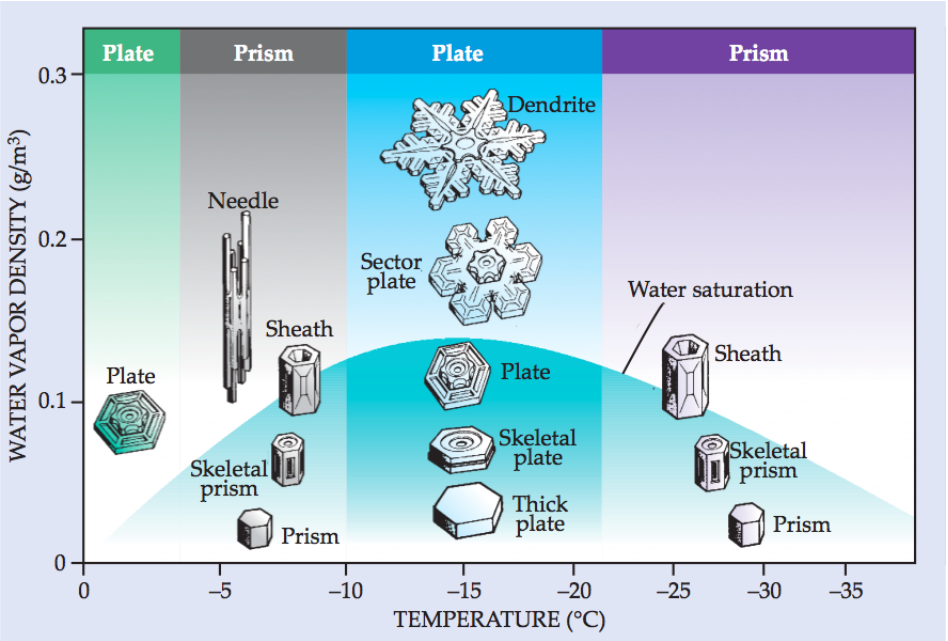

FIGURE 2.1: Overview of precipitation particles, and the environmental parameters the various forms are develop under. Figure from Furukawa and Wettlaufer 2007

Equi-temperature metamorphism, commonly known as rounding, is also a process of recrystallizing snow crystals into spherical shaped snow grains. However, this process is faster than the slow curvature effect, and is driven by a low water vapor flux that deposits mass on to the concave areas of the snow grains, and is driven by a low temperature gradient (Sommerfeld and LaChapelle 1970). This low vapor flux will not only enhance the rounding process but will also cause the snow grain to grow. Larger grains will grow on the account of smaller grains if there is a mixture of snow grain sizes (McClung and Schaerer 2006. Latent heat released when water vapor deposits on colder grains, will preferentially warm and melt smaller grains (as they take less energy to melt), and create more excess water vapor. This positive feedback causes average snow crystal size to grow (McClung and Schaerer 2006). Spherical snow grains (i.e. rounds) have high intercrystalline bonding capability and often form hard dense slabs (Colbeck 1991.

2.2.4 Kinetic-growth metamorphism

Kinetic-growth metamorphism develops snow crystals into sharp-edged crystals with flat faces, and occur in areas of the snowpack with supersaturated water vapor (LaChapelle 1969; Schweizer et al. 2003). Strong temperature gradients (from 1 °C per 10cm and higher) cause higher large vapor fluxes and consequently excess water vapor in the pore spaces. Supersaturated water vapor in the pore spaces leads to kinetic growth metamorphism that develops the crystals known as facets (see Fig. **snowgrains**) (Colbeck 1982. Faceted crystals can also develop further into to step-wise cup-shaped crystals known as depth hoar (Fig. **snowgrains**) (Pinzer et al. 2012). For this to occur, the

temperature gradient needs to be very strong and prolong for some time and the snow needs sufficient pore space for the water vapor to move.

Facets and depth hoar crystals are known to form layers of weaknesses in the snow stratigraphy. Due to their poor intercrystalline bonding capabilities and brittle behavior, they often cause the stratified snow cover to be prone to collapse and failure and cause slab avalanches (McClung and Schaerer 2006).

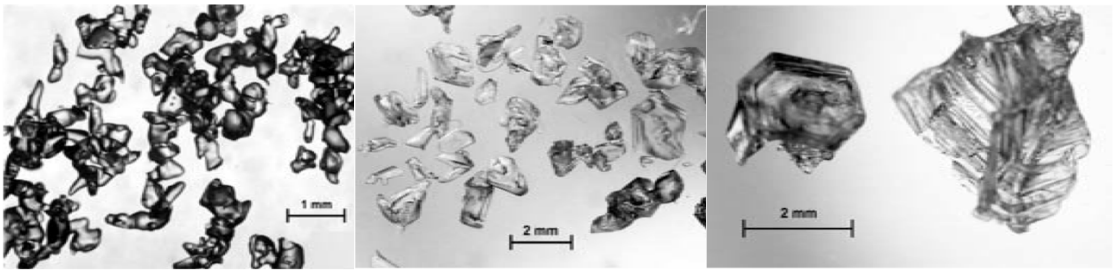

(A) Rounded snow grains. (B) faceted snow grains (C) Depth hoar crystals

FIGURE 2.2: Three examples of typical snow grains found in the Svalbard snow climate. Rounded grains (A) are spherical shapes that bounds well with neighboring grains, facets (B) have more angular corners and binds poorer with other grains, and depth hoar crystals (C) are large striated crystals that are, similarly to facets, brittle and find poorly to neighboring particles. Images from Fierz et al. 2009

2.3 Snow stratigraphy

The seasonal snow pack consists of layers with varying properties, and often, complex structures in regards to stability (Birkeland 1998). Knowledge of the stratigraphy and the properties of each layer are of interest for multiple sciences working with snow, but especially in the field of snow avalanches where unstable structures are fundamental for avalanche development (Schweizer 1999).

Each layer in a stratified snowpack is a result of a snow deposition event, either by precipitation or by wind drifted snow. Each snow deposition event is different, and consequently, each layer will also be different (Colbeck 1991). As a sum of snow crystal type, total amount accumulated, temperature, wind and topography, the newly deposited layer will get a combination of properties. If the snow layer bonds onto the snowpack, and does not get eroded away by either avalanching or wind, it becomes a part of the snow stratigraphy and possibly affects the present or future stability of the snowpack (Colbeck 1991). The initial properties of a newly deposited layer is important for how it further develops, and how neighboring layers and boundaries will change. Layers within the stratified snowpack are separated by bordering layers that have different characteristics, or by the surface at the top of the snow cover and the ground at the bottom. A boundary between two layers can be arbitrary, as some properties change gradually with depth (Colbeck 1991).

Layers of special interest to avalanche related investigations of the snowpack are cohesive slabs, weak layers and interfaces, and sliding surfaces (McClung 2002). All these are typical elements found within the snow cover, and where certain stratigraphic structures promotes avalanche risk. The attributes of snow layers are therefore important knowledge for avalanche forecasters and snow researchers. The following sections describes different types of layers and their attributes in more detail.

2.3.1 Slabs

Slabs are thick cohesive layers of snow and typically make out the majority of thickness in the snow cover (Colbeck 1991). Slabs are formed when deposited loose snow gains cohesion through intercrystalline bonding. This typically happens by rounding and settlement of the snow crystals, and formation of strong bonds between snow grains. Slabs can vary greatly in thickness, grain size, temperature, hardness and densities. All these determines slab properties, such as permeability, strength, stiffness, thermal conductivity and bonding ability with neighboring layers (Colbeck 1991).

2.3.2 Weak layers and weak interfaces

Unstable conditions commonly form in the snowpack when weak brittle layers underlay slabs (Schweizer et al. 2003). Weak layers typically develop due to kinetic-growth metamorphism in areas of the snowpack with high levels of supersaturated water vapor. The resulting faceted crystals are relatively stable shapes thermodynamically speaking, but form unstable layers as they have weak intercrystalline connections, which make the layers vulnerable to collapsing (McClung and Schaerer 2006). These layers can persist for long periods and cause prolonged problematic snow conditions. High water vapor densities are associated with imposed high temperature gradients, but can also be caused by impermeable layers that can cause high densities. Impermeable layers, e.g. rain crusts or melt-freeze crusts (see next section), can cause abnormally high levels of vapor supersaturation at unexpected areas of the snowpack (Jamieson 2006). These conditions occur as water vapor fails to penetrate through the crust, even though it is driven in that direction, and cause high saturation adjacent to the crust. Crusts are therefore often associated with weak layer formation, both above and beneath the crust. Another common weak layer is buried surface hoar (Hachikubo and Akitaya 1997). Surface hoar are crystals formed on the snow surface due to water vapor in the air depositing directly on to the snow surface. The phenomenon is the winter-equivalent of dew, and form brittle, cohesionless feathery crystals that form very weak layers if buried by subsequent snowfall (LaChapelle 1969).

During rapid deposition of snow, e.g. during wind drifts of heavy snowfall, the new snow deposition often fails to bond with the old snow surface. The interface between

the new and old snow will immediately be vulnerable to shear failure during or right after deposition, and can lead to what is called direct-action avalanches (Schweizer et al. 2003). Nevertheless, if the new snow layer does not slide, it will eventually settle and bond with the underlying snow surface, and restore stability.

2.3.3 Sliding surfaces and crusts

Slabs need a plane with low friction to slide on to form a slab avalanche. Sliding surfaces, also known as bed surfaces, can be the ground cover if the substrate is smooth, like grassy hills, but can also be hard smooth plains within the snow stratigraphy (Jamieson 2006). Common sliding surfaces within the snowpack are what often is referred to as crust, e.g. sun-crust, wind-crust, rain-crust and melt-freeze crusts. Crusts are surfaces of low friction that have limiting bonding capability caused by large grain size differences between the crystals in the crust and in the connecting layer (Colbeck and Jamieson 2001). Crusts often have associated development of weak layers below or above. However, development of weak layers above crusts are not well understood as they often seem to develop despite measurements of weak temperature gradients (Jamieson 2006). Noteworthy, Colbeck and Jamieson (2001) proposed that after the initial onset of faceting of snow grains above the crust, the thermal conductivity of the early faceted grains would fall dramatically, and the contrast in thermal conductivity between the crust and the faceted crystals would cause a strong temperature gradient to further develop fully faceted snow crystals, and even depth hoar. What causes the initial faceting is not understood. Colbeck and Jamieson (2001) argued that the decay of a wet crust could provide sufficient water vapor for initial faceting, though this requires specific weather scenarios and fails to explain all development of faceting near crusts, e.g. under dry conditions.

2.3.4 Spatial variability and scale

Snow measurements, e.g. snow height, varies spatially due to spatially variable topography and meteorological conditions. This is known as *spatial variability*, and is important for understanding avalanche patterns (Schweizer et al. 2008). Snow properties related to snow avalanches are known to vary on multiple scales, from micro-structures within a slope to more generalized, larger scale variability through a mountain range. Snow properties of layers within the snowpack varies spatially due to spatially variable environments, e.g. temperature lapse rate by elevation or incoming solar radiation by aspect, and often results in a highly complex spatially variable patterns of avalanche conditions or avalanches. Spatial variability studies have investigated snow stability within on slope scale (e.g. Jamieson and Johnston 1993) to regional scale (e.g. Birkeland **2001**), and have been discussed as one of the biggest uncertainties in regards to

forecasting snow avalanches and determining snowpack stability (Schweizer et al. 2008) and that this variability makes the biggest uncertainty of stability patterns, because of scaling issues (Kronholm, 2004). Natural processes acts over a typical scale, or a range of scales, termed the process scale (Schweizer et al. 2006). Spatial variability studies tries to measure and describe this process scale. A framework has been adapted from the field of hydrology (Blöschl and Sivapalan 1995) to describe the measurement scale in spatial variability avalanche studies. The following scaling triplet has been used to quantitatively describe sampling relevance and strategy: (1) the spatial extent (longest distance between two points, or area covered by study), (2) the spacing between samples (resolution), and (3) the integration volume of a sample (the support of an observation). Depending on sampling strategy, there will be a match or a miss-match between the measured scale and process scale. Schweizer and others (2006) acknowledged that there is a large range between measurement methods and spatial accuracy (i.e. how well different measurement techniques of snowpack properties can be extrapolated to larger areas). They specifically argued that snow layer properties are more continuous than e.g. stability scores, which implies that point measurements of layer properties can to some degree be extrapolated to a larger area.

2.4 Snow- and avalanche climate classification systems

Combinations of snowpack properties are typically determined by a regions climate, The normal combinations of snow properties over time within a region, e.g. depth of snow, type of weak layers, ice content etc., have been used to classify *snow climates*.

There is a large span in classification systems for snow, all with different perspectives and strengths. They vary in scale from grain-size scale to snow cover scale, and by objectives from vegetation growth to hydrology and snow avalanches (see Sturm et al. 1995 for overview).

2.4.1 Terminology

The term avalanche climate was first introduced by Armstrong and Armstrong (1987), and later proposed by Hägeli and McClung (2003) not to be used synonymous with the term *snow climate*. Snow climate is generally used to describe properties like snow water equivalence or average surface albedo, which are properties not relevant for avalanche researchers and forecasters. Rather than monthly averages, higher temporal resolution and detailed weather- and snow observations are of importance for avalanche research objectives and avalanche forecasting. This study will focus on avalanche climates, although an introduction of relevant snow climate classification with a brief discussion on the subject is included.

2.4.2 Snow cover classification system

To cover the whole range of snow classifications are outside the scope of this thesis. However, it is worth describing the system proposed by Sturm and Holmgren (1995), as its framework has been used to describe the snow cover of Svalbard (Eckerstorfer and Christiansen 2011a). The system proposed by Sturm and Holmgren (1995) is named "A Seasonal Snow Cover Classification System for Local to Global Application", and defined snow cover classes by: textural and stratigraphic characteristics including the sequence of snow layers, their thickness, density, and the crystal morphology and grain characteristics within eacy layer (Sturm et al. 1995). The six classes of the original system was: tundra, taiga, apline, maritime, prairie, and ephemeral. However, this system failed to classify the snow cover of some regions, and thus additions have been proposed, including one for Svalbard. The following additions were proposed: Rainy Continental (Ikeda et al. 2009), and High Arctic Maritime (Eckerstorfer and Christiansen 2011a). Overview of all classes, including descriptions, can be found in Appendix II.

2.4.3 Snow avalanche climatology system

Synoptic snow and meteorological studies over the last 50 years in NW America have lead to a classification system for avalanche climates of the region (e.g. Armstrong and Armstrong 1987; Haegeli and McClung 2003; LaChapelle 1965; Mock and Birkeland 2000). This system generalizes avalanche characteristics by region, based on snow and weather conditions, to better understand avalanche patterns and increase avalanche hazard predictability. The classes are based on regional meteorological threshold values and associated snowpack structures. The avalanche climate classes are today recognized as (1) Coastal, (2) Transitional, and (3) Continental (Haegeli and McClung 2003). Although the suggested threshold values for each class might be best suited for NW America, relative changes in associated characteristics of each class (e.g. colder conditions in continental than in coastal) apply to most regions. The system has successfully been applied to other regions, e.g. in Japan (Ikeda et al. 2009).

2.4.3.1 Coastal avalanche climates

Coastal avalanche climates have thick snow cover, high snow densities, few persistent weak layers and average temperatures close to 0°C (McClung and Schaerer 2006). Additionally can rain on snow occur at any point during the season. High precipitation amounts combined with low temperature gradients prevents development of persistent weak layers. Consequently, direct action avalanches are the most frequent form of avalanches and the largest threat in this snow climate (LaChapelle 1965). Typical areas with these characteristics are the west coast of North America and the Japan Sea side of the Japanese Alps (Ikeda et al. 2009).

2.4.3.2 Continental avalanche climates

Thin snow cover, low air temperatures and persistent weak layers characterize continental snow climates (McClung and Schaerer 2006). Low air temperatures typically cause high temperature gradients in thin snow covers, which result in weak layers of facets and depth hoar. Poorly cohesive crystals can persist for long periods when temperatures in the snowpack are low. The most common type of avalanches in this type of climate is climax-avalanches (LaChapelle 1965). Examples of continental snow climates can be found in the American Rocky Mountains and in the European Alps.

2.4.3.3 Transitional avalanche climates

Transitional snow climates have intermediate characteristics in between the maritime and the continental snow climates, and have combinations of properties from both previously mentioned categories (LaChapelle 1965). This can lead to complicated avalanche condition patterns within small distances (Haegeli and McClung 2007). Winters given the classification *transitional snow climate* are often in areas which has both frequent classifications of *continental* and *coastal*, and winters with influences of both regimes are given the transitional classification. Example of mountain ranges with this avalanche climate is Columbia Mountains in NW America (Haegeli and McClung 2003.

Chapter 3

Methods

This chapter describes the methods used to collect data, from both fieldwork and databases, and further how descriptive statistics were used to analyze, visualize and describe the data. The first sections covers how meteorological data was gathered, processed and analyzed. Next follows a description of the field study; how and when field measurements were conducted, how the data was organized, processed and later analyzed. Fig. 3.1 provides a good overview of automatic meteorological stations, location of study plots and general topography of the study area.

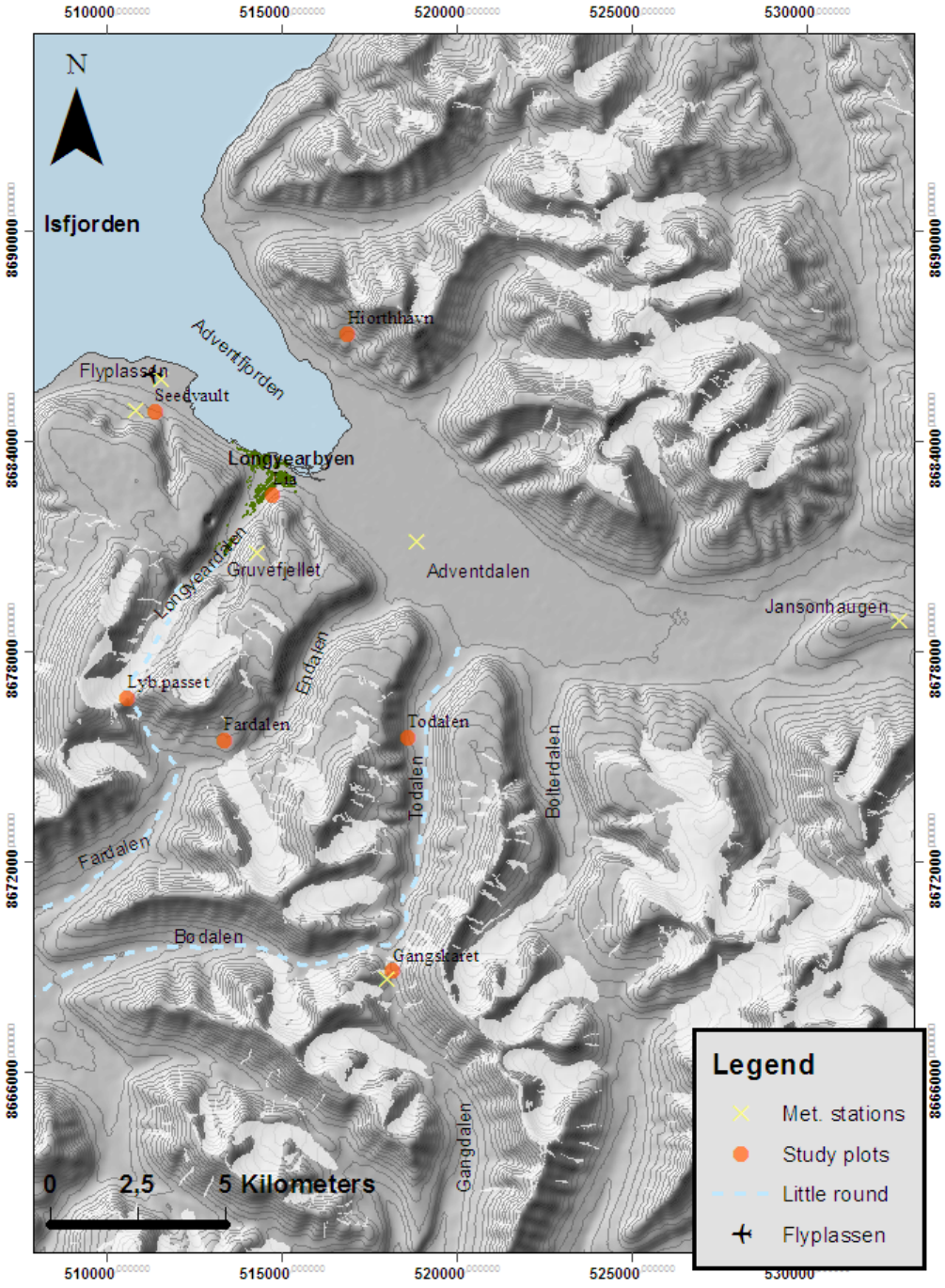

FIGURE 3.1: Map of study area displaying location of study plots, meteorological stations and topography within the study area. 50 meter contours.

3.1 Meteorological data

Six automatic meteorological stations provided relevant data for the study-area during the winter 2013-2014. The availability and location of these stations (see fig. 3.1) gave an unique opportunity to analyze the spatial- and temporal variability of weather patterns within the region of interest. Table 3.1 shows an overview of the stations used and from when data is available.

TABLE 3.1: Overview of weather stations within the study area. X- and Y-coordinates are in UTM, zone 32.

Station name	m a.s.l.	Data available from
Flyplassen	28	Oct 1964-
Adventdalen	15	Apr 1996-
Gruvefjellet	464	Dec 2006-
Janssonhaugen	251	Apr 2011-
Seedvault	125	Feb 2014
Gangskaret	460	Feb 2014

The station *Flyplassen* is operated by the Norwegian Meteorological institute (met.no 2014) and provide live online data, and historic data back to the year 1964. The station is located at low elevation and close to an open fjord, *Adventfjorden* (3.1), which normally holds no sea-ice during winters (Kilpeläinen and Sjöblom 2010). The stations in *Adventdalen,* on *Jansonhaugen* and on *Gruvefjellet* are operated by the University Center in Svalbard (UNIS), and provide both live online data and historic archives (www.unis.no). The stations *Seedvault* and *Gangskaret* are also owned by UNIS, but were idle until this study project started running them. Only manual downloads were available from the two latter stations. The stations were previously operated by the *Cryoslope project*, which monitoring avalanche activity in the area.

The data available from the different meteorological stations used in this study did not all contain the same variables and/or provide the same temporal resolution. Hourly, daily and monthly average values were used in most of the investigations - which were either calculated or provided directly from the source. Temporal resolution varied from 10 min average (standard resolution used by automatic weather stations) to hourly averages. Older data from Flyplassen did not provide hourly average or higher resolution, and thus daily average (or lower resolution) values were only used. Adventdalen, Jansonhaugen and Gruvefjellet provided an hourly average as the highest temporal resolution, and hourly maximum (max) and minimum (min) values. Seedvault and Gangskaret provide 10 min average temperature and wind values, and no max or min. Hourly averages were calculated for the latter station, and the maximum and minimum 10 min average values within that hour was used as maximum and minimum. This was not considered a large source of error, as these values were not used for further calculations. Mainly max-,

min- and average temperatures, as well as average wind speed and wind direction were investigated for this thesis. Relative humidity and air pressure measurements were also available from the stations, but were not given much focus due to low significance for the study. Only the meteorological station at Lufthavn has a precipitation gauge, and records 6 and 12-hour accumulative precipitation values. This data was included (see fig. 4.1), but was not heavily relied upon as precipitation gauges in the arctic are known to undercatch solid precipitation during winter storms (Førland and Hanssen-Bauer 2000), and because precipitation has high local variability (Humlum 2002).

3.1.1 Temporal data coverage

Some of the weather stations had gaps in their time record during the study period (October 2013 - May 2014), due to power failures or idle period. Gruvefjellet and Janssonhaugen were operational through the whole season and provided full coverage. Adventdalen had a short idle period for 243 hours between 22.04 - 02.05, due to a power failure. Flyplassen was down for a short period in October for 45 hours, between 05.10 - 07.10.2013. The Seedvault and Gangskaret weather stations were hibernating until late February, but provided good data from then and through the rest of the study period, and cover the period with consistent snow observations (February - May).

Meteorological data from the period November 2013 - April 2014 was targeted as a focus period for temporal and spatial variation analysis. The period was sought to have the most relevance for mid-winter snow cover development. Consequently were the stations with good temporal coverage over this period (Flyplassen, Adventdalen, Jansonhaugen and Gruvefjellet) chosen for the majority of the temporal investigations.

3.1.2 Spatial distribution

Spatially the weather stations cover areas in maritime fjord environments (e.g. Lufthavn) to more mountainous continental areas (e.g. Gangskaret and Gruvefjellet). The stations span in elevation from 15 to 464 m a.s.l. (table 3.1), and gives a good opportunity to investigate spatial- and temporal variability in environmental lapse rates.

The station on Gruvefjellet (464 m a.s.l.) is placed on a plateau mountain with no significant topographic influences (i.e. glacier, valley or mountain peaks) in the wind direction. This station accordingly captures the regional wind direction, not altered by topography (Christiansen et al. 2013). The station in Adventdalen (15 m a.s.l.) records the wind directions and temperatures of the air masses in the large southeast-northwest trending valley, *Adventdalen*, which terminates in to a fjord with the same orientation: *Adventfjorden* (Fig. 3.1). The station Seedvault is located on a small plateau (125 m a.s.l.) southwest of Lufthhavn meteorological station (28 m a.s.l.), close to the valley

side. The station at Gangskaret (460 m a.s.l.) is furthest southeast in the study-area. Its located at a watershed of two joining valleys, *Gangdalen* going south towards the larger *Reindalen*, and *Todalen*, a north trending valley that ends up in Adventdalen. The Jansonhaugen station (241 m a.s.l.) is located on a knoll further up Adventdalen, elevated above the valley floor. There stations range from near fjord (Lufthavn) to further inland (Jansonhaugen and Gangskaret). Gruvefjellet, though close to the fjord in distance, was considered as inland due to its high elevation, and apparently low influence by the ice-free fjord (Sect. 4.1).

3.1.3 Temperature data

3.1.3.1 Temperature interpolation

Monthly average temperatures were used for spatial and temporal analysis. Monthly average temperatures for meteorological stations without temporal coverage, Seedvault and Gangskaret for months November, December and January, were interpolated from surrounding stations. Monthly average temperatures at Seedvault and Gangskaret were calculated by using environmental lapse rates (see 3.1.3.2) between a set of weather stations with complete temporal coverage (Lufthavn-Gangskaret), and one set where one of the stations had partly coverage (e.g. Lufthavn-Gangskaret). By using the difference in lapse rates between the two sets (Lufthavn-Gruvefjellet and Lurthavn-Gangskaret) for the period where both stations had complete temporal coverage (February-April) was the lapse rate for months with partly coverage interpolated. The interpolated lapse rate value between Lufthavn and Gangskaret for the period missing data, was further used to calculate the monthly average temperature at Gangskaret. This method was used for both the Seedvault and the Gangskaret meteorological stations. The results (see 4.1) were within the range of expected values. Interpolation methods for higher resolution data (shorter periods than monthly average) were not attempted due to too high variability in daily to hourly lapse rates.

3.1.3.2 Environmental temperature lapse rates

Environmental lapse rate is the rate of decrease in temperature with altitude in the stationary atmosphere at a given location and time (Ahrens 2011). In this study were hourly and daily average temperatures recordings from meteorological stations, at different elevations, used to calculate the environmental lapse rate (ELR), using the following equation:

$$\gamma = \frac{\partial T}{\partial H} \tag{3.1}$$

where γ is the environmental lapse rate, ∂T is the difference in temperature between two meteorological stations, and ∂H is the difference in elevation between those two stations. Additionally the top and lower 15% of the total sample was identified as the strongest and weakest environmental lapse rates, and further paired with meteorological data associated with the time of recording. This was used to investigate type of weather associated with the variation in strength of the environmental lapse rates.

Data from Lufthavn (28 m a.s.l.), Jansonhaugen (251 m a.s.l.) and Gruvefjellet (464 m a.s.l.) meteorological stations were used for this purpose. They were chosen because of their highest difference in elevation (Lurthavn - Gruvefjellet) and because they had full data coverage over the whole study period. Adventdalen weather station (15 m a.s.l.) was discarded because of its high influence of cold air drainage through Adventdalen valley, recording abnormally low temperatures for its elevation, see 4.1. Data from Jansonhaugen meteorological station was used to decompose the gradient between Lufthavn and Gruvefjellet, to evaluate the linearity of the ELR.

3.1.3.3 Mid winter warm-spells

The variable *thaw hours* was used to analyze meteorological data for spatial and temporal variability of snows exposure to thawing. The variable was defined by this study as an hour with average temperature above or equal to 0 °C. The threshold temperature of 0 °C means that at least parts of the hour recorded were above freezing temperatures, allowing snow to thaw. Thawing snow leads to development of ice layers within the snowpack, when followed by negative temperatures which refreezes the snow (Jamieson 2006).

Length and number of thawing cycles were also used to study the frequency and length distribution of mid-winter warm spells. One thaw cycle was defined as a period of thaw hours, and a minimum of 24 hours of temperatures below freezing between cycles. The latter minimum requirement was used to account for a period of rapid temperature fluctuations around 0°C as one cycle. Length of a thaw cycle was measured by number of thaw hours, not total hours within a period.

Mid winter months (November-April) from the Lufthavn meteorological station were summarized for a 30-year-period. The average, maximum and mean of this period was used to determine the frequency and magnitude of mid winter warm-spells in previous seasons. Lufthavn meteorological station is the only station that holds such a long record of meteorological data in the area, and is therefore best suited for climatic scale analysis. Historic data from the Lufthavn meteorological station does unfortunately not archive hourly values, but 12 hour average values in 1980s and 1990s, and 6 hour values from about 2000 (unknown transition), in addition to daily average values (eklima.no). For consistency of variables through the whole period, daily average temperatures were

used in this study. Days of above or equal to 0°C, hereafter known as *thaw days*, were used as a proxy for temporal mid winter warm-spell variability. The method is less sensitive to shorter warm-spells or spells that overlap two days without forcing either of the daily average temperatures to above 0°C. The number of mid winter thaw-spells were also analyzed, hereafter known as *thaw cycles*, counting the number of periods with above-freezing temperatures. A minimum of one day with negative temperatures was set as criteria to separate cycles. This threshold was set after analyzing the data set, and worked well as it filtered thaw cycles where the temperatures fluctuated frequently around 0°C as one period instead of several periods.

For spatial and temporal comparison of thaw variables, were only data from Lufthavn, Jansonhaugen and Gruvefjellet meteorological stations used, for clarity in figure (Fig. 4.3) and because of the stations full temporal coverage. The stations were thought to represent low elevation maritime, medium elevation continental, and high elevation continental respectively. Data from Seedvault and Gankgskaret were comparable, in terms of thaw- hours and periods, to Lufthavn and Gruvefjellet.

3.1.3.4 Normal period

To investigating the 2013-2014 seasons representation in a climatic scale, were the 30 mid-winter seasons (1982/83 - 2012/13) leading up to the prior season analyzed. This season is henceforth referred to as the *normal* or *normal period* as it resembles a climatic normal period. The normal was described in terms of seasonal average and monthly average temperatures, thaw day temperatures, thaw days and thaw cycles; maximum and minimum temperatures and thaw cycle lengths. The results were compared to seasonal and monthly average, maximum and minimum values of the 2013-2014 mid-winter season (see table 4.1 and table 4.5)

3.1.4 Wind- speed and direction analyses

Wind- speed and direction data were examined from the weather stations within the study area. Hourly average values were primarily used, and were calculated from ten minute average data when not already available. Maximum wind speed values were also included in the data examinations. Maximum speed variables were maximum hourly average values, not max gust. Windrose diagrams were plotted for wind velocity and wind direction frequency analyses.

Wind direction for the wind rose diagrams plotted in this study, were divided in to eight sectors: north (>337.5°and 0-22.5°) northeast (22.5-67.5°), east (67.5-112.5°), southeast (112.5-157.5°), south (157.5-202.5°), southwest (202.5-247.5°), west (247.5-292.5°) and northwest (292.5-337.5 °). Wind velocities were divided in ranges according to the

Beufort scale: calm (0-0.2 m/s), light air (0.3-1.5 m/s), light breeze (1.6-3.3 m/s), gentle breeze (3.4-5.4 m/s), moderate breeze (5.5-7.9 m/s) fresh breeze (8.0-10.7 m/s) strong breeze (10.8-13.8 m/s), high wind (13.9-17.1 m/s) and gale (17.2-20.7 m/s). Each hourly average wind speed and direction recording were plotted accordingly by a percentage of total recordings. See fig. 4.5.

A moderate threshold for wind speeds causing snow drifts was assumed 8 m/s for wind velocity analysis, based on numbers by Li and Pomeroy (1997).

3.1.5 Precipitation data

Precipitation data was only available from the Lufthavn weather station, as it is currently the only station within the area with a heated precipitation gauge. However, data from this station should be considered minimum values, and not representative for the whole area, as large local variability occur (Humlum 2002). Larger regional snow fall events were recorded at the Lufthavn meteorological station, and indicated when big precipitation events occurred.

3.2 Field observations and study plots

Seven slopes were chosen for field measurements in the study area. A focus period for snow measurements of late January to early May, though some pits were investigated already in November. The focus period was chosen primarily for logistical reasons, as snow conditions for snow scooter driving are unreliable before this time. In total, eight rounds to the field study plots were completed, dividing the sites into two consecutive days – one day using snow scooter to access the more remote locations outside the road network, and one day car-driving to the less remote, more accessible locations. On occasion, were snow study plots skipped on the round-trip because of bad weather or other logistical difficulties. The field trips will in the results section be listed under one date, the first of the two consecutive days used per full round of field measurements. 51 snow pits (4.6) were investigated over the season, divided over 10 field trips.

The seven study plots (3.2 and 3.1) were strategically located based on the following criteria: (1) The slope should be representative for its region, (2) the snow cover should not be too disturbed by wind erosion/loading or human activity (e.g. snowmobile traffic, snow plowing or skiers), (3) be easy accessible for regular investigations, (4) cover a range of different elevations, (5) not be hazardous to approach or investigate, and (6) be within regions covered by meteorological stations.

Based on these criteria the seven sampling plots were placed on slopes around Adventfjorden and along the frequently used snowmobile track known as *The Little Round* (see

TABLE 3.2: Geographic description of the snow study plots. Elevation i meters above sea level (m a.s.l.), and aspect and slope in degrees (°). Distance from nearest ridge (dist ridge) in meters. Ground cover (ground) is the ground substrate underneath the snowpack. X- and y-coordiantes in UTM zone 32.

Site	Elev.	Slope	Aspect	Dist. Ridge	Ground	X-	Y-
Seedvault	250	32	340	30	Vegetation	511410	8684844
Hiorthhamn	260	20	185	15	Vegetation	516920	8687084
Lia	90	35	315	150	Vegetation	514755	8682462
Todalen	120	30	72	10	Blocky talus	518638	8675538
Gangskaret	460	25	205	40	Gravel	518203	8668876
Fardalen	430	25	148	40	Gravel	513400	8675460
Lyb.passet	615	27	78	10	Gravel	510638	8676662

fig. 3.1), covering areas in close proximity to the fjord and to higher elevation inland areas. The study area was 106km^2 i areal, within a elevatino range from 90 to 615 m a.s.l. (see table 3.2 and 3.1). The longest distance between sampling plots, Hiorthhavn to Gangskaret, is 18.2 km and a difference of 200 meters in elevation. The shortest distance is between Fardalen and Longyearbrepasset, 3 km with difference of 185 meters in elevation.

The Todalen study plot was located on a west facing rock glacier, on the side of a valley bottom in Todalen. Its short distance from its nearest ridge, which indicates degree of wind loading, was in this case not an issue due to the overall topography of the valley sheltering the slope. The ground cover at this location was blocky talus, which makes the surface rough and traps air between and beneath blocks under the snowpack. The Seedvault, Hiorthhamn and Lia sites were closest and most relevant to Longyearbyen and its infrastructure. They were also the plots closest to the fjord. Their vegetated ground surface means that the ground was relatively smooth and covered by grass, moss and/or soil. Seedvault's aspect makes it a lee side for the prevailing wind coming out of Adventdalen, though it was not as dramatically affected by wind drifts as it is located higher up from the valley bottom, and the study plot was 30 meters from the nearest ridge (slope top). Hiorthhamn was the site most affected by wind drifts, and accumulated much snow over the season, often with a wavy surface indicating wind deposition. The site was sheltered for wind erosion due to its complex adjacent terrain. Gangskaret, Fardalen and Lyb.passet had gravely smooth surfaces. The latter had also scarce blocks over the slope from rockfalls. The Gangskaret and Fardalen sites were relatively sheltered for wind loading and erosion, caused by topographic sheltering in relation to the dominant wind direction of the area. The Lyb.passet plot was also close to a ridge, but did not accumulate severe wind slabs.

3.2.1 Snow pit procedures

Snow pits were investigated by excavating vertical cuts in the snowpack and recording various snow properties according to the classification standard by (Fierz et al. 2009). The vertical stratigraphy was logged by finding clear boundaries separating layers by change in layer hardness and/or change in crystal type. Each layer was described by height (cm), grain size (mm), grain type (see table 3.3 for overview), and hardness (see table 3.4). In addition total snow depth (cm), temperatures every 10 cm through the snowpack and air temperature were recorded. Finally were stability tests applied to identify weak layers, either the Compression test (CT) and/or the Extended column test (ECT) (Jamieson 2006; Simenhois and Birkeland 2006). The stability tests were not applied to measure any value of safety, but to locate and identify reactive weak layers in the snow cover, that arguably could imply unstable conditions. Slope angle, aspect and elevation were also measured in the field using inclinometer, compass and GPS, respectively, to give a simple topographic description of the sites.

Scale and continuity of layers were issues when determining snow stratigraphy. Larger stratigraphic units were prioritized over micro-structures hard to identify by visual and physical analyzing. Horizontal discontinuities were often neglected, e.g. a small ice lense, as the goal of snow pits were to investigate the slope- to regional scale snow cover. Validation efforts were made occasionally by excavating pits adjacent to the sample plot, to investigate the extent of layers. This confirmed that layers uniform over a snow pit wall (typically 2 meters wide) were considered representable for the slope. The type of test to identify weak layers were chosen based on efficiency, snowpack structures and available assistance in the field. The most efficient is the CT, which only requires a snow saw and a shovel. The slightly more demanding ECT requires a cord (commonly known as a *Rutschblock cord*) to cut the column, preferably an assistant and a snow shovel. The CT was preferred on hard snow covers with high ice content, as the cord was inefficient cutting through thicker ice layers. The ECT is known to give more detailed information regarding stability, and was often chosen to investigate an assumed weakness further. Validation efforts were made occasionally by excavating pits adjacent to the sample plot, to investigate the extent of layers. This confirmed that layers uniform over a snow pit wall (typically 2 meters wide) were considered representable for the slope.

Snow crystal size and shape (see table 3.3) were determined by taking crystals from an identified snow layer in the snow pit, onto a crystal card (a gridded card with 1, 2 and 3 mm. squares typically used for measuring crystal size) and analyzed visually, often with a small hand held magnifying lens. Each classification type have distinct visual characteristics, see 2.2 for examples, and can usually be easily determined. Some classes were challenging to classify, like rounding facets and faceting rounds. Both shapes are of crystals undergoing development from one type to another, and look similar, and there is no easy way to determine which is what without knowing the initial crystal type.

In further analyses, the two classification (rounding facets and faceting rounds) will be grouped together to one class, *mixed forms*. Ice content was measured by pure ice layers and layers of melt forms combined.

TABLE 3.3: Classification of deposited snow on the ground. Sub-classifications were also used, e.g. rounding faceted crystals and faceting rounded crystals.

Symbol	Description
+	Precipitation Particles
/	Decomposing or Fragmented Particles
•	Rounding Grains
□	Faceted Crystals
∧	Depth Hoar
∨	Surface Hoar
◯	Melt Forms
■	Ice Formations

A hand harness test was preferred for hardness evaluation of layers. It was first introduced by De Quervain (1986) and is often used because of its efficiency and no instrument requirement. The test is based on resistance to objects being pushed into the snow. Five different objects of decreasing penetration resistance are used to assess what goes into the snow by a gentle push, not exceeding a penetration force of 10-15 N. The five steps (knife, pencil, one finger, four fingers and fist) are assigned to corresponding ram resistance measures (3.4). The test is a rather subjective measurement as both strength, shape and size of arms/hands, as well as the perception of 10-15 N, vary from person to person. It is therefore important to calibrate the technique if multiple persons are doing field investigations. In this study, the author of this thesis performed all field measurements.

TABLE 3.4: Overview of the hand hardness classification index and corresponding ram resistance range and mean value. Table adopted from Fierz et al. 2009 ** pencil is the tip-side of a sharpened pencil.*

		Hand test		Ram resistance	
Term	Hand hardness index	Object	Code	Range	Mean
very soft	1	fist	F	0-50	20
soft	2	4 fingers	4F	50-175	100
medium	3	1 finger	1F	175-390	250
hard	4	pencil*	P	390-715	500
very hard	5	knife blade	K	715-1200	1000
ice	6	ice	I	>1200	>1200

3.2.2 Snow pit data analysis

The various snow pit measurements were further evaluated by descriptive statistics. Hardness values and crystal type/ice layers were summarized using weighted averages of total snow height. Types of weak layer, position in snowpack and hardness ratios between weak layers and slab were also categorized. Types of weak layer were classified by a combination of grain types in weak layer and overlying slab. Only bottom and surface temperatures of the snowpack, and the temperature gradient between these points, were used in the snow pit descriptions. Surfaces temperatures were taken 10 cm below the surface. Typically, surface measurements are taken deeper in the snowpack (Birkeland 2001), but due to the low diurnal fluctuations on Svalbard, there were generally no need to use deeper measurements, especially early to mid season.

3.2.2.1 Hand hardness profiles

A system for classifying hardness profiles were proposed by Wiesinger and Schweizer (2000) for interpreting snow cover stability from hardness measurements. Their classification system was originally intended for classifying ramsonde (RAM) profiles, but has later been applied to hand hardness profiles (Eckerstorfer and Christiansen 2011a; Ikeda et al. 2009). RAM-profiles are not able to pick up thin layers of abrupt resistance, and thus ignores most thin weak- or hard layers (e.g. an ice crust). Eckerstorfer and Christiansen (2011a) moderated the profiles to better fit the Svalbard snow climate, by adding weak bases to profile type 7 and 9, see fig. 4.7. Relative degrees of stability are associated with the different profile types (Wiesinger and Schweizer 2000). Type 1, 5, 7 and 9 indicate potential unstable conditions, while profiles types 6 and 10 are associated with stable structures. Profiles 2, 3, 4 and 8 are not directly associated with stable or unstable conditions, but all have potential, but often less critical, weakness (Wiesinger and Schweizer 2000). This system was applied to the hand hardness profiles measured in this field study. Appropriately, thin layers of abrupt hardness changes were ignored to assess the larger hardness trends similar to a RAM-profile.

FIGURE 3.2: Schematic of hardness profile types, 1 to 10. Extent of horizontal bars imply hardness. From: Eckerstorfer and Christiansen 2011a.

3.2.2.2 Weak layer classification

Weak layers were classified based on the crystal type of the collapsing layer and its neighboring interfaces, i.e. type of base surface and type of above-lying slab or interface (e.g. ice layer or hard slab). Based on the weak layers identified six categories were established to categorize the observed weak layers, see fig. 3.3.

Depth hoar was the weak layer category used for snow columns that fracture at a weak base consisting of well-developed depth hoar crystals. *New snow/old snow* was used for categorizing fractures in the interface between softer snow from the latest storm and the harder old snow surface. The soft slabs were either of precipitation crystals or decomposing crystals. *Slab/facets/slab* was used for thin faceted layers triggered between two harder slabs. *Facets/ice* is the first ice related category, and was used for weak layers of developed facets above an ice layer and below a harder slab. The *Ice/facets* categorize the weak layers of developed facets underneath an ice layer, and *Ice/facets/ice* was used when a layer of facets was sandwiched between two ice layers, and was prone to fracturing. A criteria used for the latter category was also that there was a small gap between the two ice layers, typically less than 5 cm. This was used to distinguish between weak layers developed between ice layers from the same warm-spell period, and warm-spell periods separated by a longer period of different weather types e.g. dry precipitation.

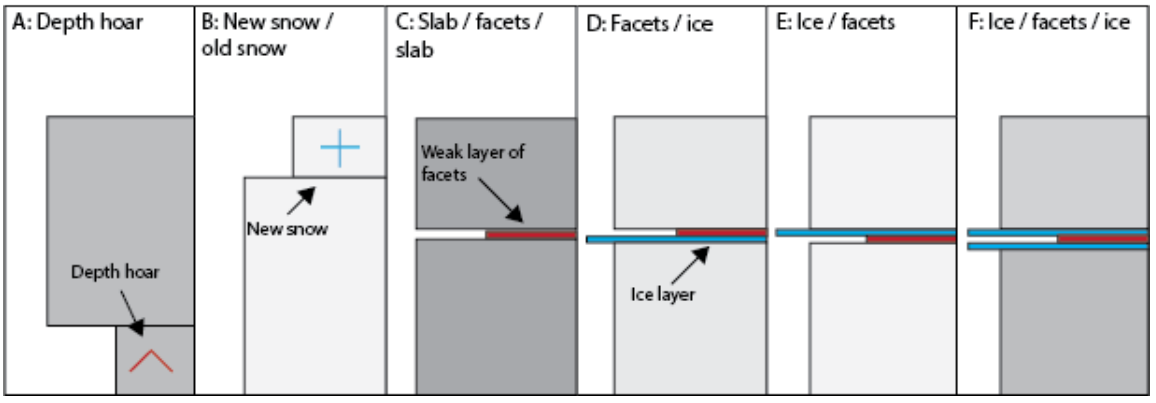

FIGURE 3.3: Schematic of the six weak layer categories. Relative hardness of layers are shown by length along the horizontal axis. Thin red layers represents weak layers of faceted crystals and thin blue layers show thin ice layers. Red caret (∧) symbolizes layer of depth hoar, blue plus sign (+) symbolizes a new snow layer of either precipitation crystals or decomposing precipitation crystals.

3.2.2.3 Weak layer hardness contrasts

Abrupt changes of hardness in the snow column can cause unstable situations. Failure in soft layers underlying a harder slab can trigger slab avalanches, and softer snow resting on harder slabs often fails before stabilizing. Large changes in hardness are therefore often used as a indicator for an unstable snow cover. For reference, it is useful to investigate the hardness contrasts between the identified weak layers and slab; and weak layer and sliding surface. The hand hardness scale (1 (fist) - 6 (ice)) was applied to all layers (slab, weak layer and sliding surface layer), and the difference between these classifications were used to determine the relative jump in hardness between the layers. E.g. a weak layer of hardness 1 (fist) and a slab of hardness 5 (pencil) would result in a hardness contrast of 4.

3.2.2.4 Weak layer depth

The position of weak layers can be decisive for determining weather or not a weak layer present a threat or if it is e.g. too deep for a skier to trigger. In this study the position of the weak layers were categorized by its position in the snowpack. This was simply done by dividing the snowpack in three even portions by dividing the snow height by three. The portions of the snowpack were termed *top*, *middle*, and *bottom* part of the snowpack.

Chapter 4

Results

4.1 Meteorological data

This chapter contains description of field measurements and meteorological data. The first half covers meteorological variables and proxies used for investigating mid-winter thaw spells. The second half describes snow measurements from field work, and further classification of snow properties.

4.1.1 Temperatures

The monthly average temperatures varied spatially between stations and temporally over the study period. This can both be seen in Fig. 4.1 and table 4.1. Lufthavn meteorological station (28 m a.s.l.) recorded on average the highest temperatures, with mid-winter average -6.7°C (table 4.1). The station measured lowest monthly average temperature in April, -9.7°C, and highest in February, -1.7°C. Gruvefjellet meteorological station (464 m a.s.l.) measured the lowest seasonal average, -10°C, also with highest monthly average temperature in February, -5.5°C, and lowest in April, -12.6°C. The temporal trend of seasonal maximum temperature in February and seasonal minimum in April was comparable for all stations. The Gangskaret meteorological stations (460 m a.s.l.) seasonal average temperature was 0.2°C higher than on Gruvefjellet, though recorded a 0.4°C lower monthly average temperature (-13°C) than Gruvefjellet in April. This was also the lowermost monthly average temperature recorded during the 2013-2014 mid-winter season. The average seasonal temperature difference between Lufthavn and Gangskaret meteorological stations was 3.1°C. The lowest hourly average temperature was recorded on Gruvefjellet, -22.6°C on December 5th (2013), and the highest recorded was at Lufthavn meteorological staion, 5.2°C on December 17th (2013).

Normal monthly average temperatures were included in table 4.1 for comparison with 2013-2014 seasons' monthly averages. The 2013-2014 mid-winter seasonal average was

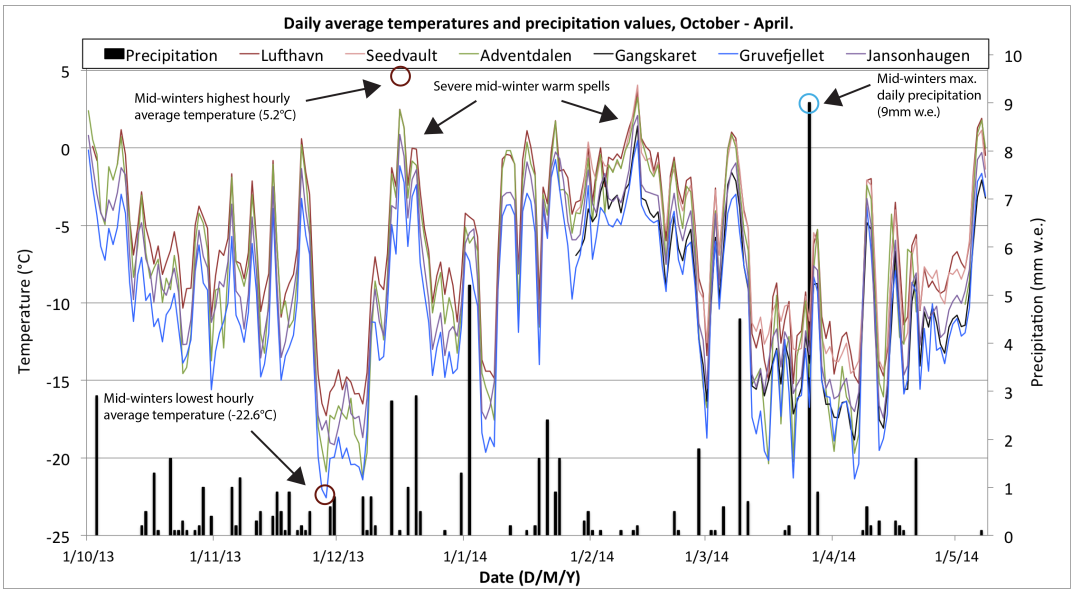

FIGURE 4.1: Daily average temperatures (colored lines) from all meteorological stations within the study area, from October to May, 2013-2014. Precipitation values (black bars) are from Lufthavn meteorological station.

4.7°C higher than the normal periods seasonal average (-11.2°C). November and April were only 0.1°C higher than the normal monthly average, but January and February were 8°and 11.3°C higher than the normal. Making February 2014 the warmest February recorded (-1.9°C) at Lufthavnen meteorological station. December (2013) and March (2014) were moderately warmer than the normal, 2.8°and 4.4°C higher respectively.

TABLE 4.1: 2013-2014 mid-winter monthly average temperatures (°C) by met stations, and last 30-year (Normal) monthly average temperatures. Normal temperatures from Lufthavn meteorological station. *Interpolated temperature values, see section 3.1.3.1 for description

Month	Normal	Lufthavn	Seedvault	Adventd.	Gangsk.	Gruvef.	Jans.haugen
November	-8.1	-8.0	-8.1*	-9.5	-11.2*	-11.5	-10.2
December	-10.9	-8.1	-8.2*	-9.8	-11.3*	-11.7	-10.4
January	-12.1	-4.1	-4.1*	-5.1	-6.7*	-7.0	-5.9
February	-13.0	-1.7	-1.9	-2.8	-4.9	-5.5	-4.0
March	-13.0	-8.6	-8.5	-10.6	-11.6	-11.8	-10.7
April	-9.8	-9.7	-9.8	-11.8	-13.0	-12.6	-12.1
Average	**-11.2**	**-6.7**	**-6.8**	**-8.3**	**-9.8**	**-10.0**	**-8.9**

4.1.2 Environmental temperature lapse rates

The ELR between Lufthavn (28 m a.s.l.) and Gruvefjellet (463 m a.s.l.) meteorological stations was on mid-winter seasonal average -0.76°C/100 m (table 4.2). However, the ELR varied temporally from -0.67°to -0.86°C/100m in monthly averages,

strongest monthly average ELR in February and the weakest in April. The ELR between Lufthavn and Gruvefjellet meteorological stations was decomposed by including Jansonhaugen meteorological station, into Lufthavn-Jansonhaugen and Jansonhaugen-Gruvefjellet. This revealed that the ELR Lufthavn-Jansonhaugen were stronger than Jansonhaugen-Gruvefjellet and Lufthavn-Gruvefjellet. The Lufthavn-Jansonhaugen ELR was on seasonal average -0.98°C/100m, 0.22°C stronger than Lufthavn-Gruvefjellet. The ELR Jansonhaugen-Gruvefjellet was the weakest, with -0.53°C/100m seasonal average, 0.45°C weaker than Lufthavn-Jansonhaugen and 0.23°C weaker than Lufthavn-Gruvefjellet. The strengths of the "decomposed" ELRs also varied temporally, e.g. February (the warmest month) was the ELR Lufthavn-Jansonhaugen -1.0°C/100m and the ELR Jansonhaugen-Gruvefjellet -0.7°C/100m, though in April, was the ELR Lufthavn-Jansonhaugen -1.08°C/100m, but Jansonhaugen-Gruvefjellet only -0.27°C/100m.

TABLE 4.2: Environmental lapse rates between meteorological stations, November - April. Montly average temperatures used for calculations. LH-JH = Lufthavn-Jansonhaugen, JH-GF = Jansonhaugen - Gruvefjellet, and LH-GF = Lufthavn-Gruvefjellet. Values in °C /100m

Month	LH-JH	JH-GF	LH-GF
November	-1.01	-0.60	-0.81
December	-1.01	-0.61	-0.81
January	-0.79	-0.54	-0.67
February	-1.00	-0.70	-0.86
March	-0.96	-0.48	-0.73
April	-1.08	-0.27	-0.68
Average	**-0.98**	**-0.53**	**-0.76**

TABLE 4.3: Top and lower 15 % of environmental lapse rate (Lr) values between FLufthavn (Lh) and Gruvefjellet (Gf), 28 and 464 m a.s.l. respectively, and meteorological values recorded simultaneously at the two meteorological stations. Meteorological variables were: avg. °C = average daily temperature, WindD = wind direction in °, and m/s = wind velocity in m/s.

Values	°C LH	°C GF	ELR	WindD LH	WindD GF	m/s LH	m/s GF
Top 15 %	-12	-17.5	-1.24	133	185	5.8	3.4
Low 15 %	-4.2	-6.4	-0.5	160	196	4.7	4.3

The top and lower 15% daily Lufthavn-Gruvefjellet ELR values, and daily average meteorological data from Gruvefjellet and Lufthavnen of days the ELR values occurred, can be seen in table 4.3.

On average were the 15% strongest ELRs -1.24°C/100m, and the average weakest ELRs were -0.5°C/100m. The difference between the average 15% strongest and weakest ELRs was thus 0.75°C/100m.

Difference in wind velocities and directions between strong (top 15%) and weak (low 15%) ELR days were moderate. Daily average wind velocities at Lufthavn were 5.8 and 3.4 m/s on Gruvefjellet during strong ELRs, while 4.7 and 4.3 m/s during the weakest

ELR values (table 4.3). Average wind velocities at Lufthavn were higher than Gruvefjellet during strong and weak ELR days, however, there were stronger difference between Lufthavn and Gruvefjellet during strong ELRs, 2.4 m/s higher at lufthavn, than during events of low ELRs, 0.4 m/s higher at Lufthavn. Daily average wind directions were from southeast at Lufthavn meteorological station, and from the south on Gruvefjellet, during strong and weak ELR days. Comparing strong and weak ELR days, the wind direction at Lufthavn was on average from 133°during strong ELR days, and 160°during weak ELR days. On Gruvefjellet the wind directions were 185°and 196°at strong and weak ELRs respectively.

Average temperatures were low at both meteorological stations, -12°C at Lufthavn and -17.5°C on Gruvefjellet, during strong ELRs. In contrast were temperatures relatively high, -4.2°C at Lufthavn and -6.4°C on Gruvefjellet, during weak ELR days. Temperature differences between the two stations were 5.5°C during strong ELRs, and 2.2°C during weak ELRs.

4.1.3 Mid winter warm-spells of 2013-2014 mid-winter season

Large variation in thaw hours and cycles were recorded at the meteorological stations through the mid-winter season of 2013/2014. Gruvefjellet weather station (464 m a.s.l.), was least exposed to thaw temperatures, recorded 47 thaw hours over four thaw cycles (see fig. 4.3 and table4.4). The Flyplassen weather station (28 m a.s.l.) recorded highest exposed to thaw, and recorded 443 thaw hours over 19 thaw cycles. Adventdalen meteorological station (15 m a.s.l), less exposed to thaw than Lufthavn in number of thaw hours, recorded 368 thaw hours, but over 20 cycles. The station at Jansonhaugen (251 m a.s.l.) recorded 102 thaw hours divided on 9 cycles. Average thaw hour temperatures were between 0.9°C and 1.5°C, highest at Jansonhaugen and lowest at Gruvefjellet. Maximum thaw temperatures were highest at Lufthavn, 5.2°C, and lowest at Gruvefjellet, 2.4°C. Adventdalen and Jansonhaugen meteorological stations measured 4.4°and 4.2°C max thaw temperatures respectively. Maximum thaw temperatures were recorded at Lufthavn and Adventdalen meteorological stations on 17.12.2013, while maximum temperatures at Jansonhaugen and Gruvefjellet were recorded on 12.02.2014. There was a large difference in thaw cycle length; the longest period was recorded at Lufthavnen, 124 thaw hours, and the shortest at Gruvefjellet, 27 thaw hours. The longest thaw cycles for all meteorological stations were recorded in the period 09.02-14.02.2014.

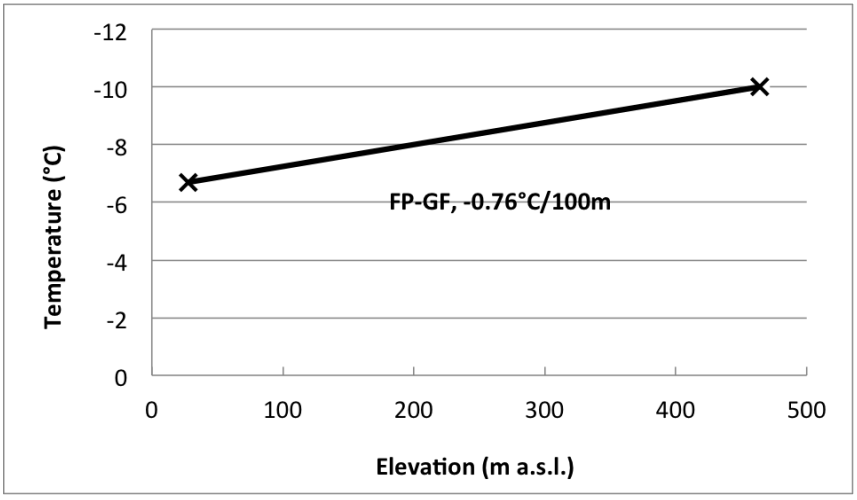

(A) Daily average ELR, Lufthavn-Gruvefjellet, -0.76°C/100m.

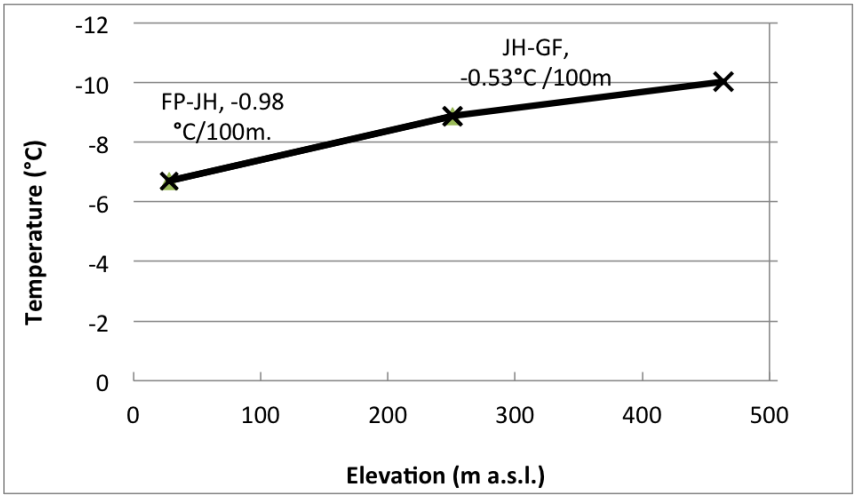

(B) Daily average ELRs, Lufthavn-Jansonhaugen and Jansonhaugen-Gruvefjellet.

FIGURE 4.2: ELRs illustrated by daily average temperature (x-axis) and m a.s.l. (y-axis) of the Lufthavn (28 m a.s.l.), Jansonhaugen (251 m a.s.l.) and Gruvefjellet (462 m a.s.l.) meteorological stations. Steepness of fitted lines imply strength of ELR between meteorological stations.

TABLE 4.4: Overview of variables and values used to describe mid-winter warm spells, November 2013 - April 2014, measured at Lufthavn, Adventdalen, Jansonhaugen and Gruvefjellet meteorological stations. Thaw hours = counted hours with average temperature >0°C, thaw cycle = number of thaw cycles counted, Avg. CycleL = average length thaw cycle, Max.HCycle = maximum length of thaw cycle, Avg. thawT = average thaw hour temperature, and Max. thawT = maximum thaw hour temperature.

	Lufthavn	Adventdalen	Gruvefjellet	Jansonhaugen
Thaw hours	443	368	47	102
Thaw cycles	19	20	4	9
Avg. cycleL	23.3	18.4	11.8	11.3
Max.HCycle	124	96	27	33
Avg. thawT	1.3	1.2	0.9	1.5
Max. thawT	5.2	4.4	2.4	4.2

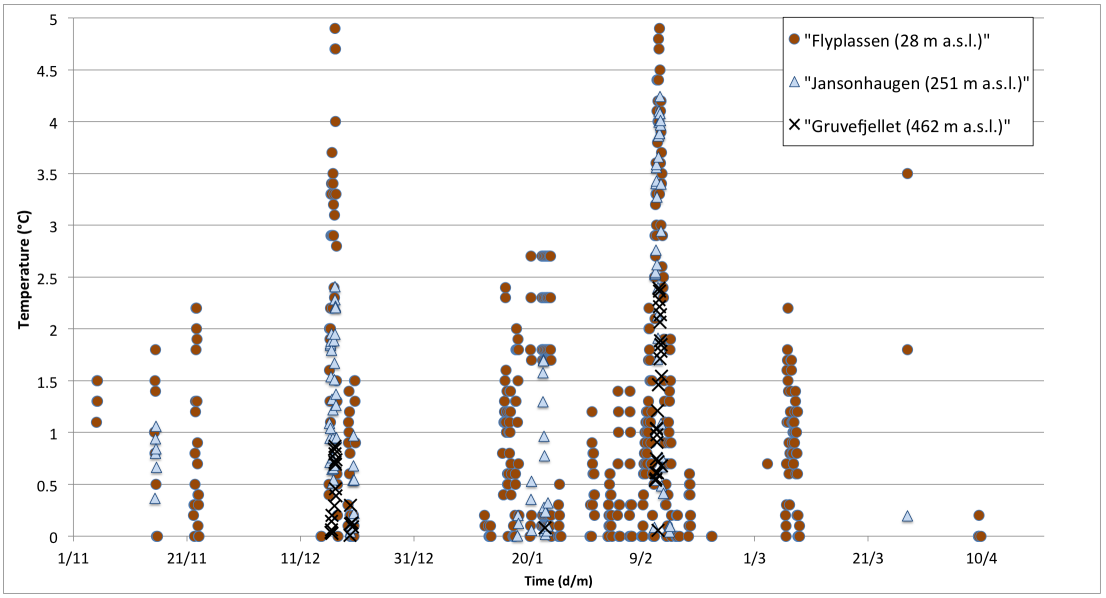

FIGURE 4.3: Distribution of thaw hours, by positive temperatures and time, recorded at the Flyplassen (28 m a.s.l.), Jansonhaugen (251 m a.s.l.) and Gruvefjellet (462 m a.s.l.) meteorological stations.

On two occasions (thaw cycles) were positive temperatures recorded at all meteorological stations, during the periods 16.12-17.12.2013 and 09.02-14.02.2014 (see Fig. 4.3). The first thaw cycle counted 40 thaw hours maximum thaw cycle length, recorded at Adventdalen meteorological station, and the second cycle counted 124 thaw hours maximum, recorded at Lufthavnen meteorological station. The shortest exposure to positive temperatures, were 14 thaw hours recorded on Gruvefjellet during during the thaw cycle, and 27 thaw hours during the second thaw cycle, also at Gruvefjellet.

4.1.4 Mid winter warm-spells: 2013-2014 season compared to norm

TABLE 4.5: Average, maximum and minimum thaw days, thaw cycles and thaw day temperatures (°C) for the mid winter months (November - April) of the normal period and the 2013-2014 season. Variables described in Sect. 3.1.3.3. Data from Lufthavn meteorological station.

	Normal period (avg / max / min)	2013/2014 -
Thaw days	11 / 44 / 1	17
Thaw cycles	6 / 19 / 1	8
Temperature	1.3 / 2.3 / 0.3	0.9

The 2013-2014 mid-winter seasons thaw days, thaw cycles, and thaw day temperatures were compared to the normal period', see table 4.5 and Fig. 4.4. The 2013/2014 mid-winter season had 17 thaw days, over 8 thaw cycles, and with an average thaw day

temperature of 0.9 °C. Average over the normal period were 11 thaw day per season, 6 thaw cycles, and average thaw day temperature of 1.3°C (table 4.5). Maximum thaw days for the normal period were recorded in the 2005/2006, with 44 thaw days (Fig. 4.4). All mid-winter seasons recorded thaw days, lowest recorded was 1 thaw day per season, recorded both in 87/88 and in 92/93. The average thaw day temperature of the 2013/2014 mid-winter season was 0.4°C lower than the normal periods average thaw day temperature.

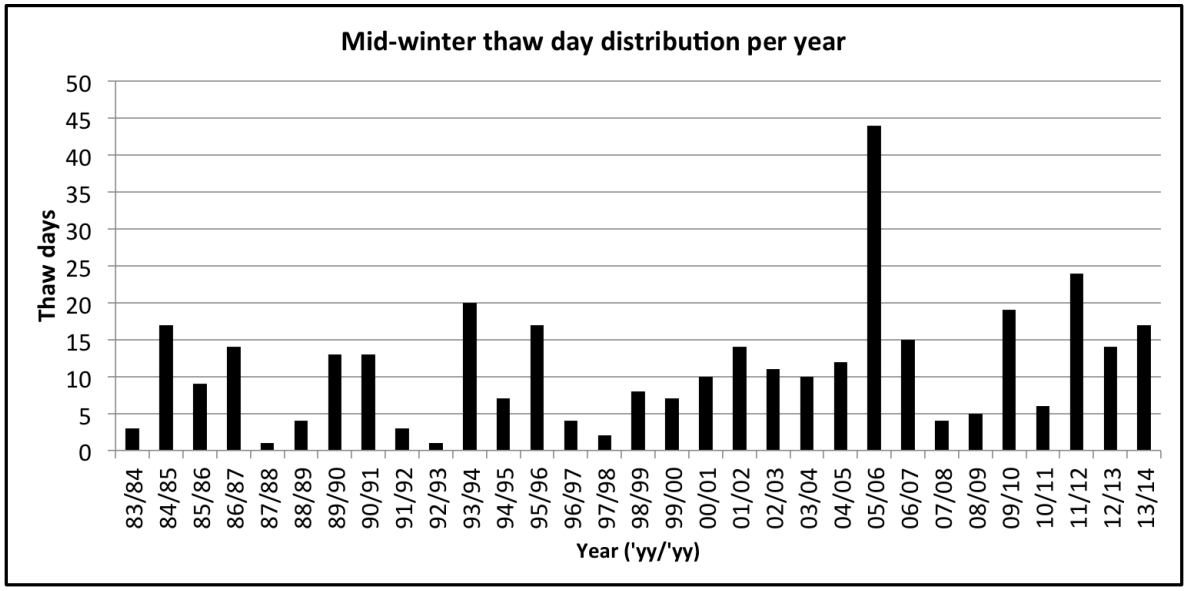

FIGURE 4.4: Frequency distribution chart of normal period mid-winter thaw days per year, including 2013-2014.

4.1.5 Wind

On Gruvefjellet there are no significant topographic influence (Fig. 3.1) on wind directions. The Gruvefjellet meteorological station is therefore sought to capture the regional wind direction (Christiansen et al. 2013). Fig. 4.5 show the frequency of wind strengths and distribution of wind directions recorded at the Gruvefjellet meteorological station. The wind direction on Gruvefjellet was predominantly from southeast during the 2013-2014 mid-winter season, and the most frequent wind velocity from this direction was gentle breeze (3.4-5.4 m/s). The Gruvefjellet meteorological station also recorded frequent winds from southwest to northwest, but typically at lower wind velocities, light breeze (1.6-3.3 m/s). Winds high enough to cause snow transport (>8 m/s, see Sect. 3.1.4) were predominantly from east to southeast, and had a few recordings from west to southwest. The average wind velocity of the mid-winter season on Gruvefjellet was 4.7 m/s, and recorded maximum hourly average velocity, 18.7m/s, from the east-southeast on 22.11.2013. Southeasterly wind direction was also reported predominant wind direction on Gruvefjellet, by Christiansen and others (2013).

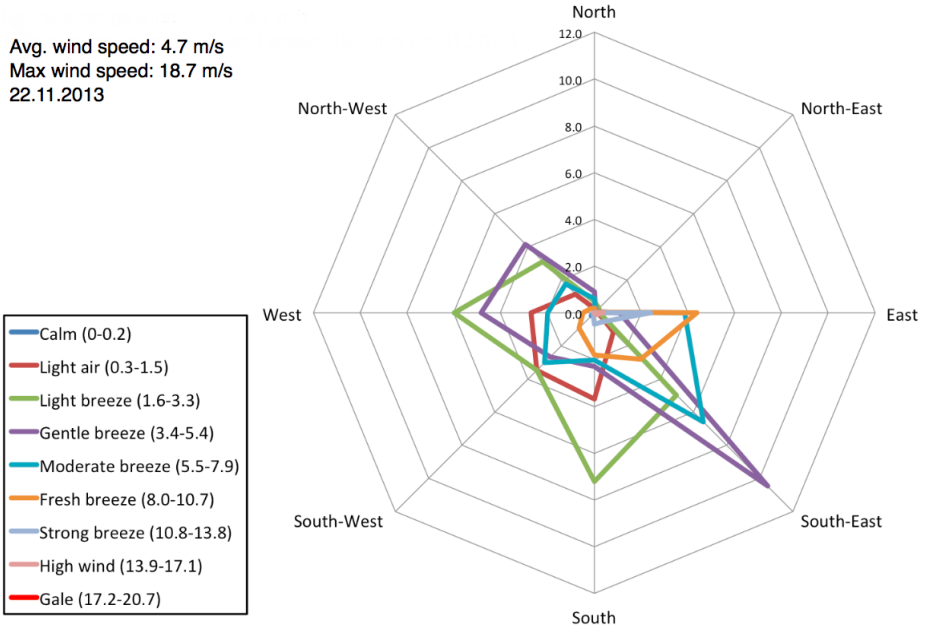

(A) Windrose plot from Gruvefjellet weather station, November 2013 - April 2014.

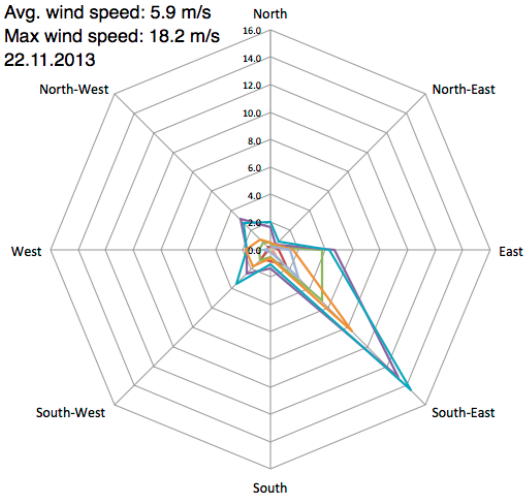

(B) Windrose plot from Flyplassen weather station, November 2013 - April 2014

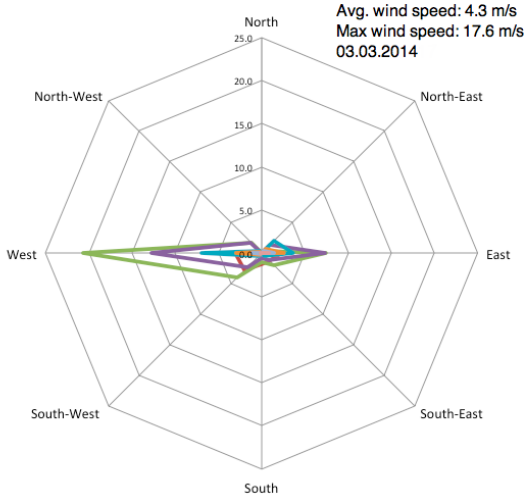

(C) Windrose plot from Gangskaret weather station, Februar - April 2014

FIGURE 4.5: Wind directions and velocities from eight sectors, N, NE, E, SE, S, SW, W and NW. Wind velocity range classification after the Beufort scale. Y-axis depicts number of hours in percentage within wind velocity range and direction.

At the Lufthavn meteorological station, during the mid-winter season of 2013-2014, were predominantly wind directions recorded from southeast, with a clear margin (Fig. 4.5). There were also scarce recorded wind directions from northwest to southwest, but much less frequent. Most dominant wind velocity from southeast was moderate breeze (5.5-7.9 m/s). Winds causing snow transport (>8 m/s) were also dominantly from southeast. Average wind velocity at Lufthavn weather station was 5.9 m/s and maximum average hourly wind velocity was 18.2m/s, from the southeast, also recorded 22.11.2013.

Gangskaret meteorological station recorded wind from two distinct directions: predominant wind directions from west, and less frequent winds from east. Most dominant range of wind velocities from west were within light breeze (1.6-3.3 m/s), and gentle breeze from east (3.4-5.4 m/s) (Fig. 4.5). Average wind velocity on Gangskaret was 4.3m/s and maximum wind velocity was 17.6m/s, recorded 03.03.2014.

4.2 Snow measurements

4.2.1 Snow height

In general, snow heights increased through the the snow season of 2013/14. Lowest snow height measurements were in December 2013, and in large, increased until the last measurements in May. The lowest snow height measured 42 cm on 04.12 (early-season) at the Lia study plot, and the highest, 152 cm, on 12.05 (late-season) at Hiorthamn study plot (table 4.6). Some measurements deviated from the trend of steady snow height increase through the snow season; Todalen measured maximum snow height (100cm) at 20.01 and 05.03, and 88 cm at late-season. These uneven snow height measurements was caused by uneven surface topography, see Fig. 4.6 for example. Seedvault also recorded seasonal maximum height, 117 cm, at mid-season, 28.01, though its average was 97 cm. Seasonal average snow height for all pits was 92 cm, Gangskaret had the lowest seasonal average snow height, 75 cm, and Hiorthhamn the highest seasonal average, 108cm. Gangskaret and Lyb.passet had the most consistent snow height increases, with only one measurement of minor snow height reduction each. Gangskaret increased from 59 cm snow height on 28.01 to 98 cm late-season, increasing 39 cm from first measurement, and Lyb.passet measured 80 cm on 11.01 and 109 cm late-season, increasing 29 cm in height over the season.

TABLE 4.6: Overview of snow height, average hardness, and hardness profiles from all snow pits included in this study, winter 2013-2014. HS = snow height, Avg. R = average hardness, R-profile = hardness profile. Pits sorted by elevation (m a.s.l.)

Date	Study plots	04.12	11.01	28.01	07.02	21.02	05.03	19.03	04.04	25.04	12.05	Avg.
Hs	Lia	42	-	77	-	84	117	80	104	109	-	87
	Todalen	-	-	100	73	68	100	81	88	90	88	86
	Seedvault	45	-	117	71	70	77	79	95	-	-	97
	Hiorthhamn	-	99	84	115	-	93	97	86	139	152	108
	Fardalen	-	-	-	101	84	86	106	-	-	132	101
	Gangskaret	-	-	59	67	66	67	74	84	90	98	75
	Lyb.passet	-	80	87	-	90	98	-	89	104	109	93
Avg. R	Lia	2.5	-	3.5	-	3.86	3.5	2.66	3.45	2.97	-	3.2
	Todalen	-	-	3.2	3.9	4.11	3.71	4.85	3.4	2.98	3.23	3.7
	Seedvault	3.1	-	3.7	3	3.2	2.74	2.9	2.65	-	3.66	3.1
	Hiorthhamn	-	2.81	2.98	2.98	-	2.8	3.59	4.4	3.25	3.28	3.3
	Fardalen	-	-	-	3	2.9	2.7	2.59	-	-	3.14	2.9
	Gangskaret	-	-	2.47	2.47	2.6	1.98	2	3.07	2.34	2.49	2.4
	Lyb.passet	-	3.67	3.6	-	1.5	3.17	-	2.87	2.21	2.95	2.9
R-profile	Lia	2	-	3	3	-	3	9	4	4	-	-
	Todalen	-	-	3	3	3	3	3	4	3	3	-
	Seedvault	2	-	9	3	2	4	9	7	-	-	-
	Hiorthhamn	-	3	2	9	-	9	3	8	3	3	-
	Fardalen	-	-	-	3	5	4	7	-	-	4	-
	Gangskaret	-	-	7	7	7	4	7	7	7	7	-
	Lyb.passet	-	3	2	-	2	3	-	3	3	3	-

4.2.1.1 Snowpack hardness

Average snow pit hardness ranged from 4.85 (pencil+), measured at Todalen study plot (120 m a.s.l) on 19.03, to 1.5 (fist) measured at Lyb.passet (615 m a.s.l.) on 21.02 (see table 4.6). The hardest seasonal average was measured at Todalen study plot, 3.7 (1F+). The softest seasonal average was measured at Ganskaret, 2.4 (4F). Lia (90 m a.s.l.), Todalen (120 m a.s.l.), Seedvault (250 m a.s.l.) and Hiorthhamn (260 m a.s.l.) recorded on seasonal average hardness of 1-finger (see table 4.6, and 3.4 for hardness index); and Fardalen (430 m a.s.l.), Gangskaret (460 m a.s.l.), and Lyb.passet (615 m a.s.l.) recorded 4-fingers on the hand hardness index.

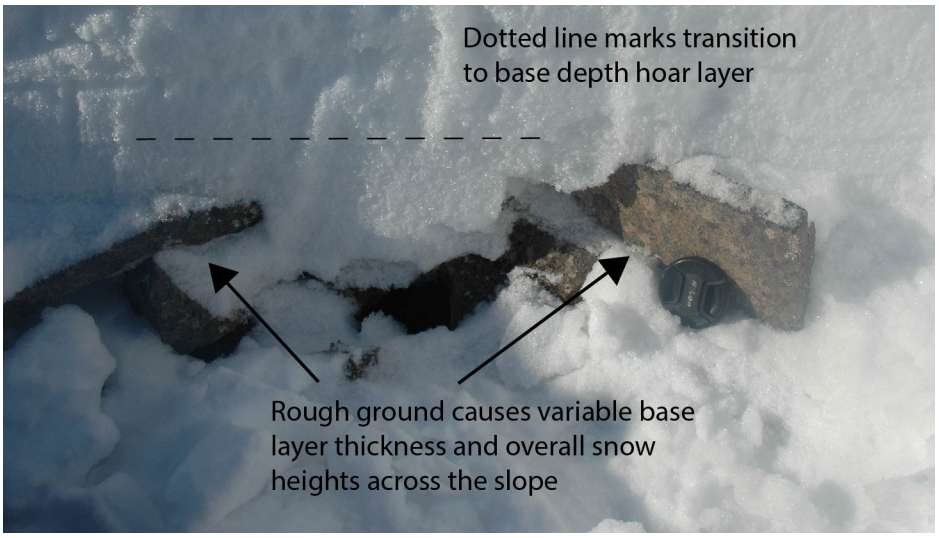

FIGURE 4.6: Image showing the base layer and surface roughness typical for the Todalen study plot. Image taken April 6th, 2014. Photo: Mikkel A. Kristiansen.

4.2.1.2 Hardness profiles

Profile 3 was the most frequent hardness profile was observed through the 2013-2014 study, assigned 41% of all snow pits, twice as many as the second most frequent profile (profile 7) (see Fig. 4.7). Profile 3 was most frequently assigned to snow pits in Todalen (7/8 pits), and Lyb.passet (5/7 pits). The second and third most observed profiles were profiles 7 and 4 (18% and 14% respectively). Profile 7 in 7/8 pits classified Gangskaret. All pits changed between different hardness profiles through the season. The most consistent were Todalen (profile 3) and Gangskaret (profile 7). Fardalen was the most inconsistent in type of profiles, having assigned the same profile only twice.

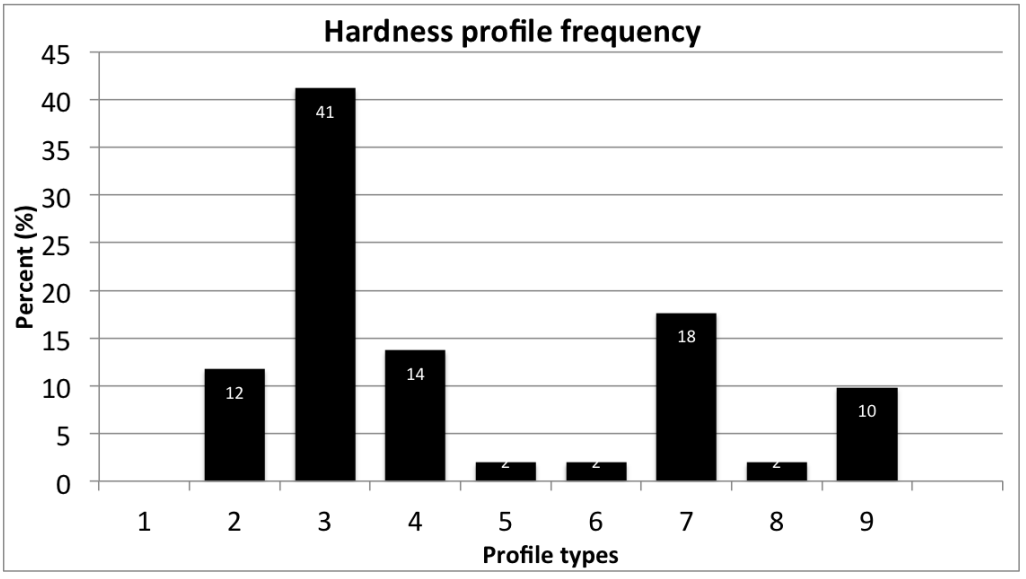

FIGURE 4.7: Hardness profile frequency distribution, in percent. See Sect. 3.2.2.1 and Fig.3.2 for description of profiles.

4.2.1.3 Measurements of snow crystal types and ice content

Fractions of snow crystal types and ice content were exemplified by: Seedvault (250 m a.s.l.) and Gangskaret (460 m a.s.l.) in Fig. 4.8, for all study plots see Appendix I. The Seedvault plot was representative for the lower elevation study plots; Lia (90 m a.s.l.), Todalen (120 m a.s.l.) and Hiorthamn (260 m a.s.l.); and Gangskaret was representative for higher elevation study plots; Fardalen (430 m a.s.l.) and Lyb.passet (615 m a.s.l.). The distinction between the two groups, termed higher elevation study plots and lower elevation study plots (>400 m a.s.l. and <300 m a.s.l.) was made due to the large difference in ice content between the two groups (see Appendix I). Variability in relative portions of snow crystals and ice content will in large be described as contrasts between the two groups.

Large fractions of ice were observed in the snowcover from late January at the Seedvault- and Todalen study plots, and from early March at Hiorthhavn and in Lia (Appendix I). From the time of these observations, and throughout the season, were average measurements of ice, 18-33%, made at these study plots. However, scarce thinner ice layers were also noted in the early-season (Appendix III). At the higher elevation study plots, were only thinner ice layers observed, typically <1cm in thickness (see Fig. 4.8 for example). This resulted in low ice content at higher elevations, seasonal average was 1% for the three study plots. Largest portions of ice content were at lower elevations measured in late February and early March. Exception to this was Hiorthhamn, where an extreme large portion of ice content (81%) was measured in early April (06.04). Seasonal average for all pits was 12% ice content, though considerable higher 21% seasonal average when excluding the higher elevation plots. Highest seasonal average was recorded in Todalen and Lia, 23%.

Relatively large fractions (of total showpack height) of depth hoar were measured early in the study period, though typically diminished through the season (Appendix I). Average fraction for all pits combined was 22%. Highest seasonal average fraction of depth hoar crystals (28%) was observed at Gangskaret study plot, followed by the study plot in Lia (23%). Largest fraction was also measured at Gangskaret (47%) on 04.03. Lowest seasonal average (12%) was recorded at Seedvault and in Todalen, though both locations had considerable higher measurements, >20%.

In large, there was gradual increase in fraction of facets by elevation (see Appendix I) or examples in Fig. 4.8). Lyb.passet and Gangskaret study plots measured the seasonal highest fractions of facets, 34 and 30% respectively; followed by Fardalen, 21%; Hiorthhamn, 22 %; and Seedvault, Todalen and Lia, 17, 16 and 13% respectively. There were, however, large variations between each rounds of measurements. Largest fraction of facets was recorded at Lyb.passet, 66% on 06.04. Recordings of no faceted crystals were also noted, both in Lia, at Seedvault, and on Hiorthhamn; on 19.03, 05.03 and 06.04 respectively.

The highest seasonal average fraction of all snow pits combined (27%) consisted of mixed forms (faceting rounds and rounding facets) (see Appendix I). Highest fraction was measured at Lyb.passet, 70% (11.01), but was also the study plot with most measurements of zero fractions of mixed forms (27.01 and 06.04). Fardalen measured the highest seasonal average fraction of mixed forms (36%) and the lowest seasonal average was at Gangskaret (17%). Rounded grains were observed as 13% of all pits. Maximum fraction of rounded grains were measured in Fardalen (38%) on 09.05, but Seedvault had the seasonal highest average, 20%.

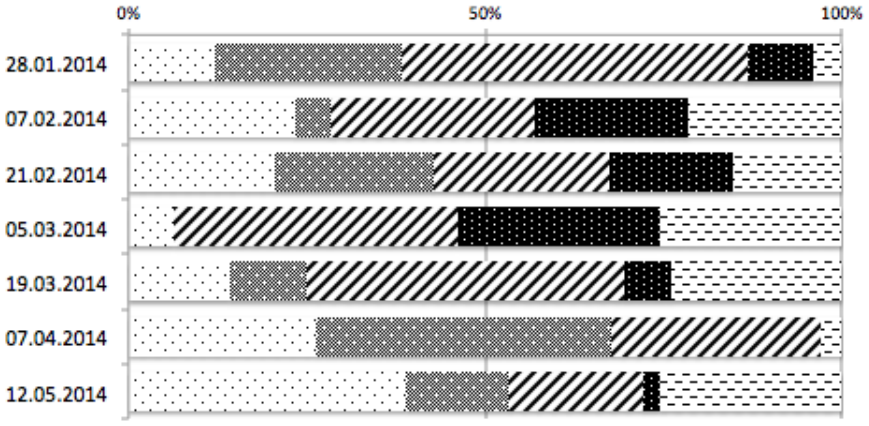

(A) Seedvault

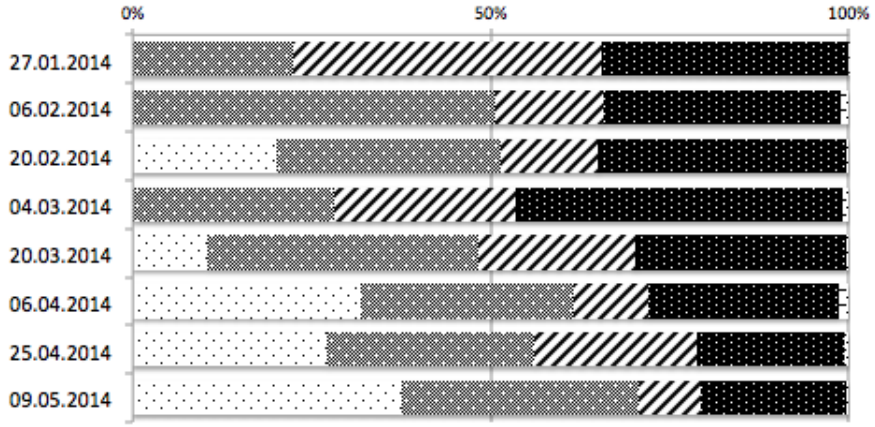

(B) Gangskaret

FIGURE 4.8: Relative amounts of rounded-, faceted-, mixed- and depth hoar particles, ice layers and melt-forms found at the Seedvault and Gangskaret study plots. Small black dots on white = rounded grains, white dots on grey=facets, oblique lines = mixed forms, white dots on black = depth hoar crystals, and short black lines on white = ice layers and melt-forms.

4.2.2 Ice content and ice layers

The contrast in ice content between lower and higher elevation study plots (section above), was a result of both number of ice layers and thickness of ice- and melt-form layers (see table 4.7). Lower elevations had both more ice layers counted per pit and

thicker layers, while higher elevations had fewer thinner layers (contrast exemplified by Fig. 4.9). Highest number of ice layers per pit (5) was observed at Seedvault, on 04.04 and 12.05, and at Hiorthhamn on 05.03. Average ice thickness per ice layers at those occurrence were 0.66 cm and 1.26 cm for Seedvault, and 1.56 cm for Hiorthhamn. Highest average ice thickness per ice layer, 20 cm, was measured in Lia on 05.03. Highest seasonal average ice thickness per ice layer, 8.6 cm, was measured both at Lia and Hiorthhamn study plots. Measurements of the lowest average ice thickness per layer, 0.2 cm, were found on Lyb.passet.

Fig. 4.9 shows good examples of how ice content presented itself late in the season.

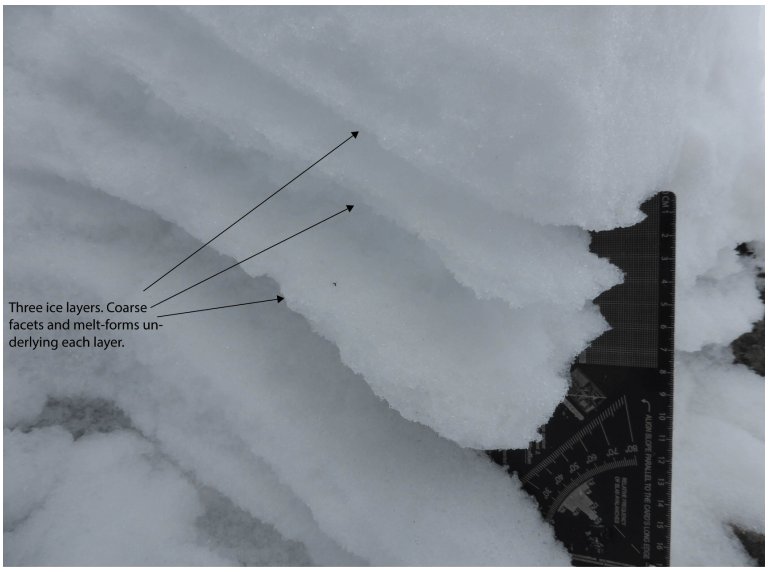

(A) Todalen late season. Three ice layers with intervening porous faceted and melt-form crystals.

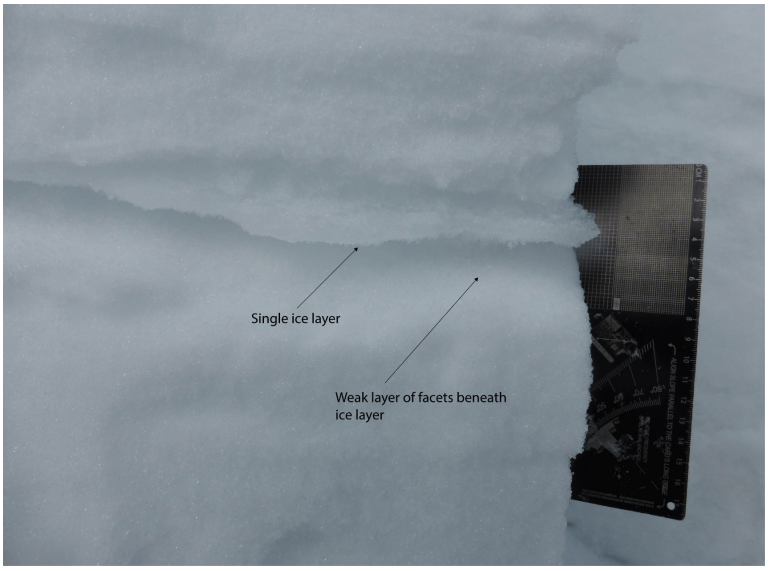

(B) Gangskaret late season. One thin ice layer with underlying weak layer of large facets.

FIGURE 4.9: Example of how ice content presented itself in (A) the lower elevated study plots and (B) higher elevated plots.

TABLE 4.7: Table of ice content (cm) and number of ice layers per snow pit through the 2013/14 study season. Avg.I = total average ice thickness per layer.

	(Ice layers / ice fraction)						
Date	Lia	Todalen	Seed-vault	Hiorth-hamn	Fardalen	Gangskaret	Lyb.passet
04.12	0/0	-	0/0	-	-	-	-
11.01	-	-	-	1/0.2	-	-	2/0.3
28.01	3/1.8	3/11.2	3/5	1/0.1	-	4/0.5	1/0.3
07.02	-	3/3.2	1/18	1/1	2/1.2	3/0.6	-
21.02	2/31	4/23	4/10.6	-	2/0.4	1/0.2	1/0.2
05.03	2/39.5	1/23	2/16	5/7.8	3/0.4	3/0.7	3/0.7
19.03	2/28	4/6	3/17	3/6.7	3/0.7	1/0.3	-
04.04	4/21.1	4/1.4	5/3.3	3/65	-	2/1.2	1/0.2
25.04	3/16.4	4/4	-	4/50	-	2/0.5	1/0.3
12.05	-	3/3	5/6.3	3/49	3/1.3	1/0.4	2/0.5
Avg. I	8.6	2.9	4.2	8.6	0.3	0.3	0.2

4.2.3 Weak layers

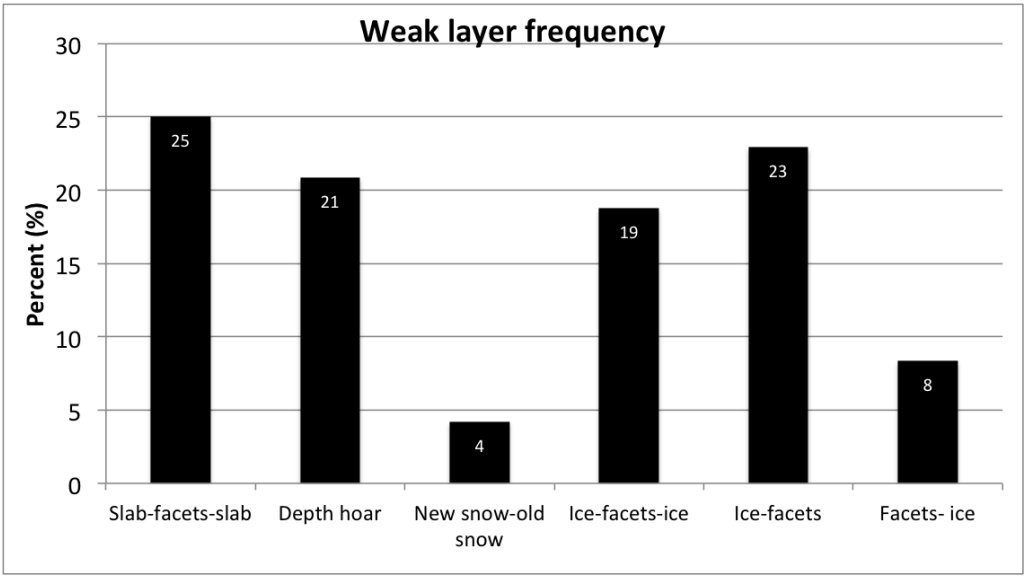

FIGURE 4.10: Frequency distribution the weak layer types. See section 3.2.2.2 for further description of the weak layer classes.

48 weak layers were identified through stability tests (CT and ECT), and classified into 6 classes (3.3). Frequency distribution of weak layers (see Fig. 4.10) show that four classes were most frequently identified in the 2013/2014 study period: slab-facets-slab (25%), base depth hoar layrs (21%), facets between ice layers (19%) and facets beneath single ice layers (23%). Combined were the weak layers connected to ice layers, the two latter and the *facets-ice* category (8%), the biggest with a total of 50% of all the observed weak layers. New snow-old snow was the least observed weak layer with 4%.

Weak layer distribution by time and elevation can be seen in Fig. 4.11. The *ice-facets-ice* weak layers were all observed at the lower elevation study plots, while the *ice-facets* category were found 80% of occurrences at higher elevations. Slab-facets-slab weak layers

were also predominantly recorded at lower elevations, by 75%. Facets-ice weak layers were only observed three times, one early season at lower elevations, and the others in late season. Lyb.passet recorded fewest weak layers per snow surveys, with only 3 observed weak layers. Weak base layers of depth hoar were, in large, recorded early in the stud period, and only 1 of 10 total recorded after 19.03 (25.04 in Lia). All study plots had occurrences of depth hoar failure, except Lyb.passet.

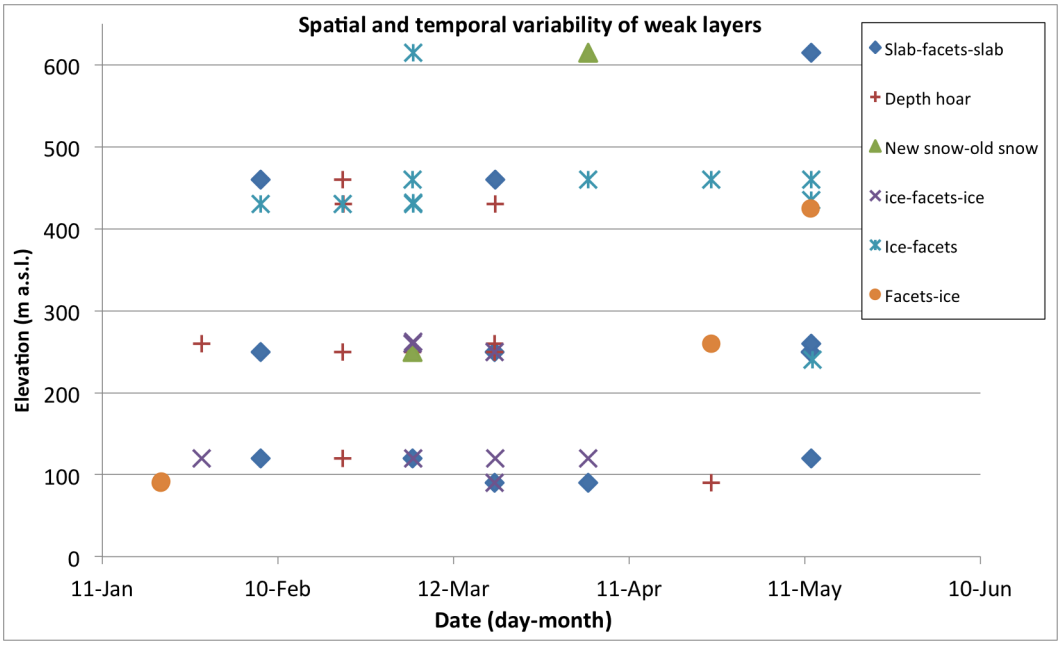

FIGURE 4.11: Plot of temporal and spatial (by elevation) distribution of weak layers observed through the 2013/2014 study period. The weak layer categories are described in detail in section 3.2.2.2. See text above for analysis of distribution. Elevation (along vertical axis) of observations are the elevation of the fixed study plots: Lia (90 m a.s.l.), Todalen (120 m a.s.l.), Seedvault (250 m a.s.l.), Hiorthavn (260 m a.s.l.), Fardalen (430 m a.s.l.), Gangskaret (460 m a.s.l.) and Longyearbrepasset (615 m a.s.l.). Temporal resolution is dictated by the timing of field campaigns (see section 4.2.1.

4.2.3.1 Steps in hardness between weak layers and slabs/base layers

The biggest hardness contrasts associated with weak layers, were between ice layers and facets (see fig. 4.12), in the ice-facets-ice weak layer category. This weak layer had a seasonal average +5 on the hardness scale (see table 3.4), from weak layer to slab, and weak layer to bed surface. I.e. *fist* (1) weak layer hardness and *ice* (6) slab and base layer hardness. The hardness step between facets and ice in the category Ice-facets was less sharp, +4 in 80% of all cases. Average hardness of the facet layer in the latter category was *4-fingers* (2), while facets were on average *fist* (1) in the ice-facets-ice category. For facets/ice was +2 (60%) the most frequent observation in hardness difference between weak layer and bed surface. For depth hoar layers were +3 and +4 the most frequent observation (both 40%). Slab-facets-slab weak layers were recorded

with seasonal average hardness difference of +2 from weak layer to slab; and weak layer to bed surface (60 and 66% of all recorded respectively).

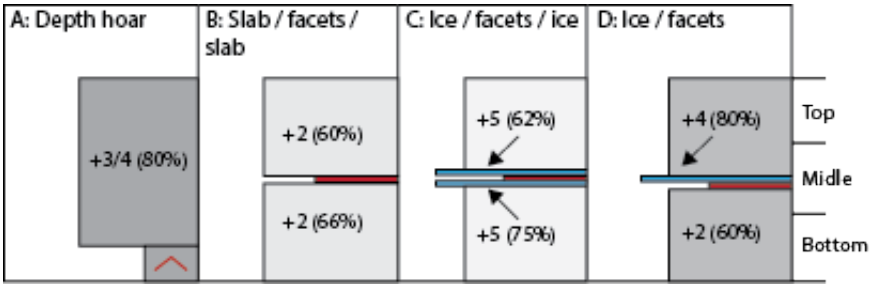

FIGURE 4.12: Illustrastion of the most frequent hardness steps on the hand hardness scale, from weak layer to slabs and weak layers to bed surfaces. The hand hardness scale is described in section 3.2.2.1. Numbers depicts the most frequent hardness difference between weak layers and slab/bed surface. Percentages of how representative the hardness difference was. Hardness difference, depth hoar to slab, was +3 and +5 equal number of times. Depth of weak layers depicts seasonal average position.

4.2.3.2 Depth of weak layers in the snowpack

40% of all weak layers were located in the middle of the snowpack, while the top and bottom parts both had 30% (see table 4.8. The main attribution to high depth weak layers were depth hoar (77%), and the remaining observations of weak layers close to the base were ice-facets (15%) and ice-facets-ice (7%). Most frequent middle depth weak layers were slab-facets-slab (33%) and ice-facets-ice (33%), followed by ice-facets (27%). Slab-facet-slab was the most frequent low depth weak layer (30%) followed by ice-facets and facets-ice (both 23%).

TABLE 4.8: Overview of weak layers by depth in the snowpack. The snowpack was divided in three equal parts: and weak layers noted according to their relative depth of the snowpack, top, middle and bottom. "-" = No Data.

	Top	Mid	Bottom
Slab-facets-slab	4	6	-
Depth hoar	-	-	10
New snow-old snow	2	-	-
Ice-facets-ice	1	6	1
Ice-facets	3	5	2
Facets-ice	3	1	-

Chapter 5

Discussion

In this chapter you find discussions of the data described in Chapter 4, Results. The first section discusses spatial variability and how spatial patterns were described by this study. Following are discussions the of results found through analyzing meteorological data. The second half covers snow properties and weak layers, and how these variables overplayed and caused spatial patterns. At the end of this chapter are study methods reviewed.

5.1 Spatial variability

It was difficult to measure precise gradients within the snow cover, or to measure precise scale of processes acting on the snow cover, due to a relative coarse sampling resolution (Fig. study-area-map), and spatial uneven distribution of snow study plots. No systematic analysis of study plots' regional representation were performed outside, except within its respective slope. It was therefore difficult to validate how representative one study plot was for its environment. However, some support was added from other study plots (e.g. study plots of same height), as they measured similar properties, or when plots followed an identified trend.

The targeted slopes for snow measurements had relatively even slope surfaces, moderate steepness and were not heavily wind affected (3.2), which are not characteristics of typical avalanche staring zones in the study area (Eckerstorfer and Christiansen 2011b). However, the environmental influences that snow structures reflected, presumably affected the snow cover, regardless of the topographic complexity it was situated in. It is therefore assumed that the documented snow structures and persistent weaknesses were representable for its snow cover, and could be extrapolated within the elevation range to some extent.

5.2 Meteorological data

5.2.1 Temperatures

The 2013/2014 mid-winter season had a considerable higher average temperature, -6.7°C, than the normal mid-season average temperature, -11.2°C (4.1). This was in large cause by very mild January and February months. 8°C and 11.3°C warmer than normal average January and February temperatures. During these months there were frequent warm cycles causing snow thaw, though primarily affected lower elevations (4.3). The remaining mid winter months (Nov, Dec, Mar, Apr) were closer to their normal month's average temperatures, but still milder than the normal averages. The remarkably high January and February was caused by frequent low-pressure centers passing Svalbard, due to blocking high-pressure building out, east of Scandinavia. There were few stable high-pressure periods with cold weather in the 2013/2014 mid-winter season. Most distinct periods were in early to mid December, and after the prolonged mild periods in January and February, in late March to early April.

In the winter season of 2013/2014 mid-winter warm spells lead to melt-freeze crusts, rain crusts, and melt form layers and will be discussed further in Sect. 5.2.3. However, it is worth mentioning how warm spells have directly caused snow avalanches earlier. Eckerstorfer and Christiansen (2012) documented two extreme mid-winter slush- and wet slab avalanche cycles, in the area surrounding Longyearbyen, as a result of mid-winter warm spells. The two avalanche cycles (January 2010 and March 2011) were attributed strong winds, positive temperatures and 100-year record monthly rainfall recordings. Although, ice layers in the snowpack played a significant part in the release of the slush flows and wet slab avalanches. Ice layers in the middle of the snowpack functioned as a water-impermeable barrier, causing water from rainfall and thawing snow to saturate the top part of the snowpack with water, and initiates slush flows. For wet slab avalanches, the ice layer was lubricated by water and created an ideal sliding surface for a heavy water saturated slabs to slide on. These avalanches released close to the base of the snowpack and are the largest avalanches described on Svalbard (2014).

Eckerstorfer and Christiansen (Eckerstorfer and Christiansen 2012) concluded that the extreme weather that lead to the slush- and wet slab avalanche cycles were caused by the frequency, magnitude and the passage time of low-pressures passing over Svalbard. However, the prolonged mild periods in January and February 2014 caused no reported or observed slush or wet slab avalanches in the surroundings of Longyearbyen, even though mild period extended for a long time and caused 100-year record high monthly average February temperature. This was assumed due to the low amounts of liquid precipitation in the period (<1 mm w.e.). The precipitation during the slush and wet slab avalanche cycle recorded 15-25 mm w.e. daily max values, during the days of avalanche initiation (Eckerstorfer and Christiansen 2012. Data from this study imply

that frequency and passage time of low-pressure passages were not important for slush and wet slab avalanche cycles, as the long lasting low-pressure systems in 2013/2014 were dry. Considering this event, it is less likely that frequency and passage time of low-pressure systems are important controls for slush and wet slab avalanche cycles, but that magnitude of low-pressure systems and transport of humidity are more decisive factors.

5.2.2 Environmental temperature lapse rates

Due to the ice-free mid-winter conditions in the Adventfjord, there were expected strong temperature gradients between the near fjord environments and the more continental mountainous areas. Environmental temperature lapse rates between the Lufthavn (28m a.s.l.) and Gruvefjellet (464m a.s.l.) meteorological stations were used to explore this idea, representing fjord near and continental mountainous environments respectively. Ideally one would choose a meteorological station further inland for continental representation, e.g. Gangskaret, but because of its limited temporal coverage (Feb, Mar, Apr), was Gruvefjellet preferred. The Jansonhaugen meteorological station (251 m a.s.l.) was also included in the analysis, to decompose the gradient. Gruvefjellet meteorological station recorded slightly warmer temperatures during April compared to the rest of the stations, this is likely due to the topography of Gruvefjellet, as the station has no terrain that cause periods of shade, and consequently receiving direct sunlight almost 24 hours of the day during cloud free conditions. This might have tilted the results slightly, causing a weaker gradient in April and moderately affecting the seasonal average.

The mid-winter season's average monthly environmental lapse rate, between Lufthavn and Gruvefjellet meteorological stations, was -0.76°C/100 m, a considerable high temperature gradient compared to the average atmospheric lapse rate of -0.65°C/100m (Ahrens 2011). However, decomposing the gradient by including temperature measurements (from Jansonhaugen (251m a.s.l.)) at an elevation in between these stations revealed that the temperature gradient was steeper at lower elevations than at higher elevations. The mid-winter average environmental lapse rate between Lufthavn and Jansonhaugen meteorological stations was -0.98°C/100m, while the rate between Jansonhaugen and Gruvefjellet stations was -0.53°C/100m. The strong temperature gradient between Lufthavnen and Jansonhaugen meteorological station means that temperatures at the Lufthavnen station, located near the fjord, was warm for its elevation, or that the Jansonhaugen station, located inland, was cold for its elevation. The latter suggestion was less plausible, as Jansonhaugen's location arguably sheltered it from the cold air masses known to drain along Adventdalen's valley bottom (3.1). A heat flux from the open water fjord, however, better explains the relative mild temperatures at Lufthavn meteorological station. Kilipelainen and Sjoblom (2010) described this layer, and measured significant heat exchange with the atmosphere. The extent of this heat source' influence

was hard to determine with the available data, making it hard to assess weather or not the snow cover on surrounding mountain/valley sides was affected. Data from Adventdalen meteorological station recorded no data suggesting influence on air temperatures from the open water fjords, though the temperature records from this station imply significant temperature control by cold air drainage from southeast, recording remarkably cold temperatures for its elevation (4.1).

To assess the temporal variability of the ELRs, top and lower 15% ELR strength occurrences, between Lufthavn and Gruvefjellet meteorological stations, were studied. The variability was investigated by identifying meteorological variables (temperature, wind direction and wind speed) at both the Lufthavn and Gruvefjellet met. stations, connected with the top and lower 15% values. Associated with the top 15% values (strong ELR), average -1.24°C/100m, were low average temperatures. On average the temperature was -12°C and -17.5°C, recorded at Lufthavn and Gruvefjellet meteorological stations, during periods of strong ELR. During the weak ELR periods (lower 15%) the average temperature was -4.2°C and -6.4°C. This finding indicates that strong ELRs occur during periods associated with stable high-pressure systems and calm cold weather (see Fig. 1.3), while weak gradients occurred during periods of relatively warm weather (-4.2°C average). This was warmer than the average 2012/2013 and the average normal period mid winter average temperature (see Fig. 4.1). It was hard to determine with certainty why strong ELR occurred during periods of cold weather and why weaker ELR occur during relatively mild weather. However, it is plausible that the strong gradients were caused by a increased heat flux from the fjord during these cold periods, as cold air temperatures could have strengthened advection between the open water fjord and surrounding low lying land areas. Kilipelainen and Sjoblom (2010) identified unstable air masses over the fjord, due to the heat flux, in periods of cold weather, supporting this explanation. The latter study also argued that topographic control on wind conditions along the fjord were important for controlling heat fluxes from open water. The monthly average ELR Lufthavn-Jansonhaugen and Jansonhaugen-Gruvefjellet were not proportionately strong during each of the mid-winter months (4.2). The strongest Lufthavnen-Gruvefjellet ELR was recorded in February, the warmest month of the study period. The maximum Jansonhaugen-Gruvefjellet ELR (-0.70°C/100m) was measured in this period, suggesting a relatively strong ELR at higher elevation during warm periods (yet still lower than at lower elevations, Lufthavn-Jansonhaugen). The lowest Jansonhaugen-Gruvefjellet ELR (-0.27°C/100m) was measured in April, the coldest mid-winter month of 2013/2014. This month also measured the lowest ELR of Lufthavnen-Gruvefjellet, possibly caused by high solar exposure influencing temperature recordings at Gruvefjellet. These results are hard to investigate further with the data available, and are outside the scope of this study.

5.2.3 Mid-winter warm spells

All meteorological stations within the study area, with significant spatial variation, recorded the meteorological signals of mid-winter warm spells by positive temperatures. The variation occurred because of height difference between the meteorological stations, and the relatively high environmental gradient. Number of thaw hours and number of thaw cycles demonstrates that lower elevations were more sensitive to warm spells than higher elevation during the 2012/2013 season (4.3), and that only severe warm-spells affect higher elevations by thawing snow. Only two of the warm spell cycles were identified simultaneously at all met. stations in the 2013/2014 season, December 17th and February 12th, both characterized by the season's max temperatures (5.2 and 4.8°C recorded at Lufthavn met. station). The first warm spell recorded at high elevations (December 17th 2013) was a rapid event (4.1, identified in the meteorological data with two days of positive temperatures (including data from lower elevations). The warm spell was initiated with a sudden large spike of approximately 20°C, leading to positive temperature records at all meteorological stations within the study area, and dropping in temperature almost as rapidly as it spiked two days afterThe second warm spell event with average hourly positive degrees recorded at all meteorological stations, was at the end of the prolonged period of mild temperatures only affecting lower elevations, from mid January to late February. At the end of this period the temperatures spiked, leading to the extensive warm spell–causing thaw at the highest elevated met. station. What caused the the prolonged mild temperature period and the sharp large spike in temperatures at the end of the period is difficult to determine.

In comparison to the normal period (11 thaw days), was the 2013/2014 season above average in number of thaw days (17) and thaw cycles (8), though slightly lower in average thaw day temperature (0.9°C). Considering the range of thaw days per season over the normal period (1 - 44), the 2013/2014 season was not extreme by any measurement, and can be considered relatively representative for an average season. However, the 100-year record mild average February temperature must be considered abnormal, as it was dramatically warmer than the average February normal temperature.

The mid-winter warm spells of the 2013/2014 season did not cause any direct avalanches similar to the slush- and wet slab avalanche cycles of 2010 and 2011, described by Eckerstorfer and Christiansen (2012). Nevertheless, there were significant ice layer development in the snow cover, which greatly affected snow properties. A subsequent reaction to one of the warm spells was a small avalanche cycle of direct action avalanches in mid January. As a result of the warm spell, there was developed a ice crust, capping the snow cover at lower elevations, which subsequent wind slabs failed to bond well onto. Several minor avalanches were observed in the mountains around Longyearbyen, most notably was a 60-meter wide avalanche at lower part of the mountain *Sukkertoppen*, in an area known as Lia (see regobs.no for report). The release area was adjacent to one of

the study plots (Lia), and is a well known location for slab avalanche releases (Delmas 2013). Although direct avalanches were not the prime focus area for this study, it is worth mentioning the observed events, as they relate to warm spells and ice content development in the snow cover. It is likely that these types of weather scenarios (ice crust formation followed by rapid slab depositions) could be a important for direct action avalanche cycles on Svalbard, as this weather scheme is regular on Svalbard. This weather/snowpack patterns connection to direct action avalanches has not been reported on before.

5.2.4 Wind patterns

Wind plays a crucial role in depositing snow, and has often been identified as the most important factor causing snow avalanches (e.g. Hendrikx et al. 2005; Eckerstorfer and Christiansen 2011c). As this study prime focus was snow stratigraphy and its variation along a environmental temperature gradient, were wind's influence on the snow cover indirectly neglected, as the study design ideally targeted slopes with low wind disturbance. Most important were the wind measurements recorded at Gruvefjellet meteorological station, as this station records the regional wind pattern, rather than local topographic controlled winds. Wind at Gruvefjellet during the 2013/2014 season was predominantly from the southeast sector, which also was documented from earlier seasons (Christiansen et al. 2013). There were however also periods with winds from the west, and both sectors had sufficient wind velocities speeds for snow transport.

The topography of the study area facilitates horizontal wind loading controlled by the regional wind patterns. The abundant flat table shaped mountains (e.g. Gruvefjellet 3.1) operate as large reservoirs for snow drifts, and are important for cornice development (Vogel et al. 2012) and wind loading onto slopes leading down from the plateaus. Topographic controlled winds on the other hand can cause severe cross loading along valley walls. Combined these two factors cause complex wind loading patterns over the study area. The predominant wind direction cause, in large, cornice development and wind loading on northwest ridge/slope aspects.

5.3 Svalbard snow cover

5.3.1 Snow height

The Todalen study sites showed the most variability in snow depths through the season, followed by Hiorthavn. The Todalen study plot (see Fig.4.6) had a rough ground surface, similar to the slope studied by Eckerstorfer and others (2014). They studied how snow height as a function of surface roughness affected slab stability on small wind affected

slopes. Their results concluded: that within the same slope (1) shallower zones of the snow cover, as a result of ground surface elevations, were potential dry slab avalanche trigger zones, and (2) that thicker areas of the snow cover potentially held more instabilities. An miniature example of this was highlighted in Fig.4.6, where larger blocks in the bed surface cause both heights and depressions, leading to deeper and shallower sections of snow cover within the same slope. In this example the base depth hoar was layer thicker in the depression, between the blocks, than above the blocks "piercing" into the snowpack.

The snow cover in the area has been characterized as thin (Eckerstorfer and Christiansen 2011a, but there are large spatial variations due to complex topography and high influence of wind. Additionally there is a precipitation gradient, where precipitation increases with elevation (Humlum 2002). One would therefore expect a thicker snow height with elevations, though the studied slopes typically showed a natural increase in snow height to around one meter, and no noticeable trend of thicker snow cover with elevation. However, the sampling strategy chose slopes with expected high snow depths, excluding overall representative snow depth measurements for the study area.

5.3.2 Snow hardness and hardness profiles

Snow hardness varied spatially, and was in large controlled by the amount of ice and facets in the snowpack. Lower elevations gained melt forms in addition to numerous ice layers, while higher elevations only gained scarce and thinner ice layers. This spatial distribution was due to lower exposure to warm spells at higher elevations than at lower. Higher elevations also measured higher fractions of faceted snow grains. Combined this lead to a contrast of hardness between higher and lower elevations.

Both profile 7 and 9 were frequently applied to hardness structures in the 2013/2014 seasons. Profile 9 was least frequently observed of the two profiles, applied five times to lower elevation study plots (Seedvault, Hiorthavn and Lia). Profile 7 was most frequently applied to the Gangskaret plot, where seven of eight snowpits investigated were assigned the profile. This implied a consistent weakness present in the snow stratigraphy throughout the season. The snowpack at Gangskaret (and profile 7) typically presented two sharp contrasts in hardness, one at the middle and one at the base, due to both faceting underneath a harder slab and a weak base of depth hoar crystals. The Hardness profile 3 was most frequently assigned through the season, 41% of all pits. The profile is described as less definite in terms of stability, as it shows less critical, but conditional weaknesses. The profile was applied frequently at all elevations through the season. This profile shape was a natural cause of the snow cover's developed in the 2013/2014 season, especially at lower elevations where mid-winter warm spells were severe. The bell shaped form developed as follows: the snow cover early developed a weak base with depth hoar, and later gained a severe hard slabs in the middle due to mid-winter warm spells, and

later accumulated softer snow layers at the top. The conditional weakness associated with this profile depends on the properties of the hard middle section, as a weak layer of depth hoar is not conclusive in determining instabilities on its own (Wiesinger and Schweizer 2000). If the middle section was well consolidated (hard), as often was the case during this study, profile 3 implies stability rather than weaknesses. Hardness of slabs has been identified as an important consideration when determining snowpack weaknesses, as hard slabs can "shelter" a weak layer from any realistic artificial trigger (e.g. skier or snowscooter). This will be discussed further under the Weak layer discussion (Sect. 5.4)

The high number of profile 3 and 7 is comparable to the results of Eckerstorfer and Christiansen (2011a). Most of their hardness measurements were on average over two seasons (2007/2008 and 2008/2009) classified as profile 3, their second most applied profile was profile 4, which in this study was the third most applied profile. Profile 2 and 7 was their third most used profiles, profile 7 was in this study the second most common and profile 2 the forth most common. The 2013/2014 season's hardness profile distribution were similar to to the latter study, implying that the slabs and weakness structures found in this study are representative for the norm of the snow climate, and that varies little from year to year.

5.3.3 Snow grain types and ice layers

A lot of effort was put into measuring the content of various snow grains and ice in the snowpack. Spatial trends of snowpack content were identified, like the contrast in ice content between high and low elevation study plots, and a gradual increase of facets by elevation. Ice content affected the snowpack in two direct ways in regards to snowpack stability: (1) ice content hardens the snowpack, making it harder to trigger deep weak layers, underlying ice layers; and (2) ice layers are vapor-impermeable layers, typically resulting in faceting just below or above ice layers. How this affected stability will be further discussed in the next section (Sect.XX).

The average larger portion of facets measured at higher elevations, combined with less ice content, explains the hardness contrast between high and low elevations. Depth hoar crystals were consistently found at the base of almost all studied snow pits, though there were found no spatial patterns of magnitude or temporal development along the climatic gradient. The temporal pattern of thicker depth hoar layers early season than late season, (see Appendix I), was not caused by increased thickness of depth hoar layers, but rather increased snow heights over the season. The actual height of depth hoar layers varied little from first observation to the end of the season, and the variations observed could be explained by variation in surfaces roughness, as depressions tend to create pockets of thicker depth hoar layers.

The development of ice layers during warm spells event, occurred in the top part of the snowpack. The more severely impacted lower elevated developed several ice layers and intervening melt form layers. As the snowpack refroze these layers were almost uniform in hardness, as the ice layers and the intervening melt forms layeres measured relatively hard layers (P to I). As time progressed, the melt form layers intervening ice layers, recrystallized in to faceted crystals. This caused great hardness contrast between the hard ice layers and the intervening and underlying coarse soft layers of facets. These layers resulted in reactive weaknesses later in the season

Table 4.7 shows an overview of the ice content and number of ice layers measured in the stratigraphy at each study plot through the study period. In late January there is a noticeable trace of the warm spells occurring earlier in the month and from late 2013 (see fig. 4.3), and slight but noticeable contrast between lower elevations andhigher elevations in ice content. This contrast peeked by late February due to the extensive warm spell that dominated that month. Late February and early March shows large ice content at lower elevations, between 7 - 39 cm at the Seedvault, Hiorthhavn, Lia and Todalen study plots. This high measurement is due to the extreme hardness of ice layers and layers saturated with melt-forms, causing them to be categorized as ice (I) on the hand-hardness scale. Noteworthy is that the layers of high melt form content later diminish as the snow crystals recrystallize in to either purely faceted crystals or a mix of facets and melt forms. This caused high hardness contrasts between ice layers and formed into weak layers. Number of ice layers both increased and decreased through the season, the prior was caused by warm spells forming new ice layers. Thinner layers can diminish by sublimation, explains partly why there were noted decreased numbers of ice layers (Jamieson 2006.

5.4 Weak layers

Six categories were used to characterize the weak layers identified during the 2013/2014 study season, but for simplicity they are here divide in three: (1) weak base layers of depth hoar, (2) weak layers connected to ice formations, and (3) faceted crystals below hard slabs (slab/facets/slab). Distinctions within ice related weaknesses will be discussed separately below, and new snow / old snow interfaces are neglected as they were few observed cases and not the prime focus of this study (as they are related to direct action avalanches).

Depth hoar layers were found at all study plots, and were observed from early to late in the season. However, even though the layer was the third most frequent weak layer, it had only one observed failure after March, indicating that depth hoar layers got less sensitive to failure towards the end of the winter season. The reason for low sensitivity could be caused by a higher snowpack towards the end of the season, buffering more

of the applied force from stability tests used to identify weak layers. Hardness of the snowpack was also a likely cause for increased stability at the base of the snowpack towards late season. Well sintered slabs and ice layers typically increase stability in the snowpack, as these layers are typically less brittle and increases the force necessary to reach a weak layer, and increases stability by "bridging"[1] (Brattlien and Ellesvold 2010). This is a important topic for hard snow climates, as weaknesses identified by stability tests are often overestimated if underlying a hard slab. Slopes with hard thick slabs overlying weak layers can be nearly impossible to trigger, but are often identified as unstable through stability testing. This occurs as cut snow coulombs loose strength when isolated from the snow cover, by lowered ability to "bridge" force.

Thin layers of facets sandwiched between two harder slabs ere typical weak layers through the season, and were only observed at lower elevations. This weakness requires two hard slabs and well developed facets in between, a structure seldom observed at higher elevations. Why this structure was more typical for lower elevations is difficult to reason, but could possibly be explained by more faceting within slabs at higher elevations, causing average softer contrasts to interface below a weak layer. Although the hardness contrasts associated with this weak layer was relatively low (see Fig. 4.12).

Combined were weak layers connected to ice formation the biggest group, implying that ice formations had a important role in development of weak layers. However, clear distinctions between the weak layers connected to ice were identified. Facets developing beneath ice layers and facets sandwiched between two ice layers had spatial pattern of importance, as they imply different weaknesses at higher elevations than at lower elevations. Facets developing below a single ice layer have potentially a much larger water vapor reservoir, as vapor can travel through the underlying slab and contribute to faceting. Facets developing between two ice layers were limited by vapor-impermeable layers above and below.

It was difficult to determine which of the two categories presented the biggest threat in regards to slab avalanches. In a way, ice formations were contradictory, as they both caused stability and instability. They caused instabilities as ice layers were vapor-impermeable barriers, facilitating frequent development of facets underneath; and caused stability by strengthening the overlying slab. The hardness property was in large neglected by stability tests. Larger steps in hardness were identified in the ice-facets-ice category than in the ice-facets category, implying a more severe weakness in the prior category. However, the snowpack where the latter category most frequently was observed, at higher elevations, was on average softer than lower elevation snow cover. Softer snowpack is in theory easier to trigger than hard snowpack, implying that the high elevation snow conditions presented a bigger threat than lower elevations. The slightly larger hand hardness contrast between facets and ice layer in the ice-facets category was a result of the harder facet layers, not harder ice layers. This hardness (4F) imply a higher density

[1] Bridging refers to spreading of force horizontally through the slab

in the layer of facets linked to this category (ice-facets), and although speculative, it is reasonable to believe that a relatively dense layer of well developed facets would initiate fracture propagation easier than a less dense layer of facets and melt forms.

5.5 Review of study design and methods

Using meteorological data to describe a climatic gradient, and point measurements of snow properties to study spatial variability of the snow cover along this gradient, proved to be a complex and challenging study design. Meteorological data and snow measurements were successfully connected, as the outcome of the environmental gradient described through meteorological data was identifiable in the snowpack measurements. However, the snow data only succeeded in describing the contrast between the outer extends of the gradient (i.e. ice content), and failed to identify the rate of transition. This is due to the scarce sample resolution of snow properties, resulting in too large spatial integration per sample, and failing to describe a gradual transition of properties (e.g. ice content). This is of course also a logistical issue, as it would be near impossible to have a perfect sampling resolution over such a large area by this study design.

Snow pits provided many types of data per site (e.g. crystal types, temperatures, snow heights etc.), and provided good quality data as a exploratory field methods. Data analysis was slightly limited by this approach, as there was not given any special emphasis on measuring one particular snow property. A more targeted approach could thus have provided more detailed descriptions of one topic (e.g. ice layers or weak layers), by using more efficient methods, allowing higher resolution measurements.

Using fixed locations for snow measurements, and investigating the sites continuously over the study period, provided good data for documenting the snowpack development. This method provided good control over the sampling sites, as one could document how layers evolved through the season by tracing the snowpack history back to early mid season. However, the temporal nature of the data series limited the available data analysis tools, e.g. was multiple regression analysis not easily applied, which is common applied approach to spatial variability studies.

Chapter 6

Conclusion

This study combined field measurements and meteorological data to describe how snow properties and environmental parameters affecting snow properties, varied spatially and temporally within areas surrounding Longyearbyen, Svalbard, during the mid-winter season of 2013/2014. Emphasis was put on how this variability appeared along a local climatic gradient, from areas near the sea-ice free Adventfjorden, to higher elevation inland areas. The gathered data was processed and analyzed to answer the research questions introduced in chapter 1, and concluded the following:

- Spatial and temporal meteorological data from the study area described a strong environmental temperature gradient from near fjord areas to higher elevation inland areas. Decomposing this gradient, further revealed that the gradient was stronger at lower elevations near the fjord, implying that heat fluxes from the open fjord affected air temperatures in its nearby environment. By comparing the mid-winter period of 2013/2014 with a normal period, it was evident that 2013/2014 was just slightly over average regarding mid-winter warm spell influence, but that the season was considerably warmer (by 4.5°C) than the normal period (3.1.1). This was mainly due to remarked warm January and February months, with highest average February temperatures recorded since meteorological measurements started in Longyearbyen.

- Spatial snow measurements reflected the gradient described by meteorological data, in the following ways: (1) the amount of faceted crystals, in large, increased gradually with elevation; (2) there was a large contrast between lower elevation study plots and higher elevation study plots in total ice content, and in how ice content was presented in the snowpack; and (3) as a result of the two prior properties, the snowpack was softer in higher elevations than lower elevations.

- The contrasts in ice content and ice structure, between higher and lower elevations, resulted in different type of weak layers in the respective areas. This variability of

weak layer types caused a spatial pattern of snowpack weaknesses. The dominant weak layer type at higher elevations, combined with a softer snowpack, arguably caused more unstable snowpack conditions than at lower elevations.

Chapter 7

Appendix

7.1 Appendix I

Stacked snow crystal type / ice and melt-form content column charts from all pits

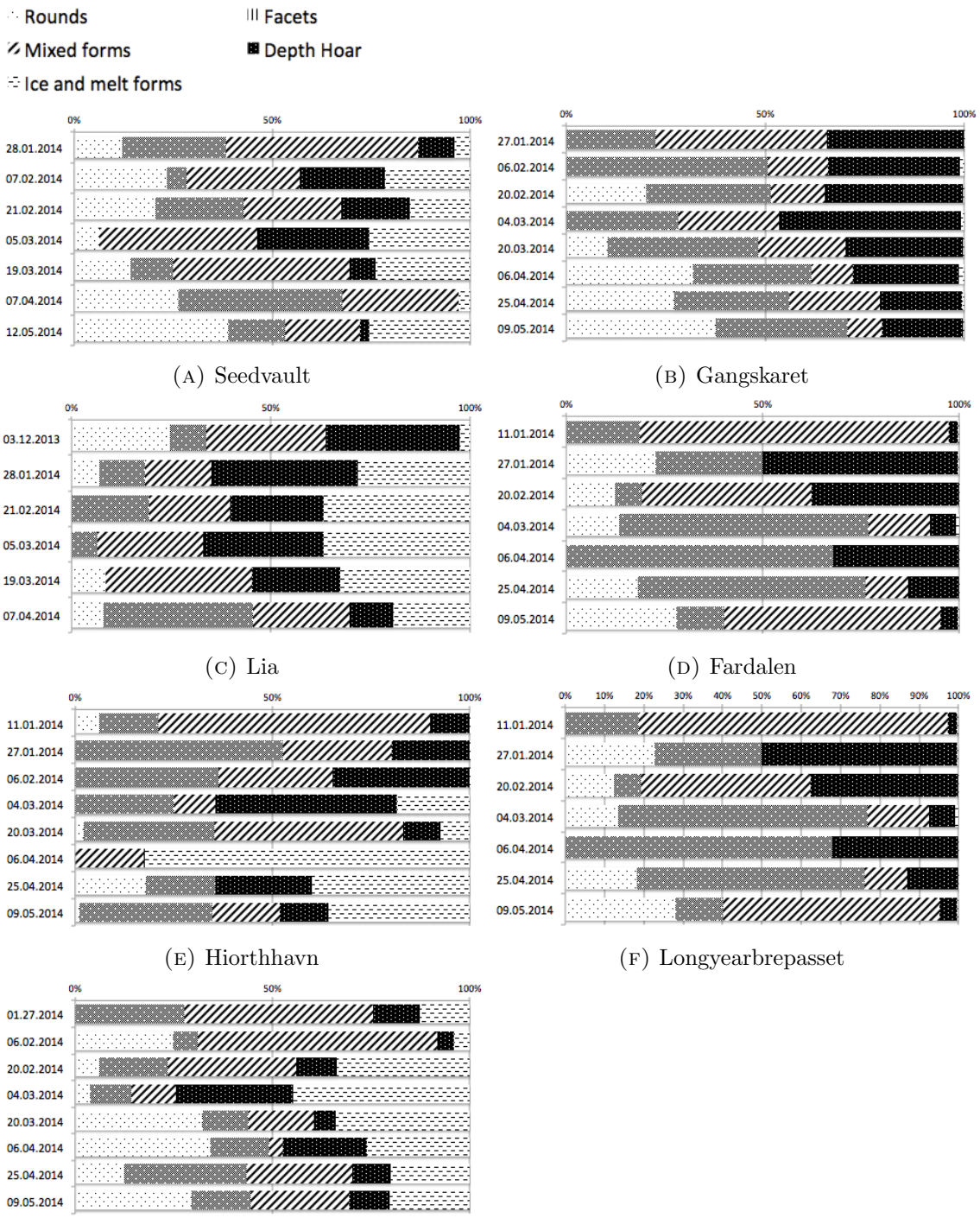

(A) Seedvault

(B) Gangskaret

(C) Lia

(D) Fardalen

(E) Hiorthhavn

(F) Longyearbrepasset

(G) Todalen

FIGURE 7.1: Distribution charts of snow crystal type and ice amount observed per pit through the study period

7.2 Appendix II

TABLE 7.1: Description of snow climate classes

Snow cover class	Description	Depth range (cm)	Bulk density (g cmˆ3)	Number of layers
Tundra	A thin, cold, wind-blown snow. Max. depth approx. 75 cm. Usually found above or north of tree line. Consists of a basal layer of depth hoar verlain by multiple wind slabs. Surface sastrugi common. Melt features rare.	10-75	0.38	0-6
Taiga	A thin to moderately deep low-density cold snow cover. Max. Depth: 120 cm. Found in cold climates in forests where wind, initial snow density, and average winter air temperatures are all low. By later winter consists of 50% to 80% depth hoar covered by low-density new snow.	30-120	0.26	15
Alpine	An intermediate to cold deep snow cover. Max. depth approx. 250 cm. Often alternate thick and thin layers, some wind affected. Basal depth hoar common, as well as occasional wind crusts. Most new snowfalls are low density. Melt features occur but are generally insignificant.	75-250	no data	15
Maritime	A warm deep snow cover. Max depth can be in excess of 300 cm. Melt features (ice layers, percolation columns) very common. Coarse-grained snow due to wetting ubiquitous. Basal melting common.	75-500	0.35	15
Ephemeral	A thin, extremely warm snow cover. Ranges from 0 to 50 cm. Shortly after it is deposited, it begins melting, with basal melting common. Melt features common. Often consist of a single snowfall, which melts away, then a new snow cover reforms at the next snowfall.	0-50	no data	1-3
Prairie	A thin (except in drifts) moderately cold snow cover with substantial wind drifting. Max. depth approx. 1 m. Wind slabs and drifts common.	0-50	no data	1-3
Mountain	A highly variable snow cover, depending on solar radiation effects and local wind patterns. Usually deeper than associated type of snow cover from the adjacent low-lands.		no data	variable
High Arctic Maritime*	Very thin and cold snowpack. Rain and melting events not uncommon mid winter. Typical are persistent weak basal layers of depth hoar with winds slabs and ice layers on top.	N/A	N/A	N/A
Rainy Continental*	Relatively thin snowpack and cold air temperatures. Heavy rainfall. Persistent structural weaknesses caused by facets and depth hoar. Dominance of facets and wet grains.	N/A	N/A	N/A

7.3 Appendix III

7.3.1 Lia 1/2

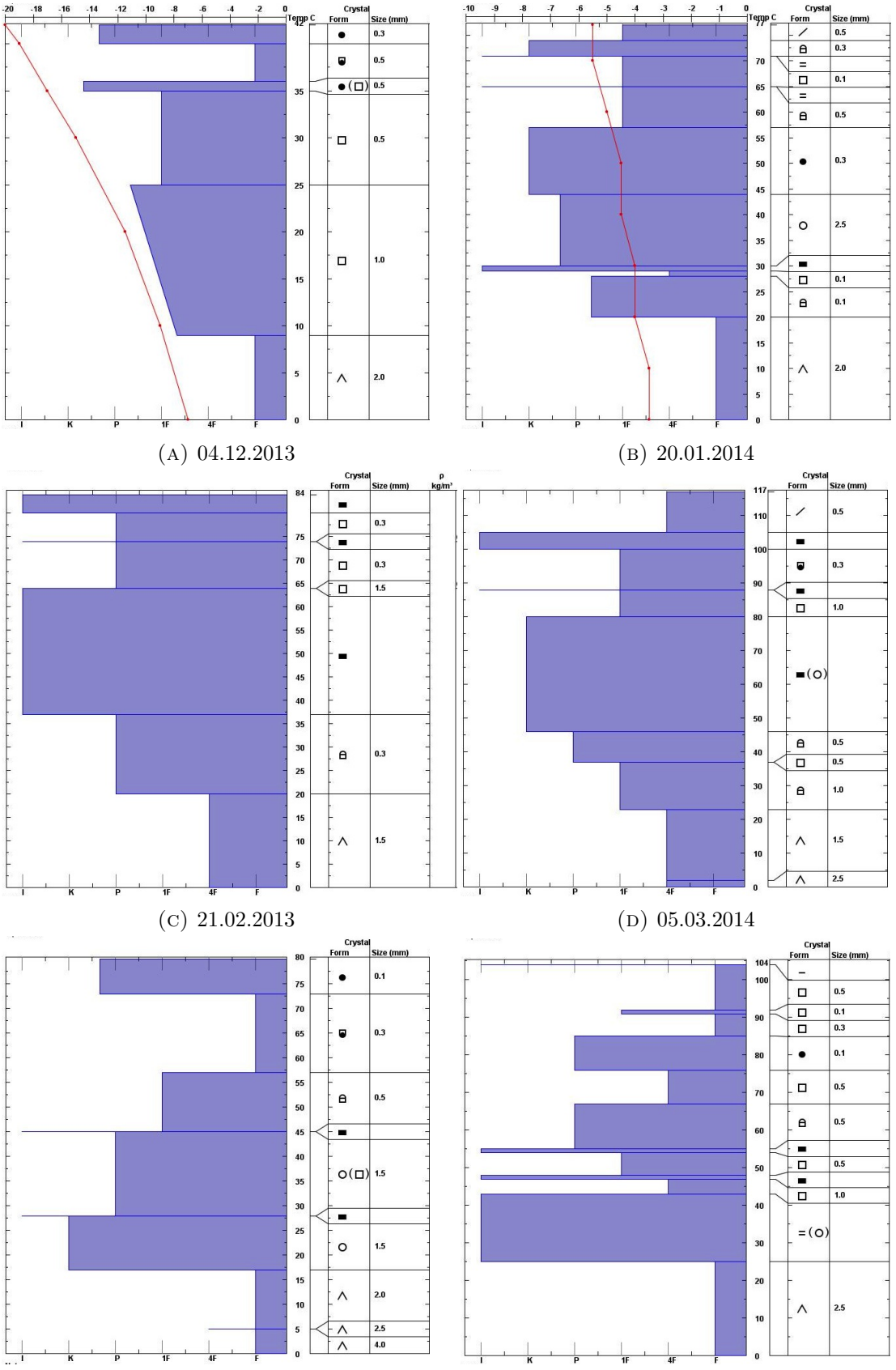

(A) 04.12.2013 (B) 20.01.2014

(C) 21.02.2013 (D) 05.03.2014

(E) 19.03.2013 (F) 04.04.2014

FIGURE 7.2: Snow pit profiles from Lia, 90 m a.s.l., 04.12.2013-04.04.2014.

7.3.2 Lia 2/2

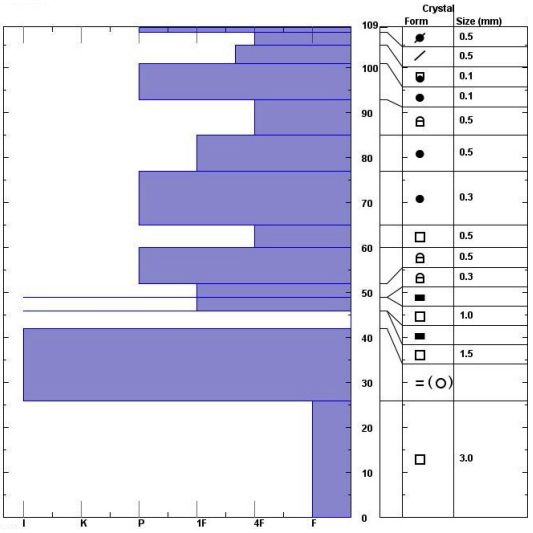

(A) 25.04.2014

FIGURE 7.3: Snow pit profiles from Lia, 90 m a.s.l., 25.04.204.

7.3.3 Todalen 1/2

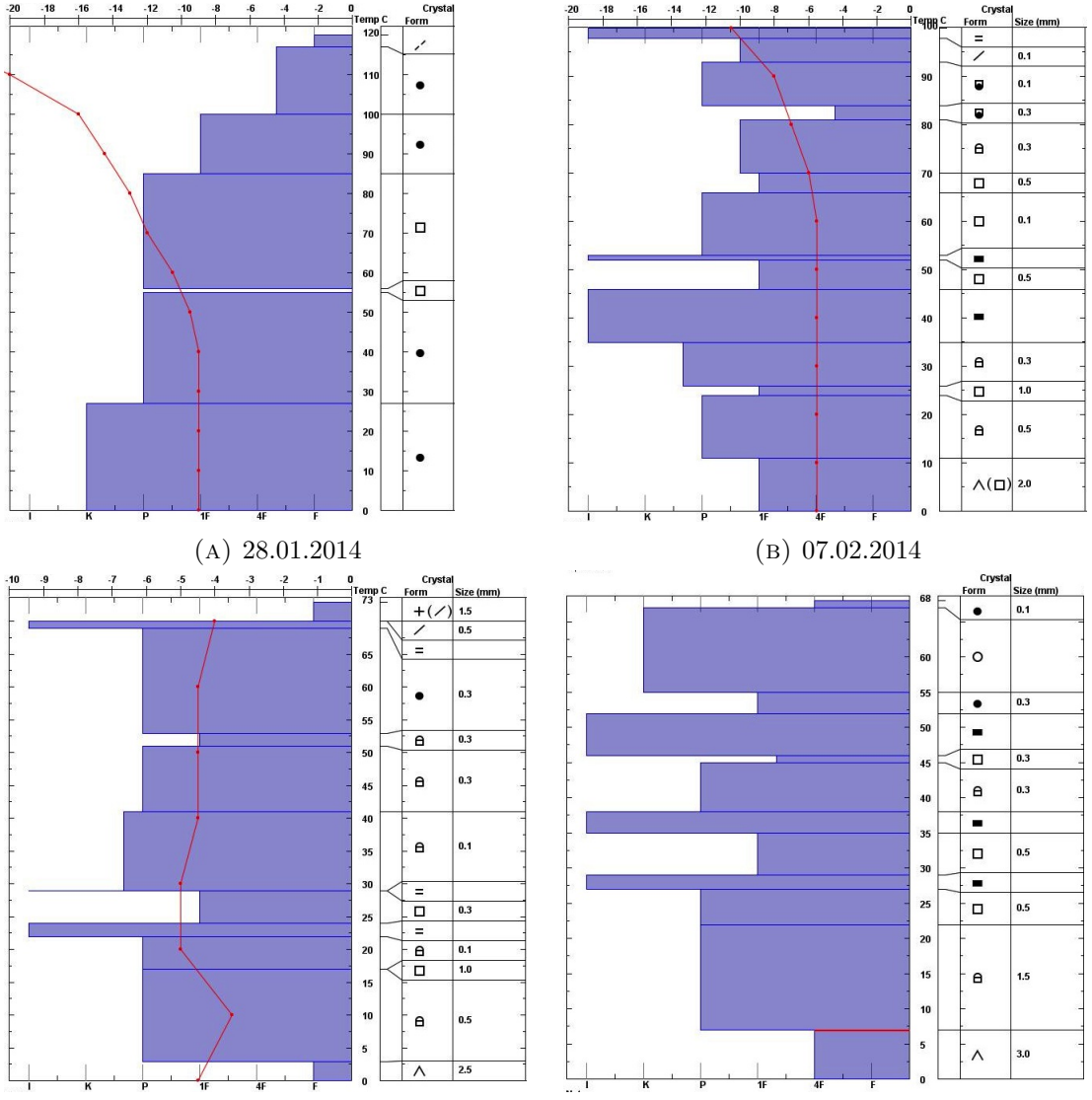

(A) 28.01.2014 (B) 07.02.2014

(C) 21.02.2014 (D) 05.03.2014

FIGURE 7.4: Snow pit profiles from Todalen, 120 m a.s.l., 28.01.2014-05.03.2014.

7.3.4 Todalen 2/2

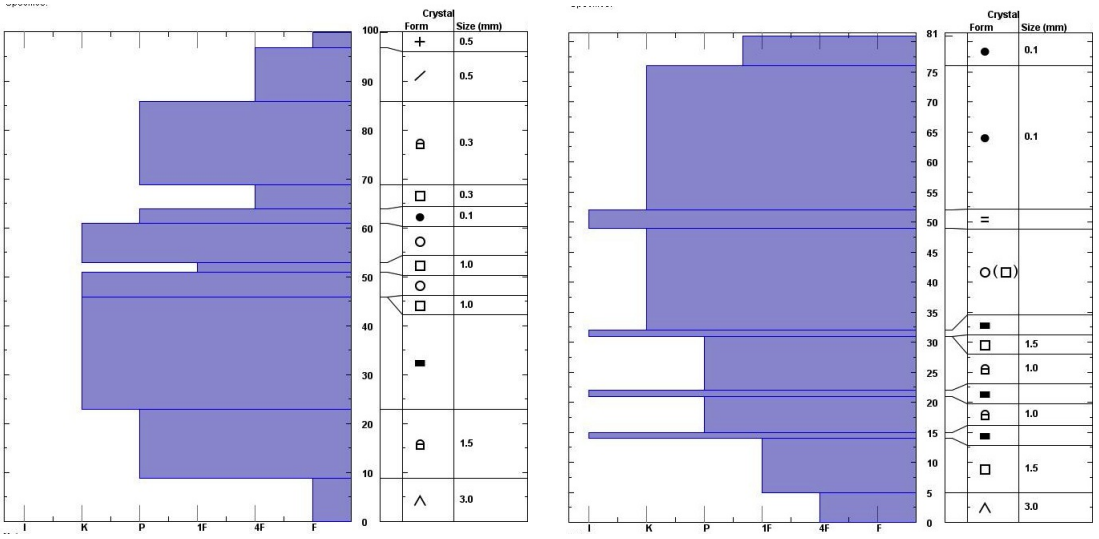

(A) 19.03.2014 (B) 04.04.2014

FIGURE 7.5: Snow pit profiles from Todalen, 120 m a.s.l., 28.01.2014-04.04.2014.

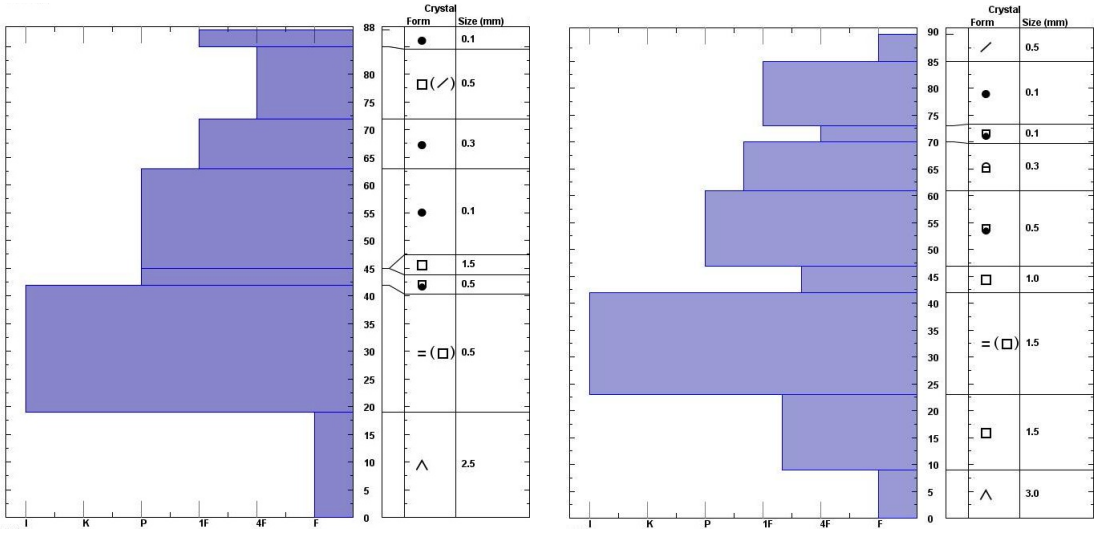

(A) 25.04.2014 (B) 12.05.2014

FIGURE 7.6: Snow pit profiles from Todalen, 120 m a.s.l., 19.03.2014-12.05.2014.

7.3.5 Seedvault 1/2

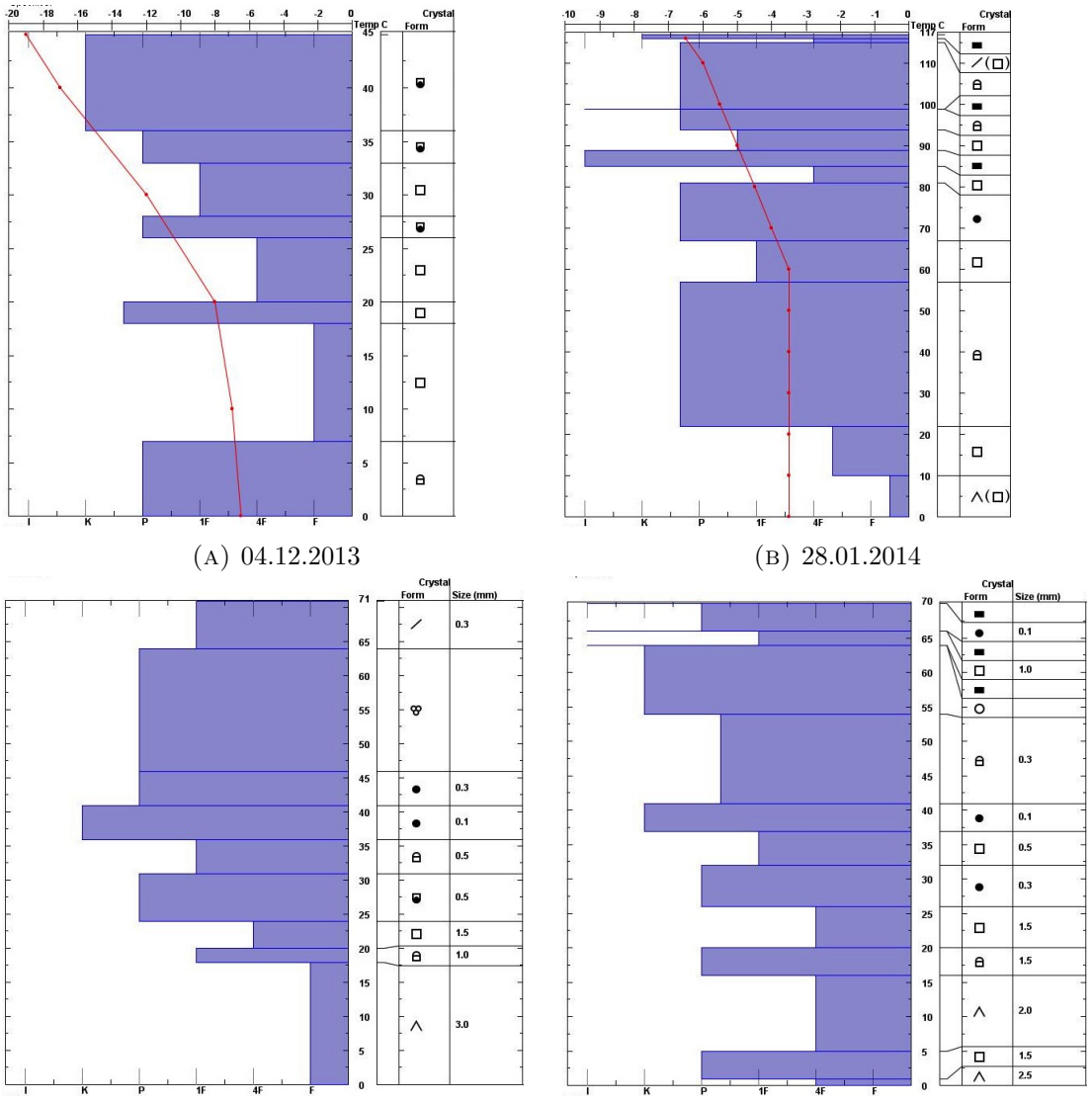

(A) 04.12.2013

(B) 28.01.2014

(C) 07.02.2014

(D) 21.02.2014

FIGURE 7.7: Snow pit profiles from Seedvault, 250 m a.s.l., 04.12.2013-21.02.2014.

7.3.6 Seedvault 2/2

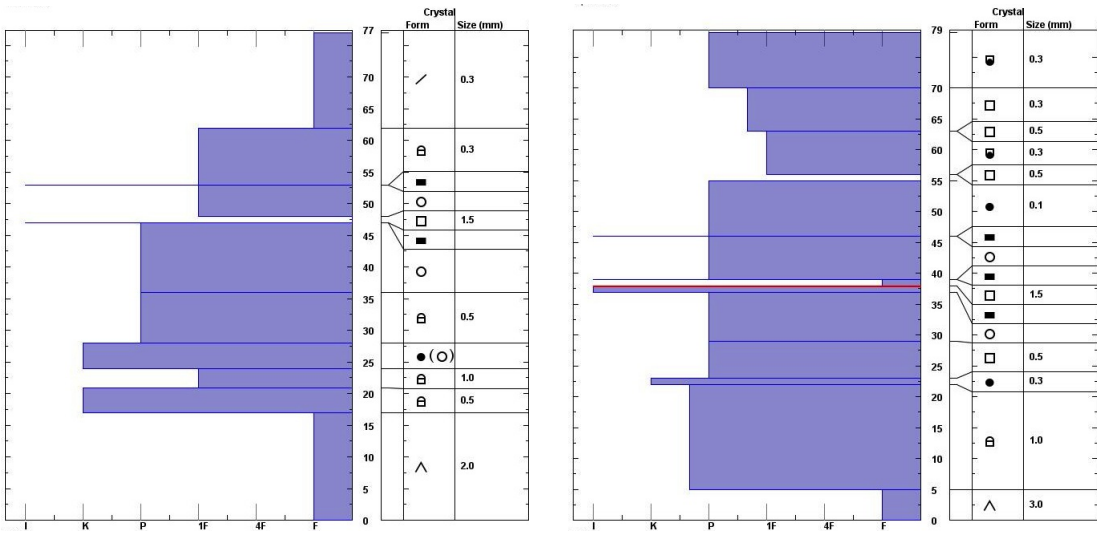

(A) 05.03.2014

(B) 19.03.2014

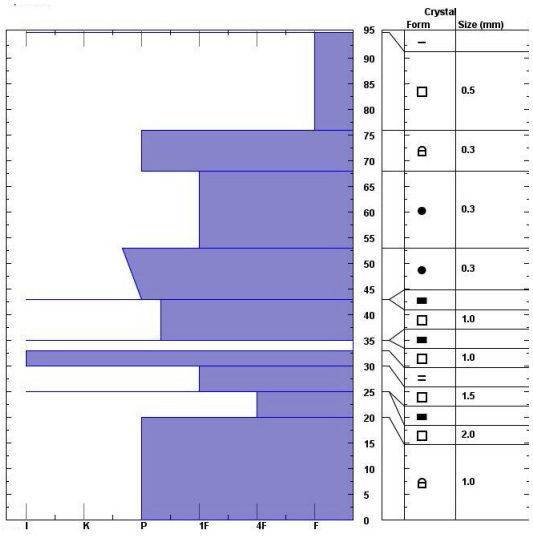

(C) 04.04.2014

FIGURE 7.8: Snow pit profiles from Seedvault, 250 m a.s.l., 05.03.2014-04.04.2014

7.3.7 Hiorthhamn 1/2

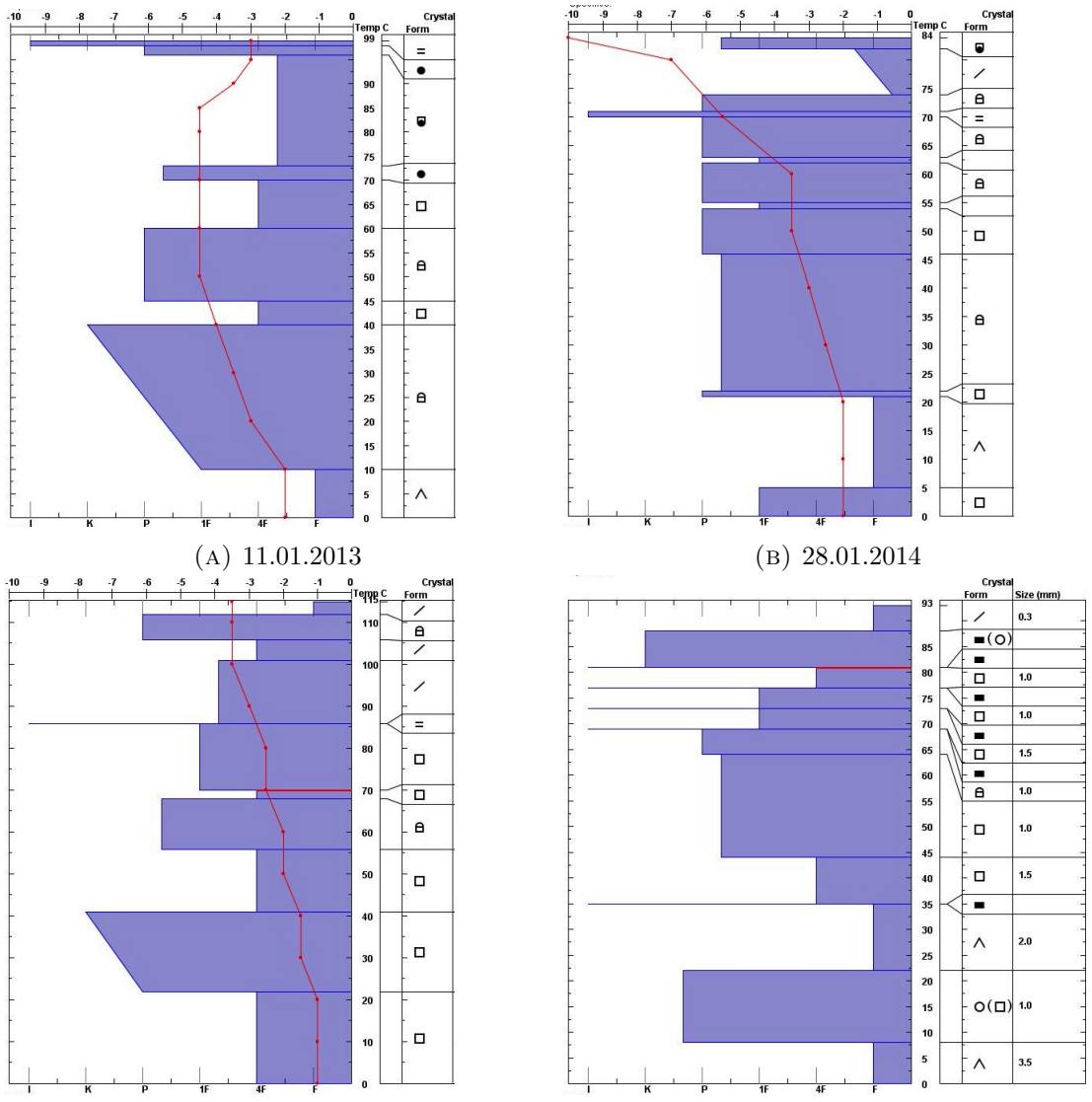

(A) 11.01.2013

(B) 28.01.2014

(C) 07.02.2014

(D) 05.03.2014

FIGURE 7.9: Snow pit profiles from Hiorthhamn, 260 m a.s.l., 11.01.2014-05.03.2014.

7.3.8 Hiorthhamn 2/2

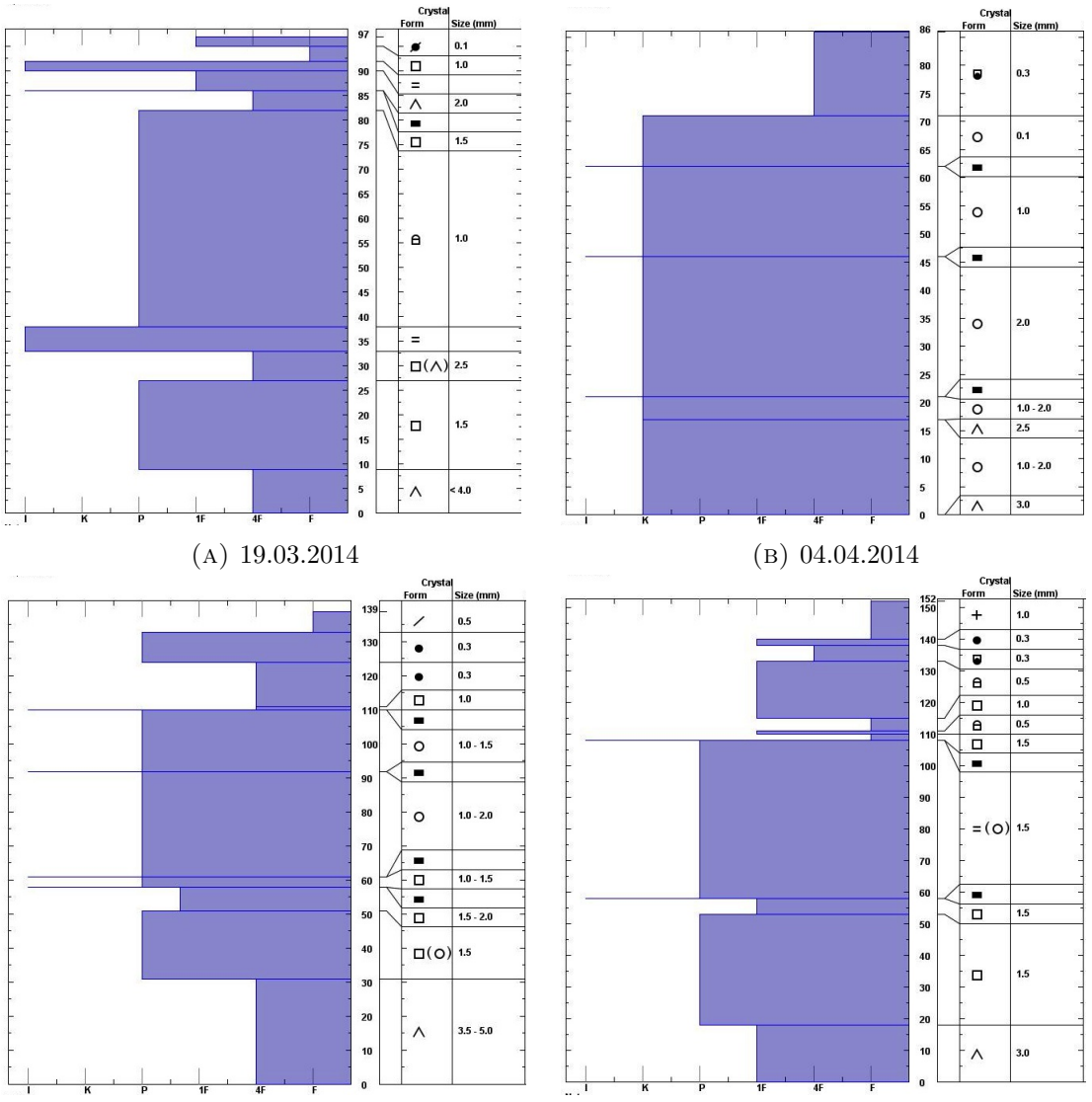

(A) 19.03.2014

(B) 04.04.2014

(C) 25.05.2014

(D) 12.05.2014

FIGURE 7.10: Snow pit profiles from Hiorthhamn, 260 m a.s.l., 19.03.2013-15.05.2014.

7.3.9 Fardalen 1/2

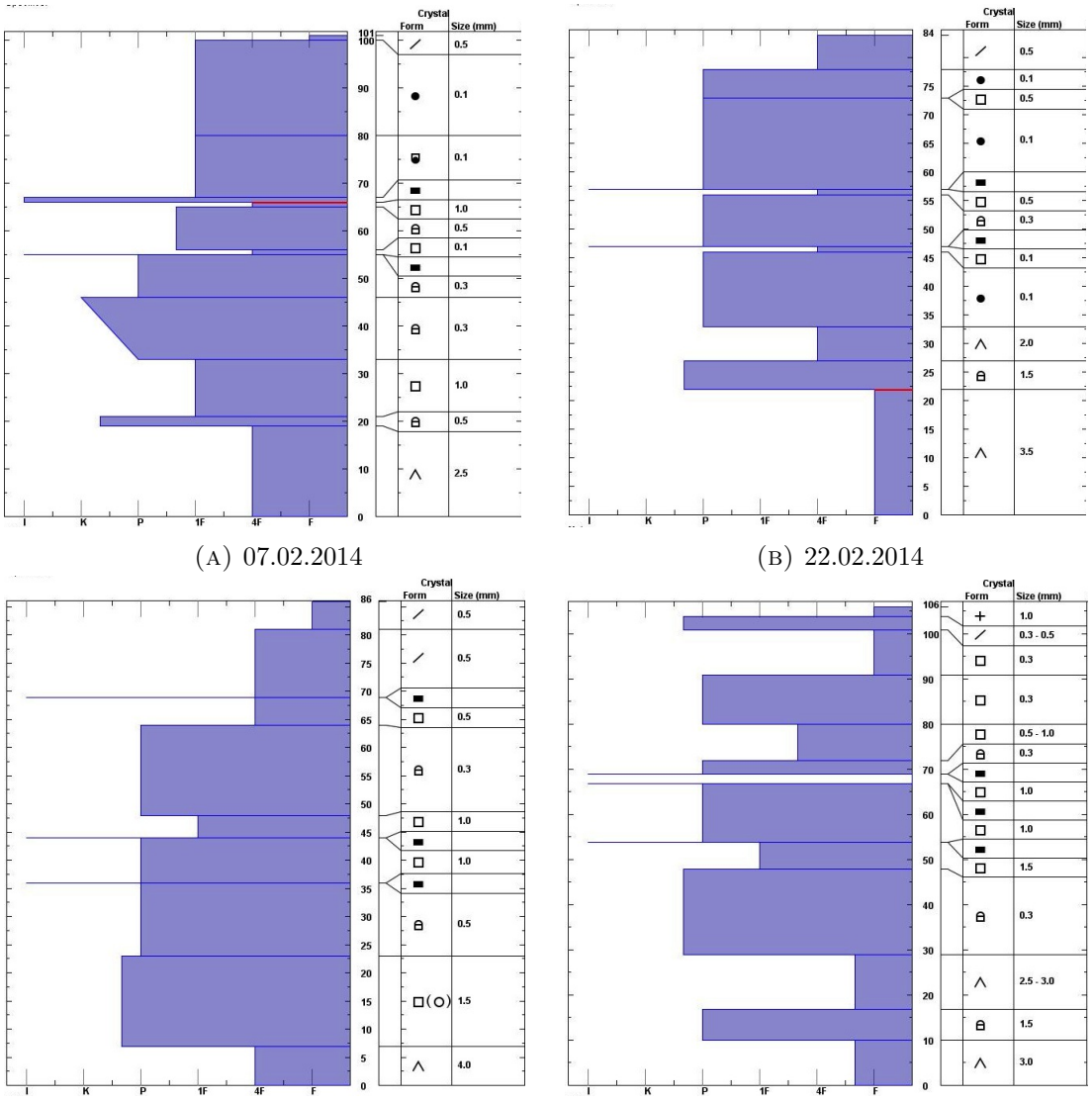

(A) 07.02.2014

(B) 22.02.2014

(C) 05.03.2014

(D) 19.03.2014

FIGURE 7.11: Snow pit profiles from Fardalen, 430 m a.s.l., 07.02.2014-19.03.2014.

7.3.10 Fardalen 2/2

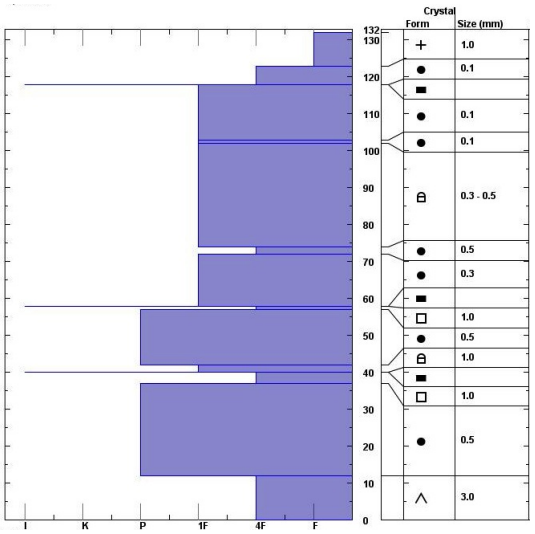

(A) 12.05.2014

FIGURE 7.12: Snow pit profiles from Fardalen, 430 m a.s.l., 12.05.2014.

7.3.11 Gangskaret 1/2

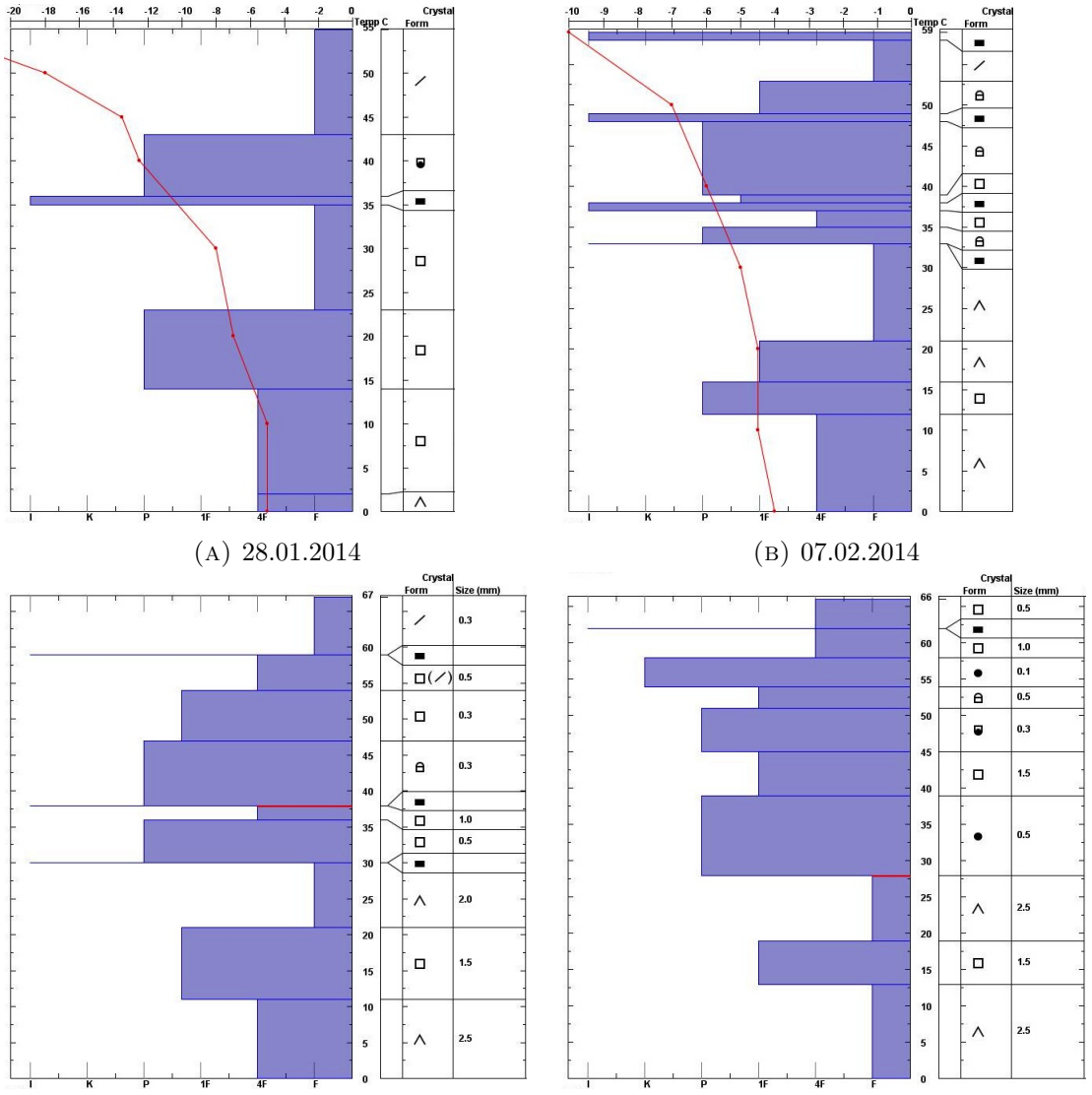

(A) 28.01.2014

(B) 07.02.2014

(C) 21.02.2014

(D) 05.03.2014

FIGURE 7.13: Snow pit profiles from Gangskaret, 460 m a.s.l., 28.01.2014-05.03.2014.

7.3.12 Gangskaret 2/2

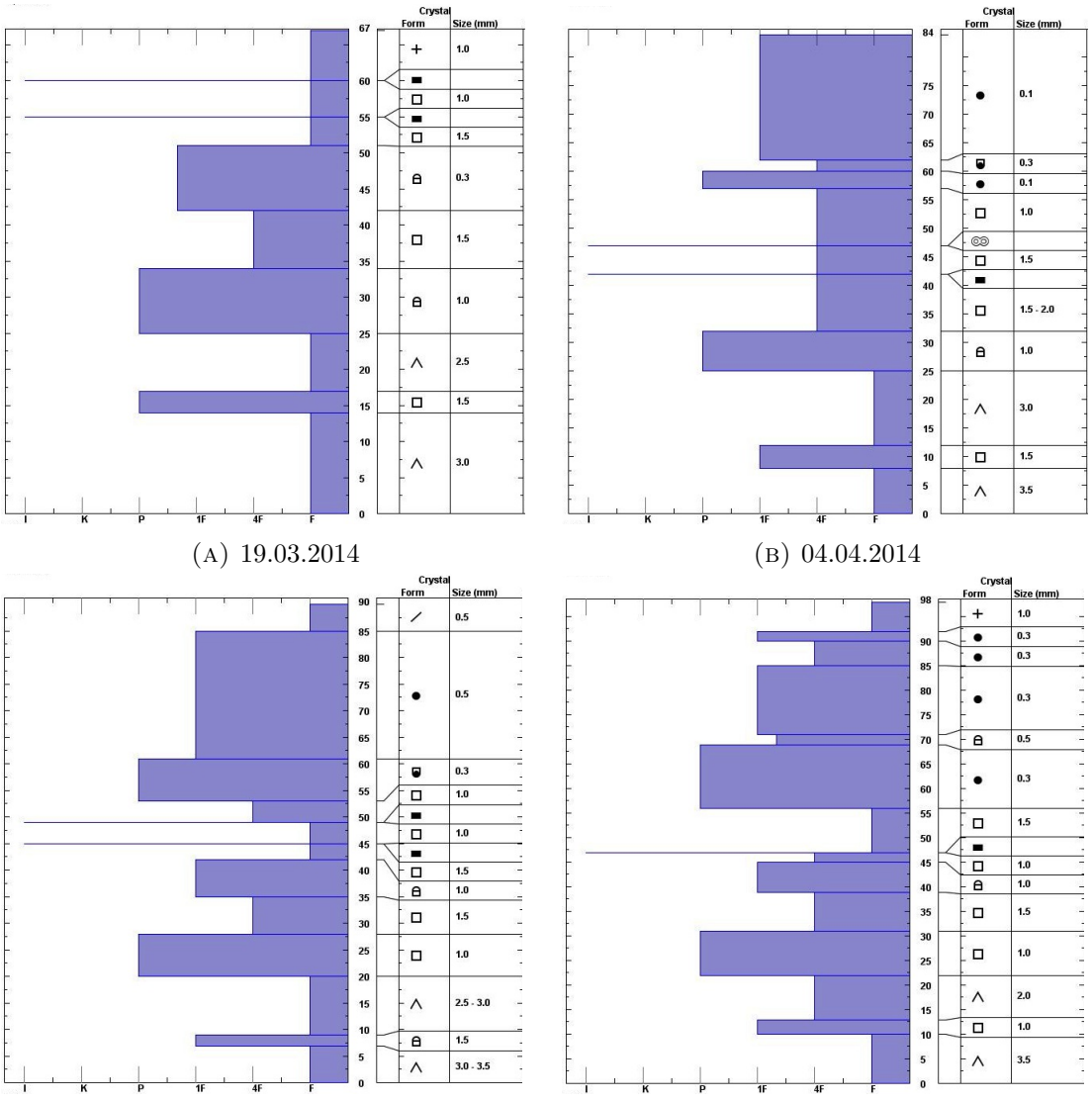

(A) 19.03.2014

(B) 04.04.2014

(C) 25.04.2014

(D) 12.05.2014

FIGURE 7.14: Snow pit profiles from Gangskaret, 430 m a.s.l., 19.03.2014-12.05.2014.

7.3.13 Lyb.passet 1/2

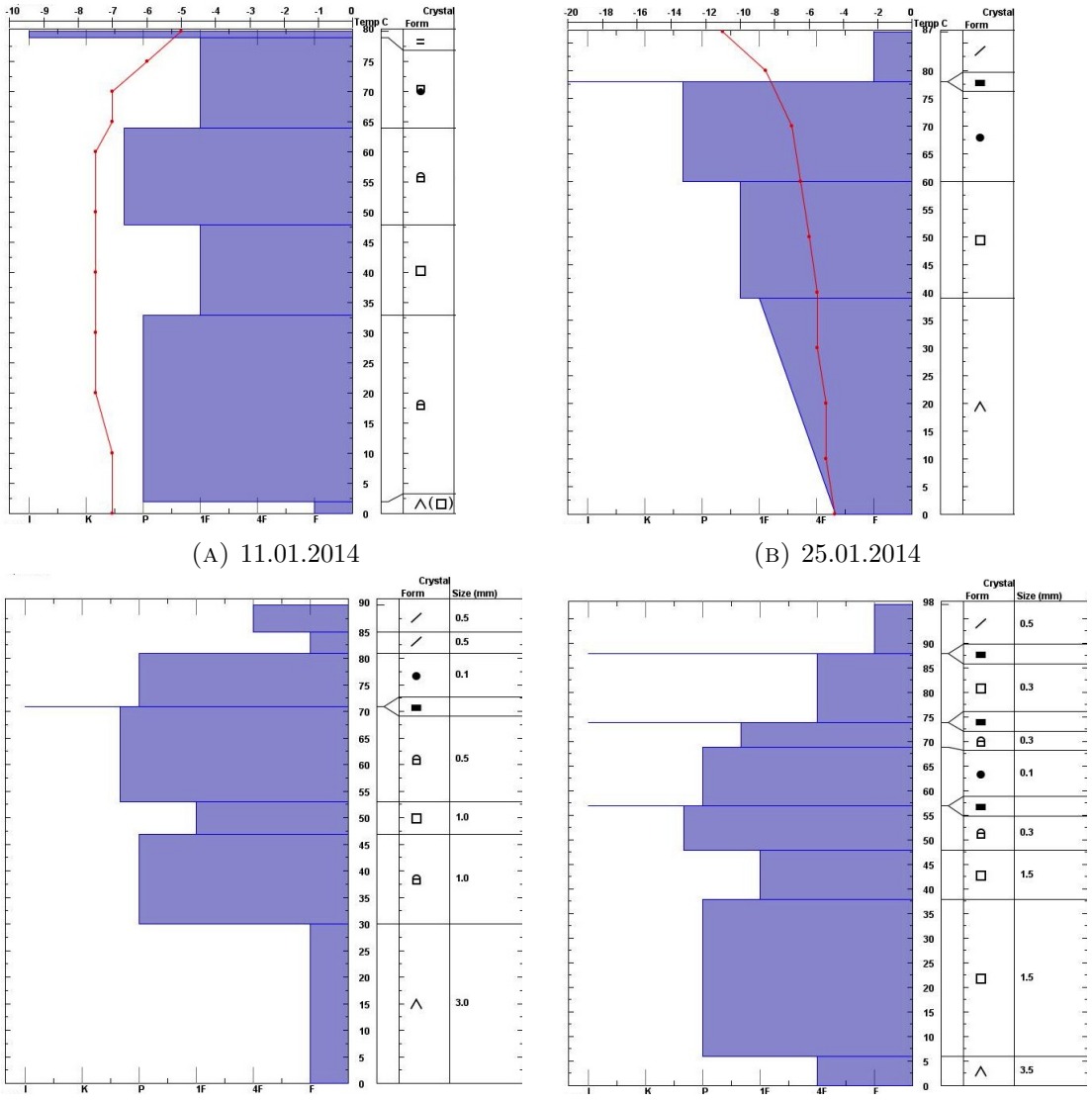

(A) 11.01.2014

(B) 25.01.2014

(C) 21.02.2014

(D) 05.03.2014

FIGURE 7.15: Snow pit profiles from Lyb.passet, 630 m a.s.l., 11.01.2014-05.03.2014.

7.3.14 Lyb.passet 2/2

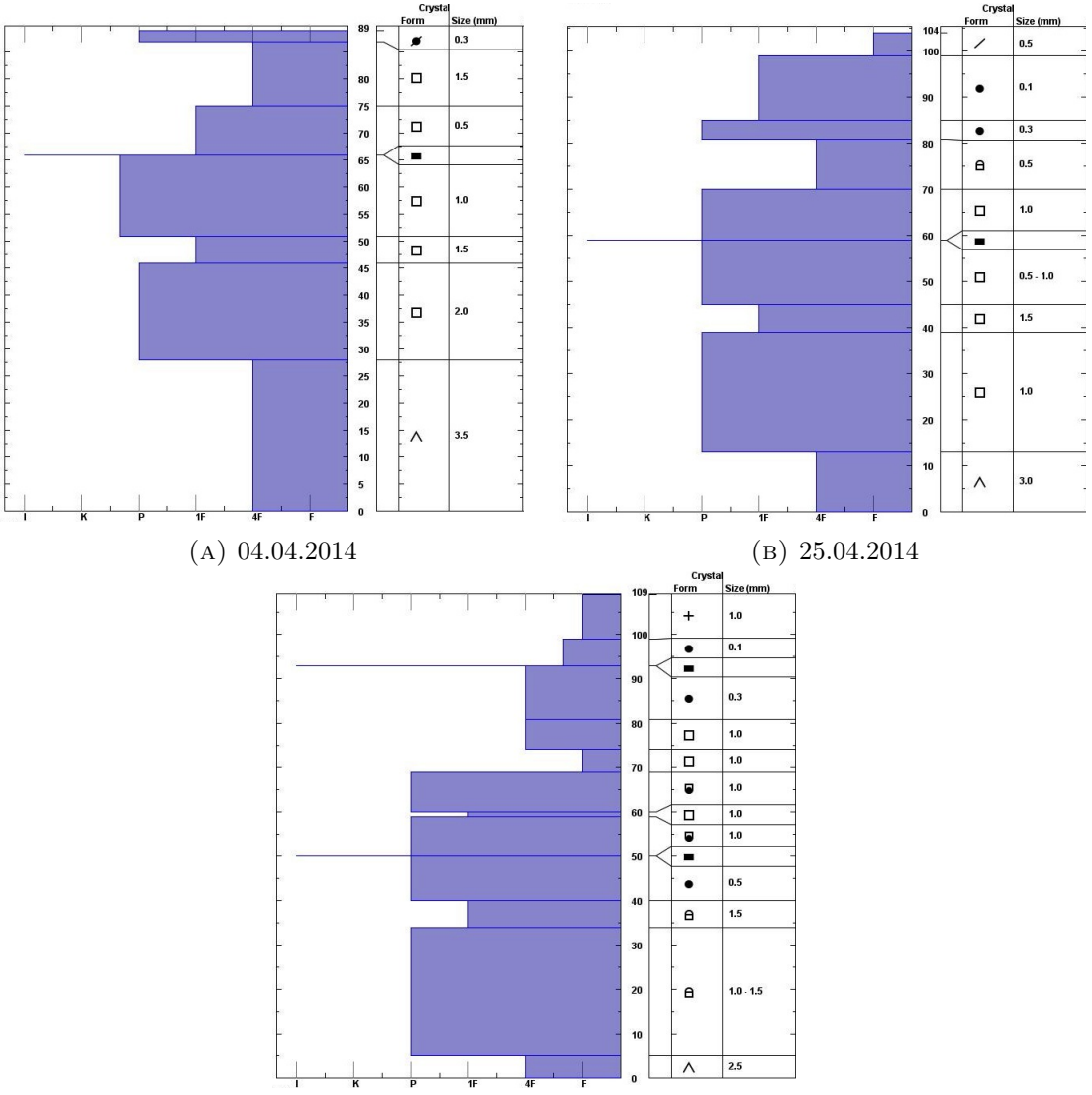

(A) 04.04.2014

(B) 25.04.2014

(C) 12.05.2014

FIGURE 7.16: Snow pit profiles from Lyb.passet, 430 m a.s.l., 07.02.2014-19.03.2014.

Bibliography

[1] Jennifer C Adam and Dennis P Lettenmaier. "Adjustment of global gridded precipitation for systematic bias". In: *Journal of Geophysical Research: Atmospheres (1984–2012)* 108.D9 (2003).

[2] C Donald Ahrens. *Essentials of meteorology: an invitation to the atmosphere*. Cengage Learning, 2011.

[3] Marie-Françoise André. "Geomorphic impact of spring avalanches in Northwest Spitsbergen (79 N)". In: *Permafrost and Periglacial Processes* 1.2 (1990b), pp. 97–110.

[4] Marie-Franfoise André. "Frequency of debris flows and slush avalanches in Spitsbergen: a tentative evaluation from lichenometry". In: *Polish Polar Research* 11.3-4 (1990a), pp. 345–363.

[5] RICHARD L Armstrong and BETSY R Armstrong. "Snow and avalanche climates of the western United States: a comparison of maritime, intermountain and continental conditions". In: *IAHS Publication* 162 (1987), pp. 281–94.

[6] RE Benestad et al. "Associations between sea-ice and the local climate on Svalbard". In: *Oslo: Norwegian Meteorological Institute Report* 07/02 (2002), pp. 1–7.

[7] Karl W Birkeland. "Terminology and predominant processes associated with the formation of weak layers of near-surface faceted crystals in the mountain snowpack". In: *Arctic and Alpine Research* (1998), pp. 193–199.

[8] KW Birkeland. "Spatial patterns of snow stability throughout a small mountain range". In: *Journal of Glaciology* 47.157 (2001), pp. 176–186.

[9] Günter Blöschl and M Sivapalan. "Scale issues in hydrological modelling: a review". In: *Hydrological processes* 9.3-4 (1995), pp. 251–290.

[10] K Brattlien and J.G. Ellesvold. "The SLAB test - The missing link in stability testest?" In: *International Snow Science Workshop* Lake Tahoe, Ca. (2010), pp. 61–65.

[11] Hanne H Christiansen, Hugh M French, and Ole Humlum. "Permafrost in the Gruve-7 mine, Adventdalen, Svalbard". In: *Norsk Geografisk Tidsskrift* 59.2 (2005), pp. 109–115.

[12] Hanne H Christiansen, Ole Humlum, and Markus Eckerstorfer. "Central Svalbard 2000-2011 meteorological dynamics and periglacial landscape response". In: *Arctic, Antarctic, and Alpine Research* 45.1 (2013), pp. 6–18.

[13] Samuel C Colbeck and J Bruce Jamieson. "The formation of faceted layers above crusts". In: *Cold Regions Science and Technology* 33.2 (2001), pp. 247–252.

[14] SC Colbeck. "An overview of seasonal snow metamorphism". In: *Reviews of Geophysics* 20.1 (1982), pp. 45–61.

[15] SC Colbeck. "The layered character of snow covers". In: *Reviews of Geophysics* 29.1 (1991), pp. 81–96.

[16] SC Colbeck. "The vapor diffusion coefficient for snow". In: *Water resources research* 29.1 (1993), pp. 109–115.

[17] MARCEL DE QUERVAIN and ROLAND MEISTER. "50 years of snow profiles on the Weissfluhjoch and relations to the surrounding avalanche activity (1936/37-1985/86)". In: *Avalanche Formation, Movement and Effects IAHS Publ. 162, September 14–19* (1986), pp. 161–181.

[18] Louis Delmas. "Spontaneous Avalanche Releases in Svalbard, Influence of Climate Parameters on Snow Mechanical Properties". In: (2013).

[19] M Eckerstorfer and HH Christiansen. "Relating meteorological variables to the natural slab avalanche regime in High Arctic Svalbard". In: *Cold Regions Science and Technology* 69.2 (2011c), pp. 184–193.

[20] M Eckerstorfer and HH Christiansen. "Meteorology, Topography and Snowpack Conditions causing Two Extreme Mid-Winter Slush and Wet Slab Avalanche Periods in High Arctic Maritime Svalbard". In: *Permafrost and Periglacial Processes* 23.1 (2012), pp. 15–25.

[21] Markus Eckerstorfer and Hanne H Christiansen. "The" High Arctic Maritime Snow Climate" in Central Svalbard". In: *Arctic, Antarctic, and Alpine Research* 43.1 (2011a), pp. 11–21.

[22] Markus Eckerstorfer and Hanne H Christiansen. "Topographical and meteorological control on snow avalanching in the Longyearbyen area, central Svalbard 2006–2009". In: *Geomorphology* 134.3 (2011b), pp. 186–196.

[23] Markus Eckerstorfer et al. "Snow cornice dynamics as a control on plateau edge erosion in central Svalbard". In: *Earth Surface Processes and Landforms* 38.5 (2013), pp. 466–476.

[24] Markus Eckerstorfer, Wesley R Farnsworth, and Karl W Birkeland. "Potential dry slab avalanche trigger zones on wind-affected slopes in central Svalbard". In: *Cold Regions Science and Technology* 99 (2014), pp. 66–77.

[25] Wesley R Farnsworth, Markus Eckerstorfer, and Hanne H Christiansen. "SPATIAL VARIABIITY OF SNOWPACK ON SMALL WIND EFFECTED SLOPES, CENTRAL SVALBARD". In: (2013).

[26] Charles Fierz et al. *TheInternational Classificationi for Seasonal Snow on the Groun*. UNESCO/IHP, 2009.

[27] Eirik J Førland and Inger Hanssen-Bauer. "Increased precipitation in the Norwegian Arctic: True or false?" In: *Climatic Change* 46.4 (2000), pp. 485–509.

[28] Yoshinori Furukawa and John S Wettlaufer. "Snow and ice crystals". In: *Physics Today* 60.12 (2007), pp. 70–71.

[29] Akihiro Hachikubo and Eizi Akitaya. "Effect of wind on surface hoar growth on snow". In: *Journal of Geophysical Research: Atmospheres (1984–2012)* 102.D4 (1997), pp. 4367–4373.

[30] Pascal Haegeli and David M McClung. "Avalanche characteristics of a transitional snow climate–Columbia Mountains, British Columbia, Canada". In: *Cold Regions Science and Technology* 37.3 (2003), pp. 255–276.

[31] Pascal Haegeli and David M McClung. "Expanding the snow-climate classification with avalanche-relevant information: initial description of avalanche winter regimes for southwestern Canada". In: *Journal of Glaciology* 53.181 (2007), pp. 266–276.

[32] Walter Brian Harland et al. "The geology of Svalbard". In: (1997).

[33] Jordy Hendrikx et al. "Avalanche activity in an extreme maritime climate: The application of classification trees for forecasting". In: *Cold Regions Science and Technology* 43.1 (2005), pp. 104–116.

[34] Ole Humlum. "Modelling late 20th-century precipitation in Nordenskiold Land, Svalbard, by geomorphic means". In: *Norsk geografisk tidsskrift* 56.2 (2002), pp. 96–103.

[35] Ole Humlum, Arne Instanes, and Johan Ludvig Sollid. "Permafrost in Svalbard: a review of research history, climatic background and engineering challenges". In: *Polar Research* 22.2 (2003), pp. 191–215.

[36] Ole Humlum, Hanne H Christiansen, and Håvard Juliussen. "Avalanche-derived rock glaciers in Svalbard". In: *Permafrost and Periglacial Processes* 18.1 (2007), pp. 75–88.

[37] Shinji Ikeda et al. "Study of snow climate in the Japanese Alps: Comparison to snow climate in North America". In: *Cold Regions Science and Technology* 59.2 (2009), pp. 119–125.

[38] Bruce Jamieson. "Formation of refrozen snowpack layers and their role in slab avalanche release". In: *Reviews of Geophysics* 44.2 (2006).

[39] JB Jamieson and CD Johnston. "Rutschblock precision, technique variations and limitations". In: *Journal of Glaciology* 39 (1993), pp. 666–674.

[40] Tiina Kilpeläinen and Anna Sjöblom. "Momentum and sensible heat exchange in an ice-free Arctic fjord". In: *Boundary-layer meteorology* 134.1 (2010), pp. 109–130.

[41] Edward R LaChapelle. *Avalanche forecasting-a modern synthesis*. US Department of Agriculture, 1965.

[42] Edward R LaChapelle. "Field guide to snow crystals". In: (1969).

[43] Long Li and John W Pomeroy. "Estimates of threshold wind speeds for snow transport using meteorological data". In: *Journal of Applied Meteorology* 36.3 (1997), pp. 205–213.

[44] maps.grida.no. *http://www.grida.no/graphicslib/detail/permafrost-extent-in-the-northern-hemisphere$_1$266*. 2014.

[45] David McClung and Peter A Schaerer. *The avalanche handbook*. The Mountaineers Books, 2006.

[46] DM McClung. "The elements of applied avalanche forecasting, Part II: the physical issues and the rules of applied avalanche forecasting". In: *Natural Hazards* 26.2 (2002), pp. 131–146.

[47] met.no. *Norwegian meteorological institute*. Internet. 2014.

[48] Cary J Mock and Karl W Birkeland. "Snow avalanche climatology of the western United States mountain ranges". In: *Bulletin of the American Meteorological Society* 81.10 (2000), pp. 2367–2392.

[49] Christine Pielmeier and Martin Schneebeli. "Developments in the stratigraphy of snow". In: *Surveys in Geophysics* 24.5-6 (2003), pp. 389–416.

[50] BR Pinzer, M Schneebeli, and TU Kaempfer. "Vapor flux and recrystallization during dry snow metamorphism under a steady temperature gradient as observed by time-lapse micro-tomography". In: *The Cryosphere Discussions* 6.3 (2012), pp. 1673–1714.

[51] Martin Schneebeli and Sergey A Sokratov. "Tomography of temperature gradient metamorphism of snow and associated changes in heat conductivity". In: *Hydrological Processes* 18.18 (2004), pp. 3655–3665.

[52] Jürg Schweizer. "Review of dry snow slab avalanche release". In: *Cold Regions Science and Technology* 30.1 (1999), pp. 43–57.

[53] Jürg Schweizer, Kalle Kronholm, and Thomas Wiesinger. "Verification of regional snowpack stability and avalanche danger". In: *Cold Regions Science and Technology* 37.3 (2003), pp. 277–288.

[54] Jürg Schweizer et al. "SPATIAL VARIABILTY–SO WHAT?" In: (2006).

[55] Jürg Schweizer et al. "Review of spatial variability of snowpack properties and its importance for avalanche formation". In: *Cold Regions Science and Technology* 51.2 (2008), pp. 253–272.

[56] Ron Simenhois and KW Birkeland. "The extended column test: A field test for fracture initiation and propagation". In: *Proceedings ISSW*. 2006, pp. 79–85.

[57] RA Sommerfeld and Edward R LaChapelle. *The classification of snow metamorphism*. British Glaciological Society, 1970.

[58] Matthew Sturm, Jon Holmgren, and Glen E Liston. "A seasonal snow cover classification system for local to global applications". In: *Journal of Climate* 8.5 (1995), pp. 1261–1283.

[59] S Vogel, M Eckerstorfer, and HH Christiansen. "Cornice dynamics and meteorological control at Gruvefjellet, Central Svalbard". In: *The Cryosphere* 6.1 (2012), pp. 157–171.

[60] Thomas Wiesinger and Jürg Schweizer. "Snow profile interpretation". In: *Montana* 2 (2000), p. 6.

[61] Zyungo Yosida et al. "Physical Studies on Deposited Snow. I.; Thermal Properties." In: *Contributions from the Institute of Low Temperature Science* 7 (1955), pp. 19–74.